1-1-2017

Influence of Land Use, Land Cover, and Hydrology on the Spatial and Temporal Characteristics of Dissolved Organic Matter (DOM) in Multiple Aquatic Ecosystems

Shatrughan Singh

Influence of land use, land cover, and hydrology on the spatial and temporal characteristics of dissolved organic matter (DOM) in multiple aquatic ecosystems

By

Shatrughan Singh

A Dissertation
Submitted to the Faculty of
Mississippi State University
in Partial Fulfillment of the Requirements
for the Degree of Doctor of Philosophy
in Earth and Atmospheric Sciences
in the Department of Geosciences

Mississippi State, Mississippi

August 2017

Influence of land use, land cover, and hydrology on the spatial and temporal characteristics of dissolved organic matter (DOM) in multiple aquatic ecosystems

By

Shatrughan Singh

Approved:

_____

Padmanava Dash
(Major Professor)

_____

William H. Cooke III
(Committee Member)

_____

John C. Rodgers III
(Committee Member)

_____

Andrew E. Mercer
(Committee Member)

_____

Renee M. Clary
(Graduate Coordinator)

_____

Rick Travis
Dean
College of Arts & Sciences

Name: Shatrughan Singh

Date of Degree: August 11, 2017

Institution: Mississippi State University

Major Field: Earth and Atmospheric Sciences

Major Professor: Padmanava Dash

Title of Study: Influence of land use, land cover, and hydrology on the spatial and temporal characteristics of dissolved organic matter (DOM) in multiple aquatic ecosystems

Pages in Study 159

Candidate for Degree of Doctor of Philosophy

Spatial and temporal patterns of dissolved organic matter (DOM) were characterized using a combination of spectro-fluorometric measurements and multivariate analysis techniques. The study was conducted over a four-year (2012-2016) period in multiple watersheds located in the Gulf-Atlantic Coastal Plain Physiographic region of the southeast USA as well as in the Indo-Gangetic Plain of India. Surface water samples were collected from five major lakes in the Mississippi, an estuarine region in the southeastern Louisiana, and from the coastal region in the eastern Mississippi Sound in the USA, and a large river (Ganges River) in India. Absorption and fluorescence measurements were performed to generate absorption spectra and excitation-emission matrices (EEMs). Using parallel factor analyses (PARAFAC), EEM models were developed to characterize the biogeochemistry of DOM in three studies in this project. Principal component analysis and regression analyses of DOM data indicated that the northern Mississippi lakes were majorly influenced by agricultural land use, estuarine region was affected by natural DOM export from forests and wetlands, while the coastal waters were affected by a mix of anthropogenic and natural inputs of DOM. Spatial

analyses indicated that DOM derived from watershed with increased wetland coverage was humic and aromatic while the DOM derived from agricultural watersheds was bioavailable. Temporal patterns of DOM in the estuary indicated the influence of hydrologic conditions and summer temperatures, and revealed strong seasonality in DOM evolution in the watershed. During high discharge periods (spring), aromatic and humic DOM was exported from the watershed while strong photochemical degradation during summer resulted bioavailable DOM. Comparison between two river systems, a highly urbanized large river and a small pristine river, indicated the influence of anthropogenic inputs of DOM in the large river system. DOM was bioavailable during summer due to anthropogenic activities in the large river system while it varied with hydrological connectivity in a small river system during summer and winter. In conclusion, this study has improved my understandings of the DOM properties, which are critical for a comprehensive assessment of biogeochemical processes undergoing in important water bodies on which our society is heavily dependent upon.

ACKNOWLEDGEMENTS

This dissertation has only been possible with the continuous guidance, support, and encouragement from my advisor, Dr. Padmanava Dash. I am thankful to him for providing me the opportunity and his valuable support and guidance throughout this work. I would also like to thank my committee members, Dr. Bill Cooke, Dr. John Rodgers, and Dr. Andrew Mercer, for their support and encouragement throughout this research dissertation. Dr. Cooke has been very kind and inspiring to me, and has provided his intellectual inputs. Dr. Rodgers helped me with my teaching obligations, in addressing student related issues, and with geospatial techniques. Dr. Mercer helped me in understanding many complex statistical methods.

I would like to extend my appreciation to Prof. Ramesh Singh, Chapman University, for his kind encouragements and helpful discussions during this project. Prof. Singh not only helped me with academic discussions but also brought me water samples from India that was used as a part of this project.

I am grateful to my colleagues – Saurav Silwal (Sauree), Sankar M. Sasidharan, Pushkar Inamdar, Mary G. Chambers, and Kate Grala – for their friendship and support. It would be unfair if I do not mention especially my lab mates Sauree as she has helped in water sampling and filtering, and Sankar who helped in processing the water samples. I thank Christopher Zarzar, Department of Geosciences, and Gray Turnage, Geosystems Research Institute at the Mississippi State University for their help with water sampling. I

gratefully acknowledge the field sampling costs supported by the faculty start-up grant to Dr. Padmanava Dash and by a funding to Dr. Robert Moorhead from the NOAA Unmanned Aerial Systems Program Office through the Northern Gulf Institute, a NOAA Cooperative Institute (grant no. NA11OAR4320199).

I thank Dr. Gary Feng and Dr. Ardeshir Adeli for allowing me to use their labs and their staff Trey Robinson, Mary Hardy, and Nicole Barksdale at the Genetics and Sustainable Agriculture Research Unit, Agricultural Research Service, United States Department of Agriculture, Mississippi State, MS, for nutrient analysis.

I thank Dr. Yuehan Lu, University of Alabama, for allowing me to use her laboratory to measure DOC and TDN concentrations, and Peng Shang for helping me with the training and processing of the samples. Both Dr. Lu and Peng were exceptionally generous with the equipment, materials, and time.

I would like to thank the faculty, staff and graduate students of the Department of Geosciences at the Mississippi State University for their contribution towards the success of this project. A special thanks is extended to Dr. Jamie Dyer for providing the multi-sensor precipitation estimates data for my study region.

Finally, I would like to thank all my friends and family for their continuous support, warm encouragements, and motivation during this dissertation research.

TABLE OF CONTENTS

LIST OF TABLES

LIST OF FIGURES

CHAPTER I

INTRODUCTION

Dissolved organic matter (DOM) is a complex heterogeneous mixture of organic molecules composed of humic (e.g., humic and fulvic acids) and non-humic (e.g., carbohydrates and amino acids) substances and is abundant in aquatic environments (Coble 2008; Fellman et al. 2010; McKnight et al. 2001; Thurman 1985). DOM plays an important role in modifying water quality through various biogeochemical processes (Aiken et al. 2011; Bolan et al. 2011). It also plays a vital role in terrestrial and aquatic ecosystems by serving as carbon and energy source for the microbial food web (Bano et al. 1997; Findlay 2010), and by absorbing damaging ultraviolet radiations in order to protect benthic ecosystems (Vahatalo and Zepp 2005; Zepp et al. 2006). Nitrogen and phosphorous compounds of DOM (i.e., DON and DOP) can become bioavailable and stimulate algal growth or eutrophication in aquatic ecosystems (Boyer et al. 2006; Qualls 2013; Schrumpf et al. 2006; Wagner et al. 2008; Williams et al. 2006). DOM interacts strongly with pollutants and trace metals, thereby enhancing their water solubility and transport (Aiken et al. 2011; Jansen et al. 2014). Understanding of chemical composition of DOM is imperative to understand the contributions of DOM in biogeochemical reactions and transport of pollutants and their role in regional and global carbon and nutrient cycles (Aiken et al. 2011; Coble 2007, 1996; Cory and McKnight 2005). Spectral properties (absorption and fluorescence) of DOM are related to its molecular

arrangements and chemical nature, and these spectral characteristics have been used to trace DOM origin, chemical composition, and photo- and bio-chemical reactions and also to understand carbon and nutrient cycles in aquatic ecosystems (Cory et al. 2011; Fellman et al. 2010; Murphy et al. 2013; Stedmon et al. 2011).

Characterizing DOM constituents and determining their concentration has been difficult using traditional laboratory techniques since the analytical methods are laborious, time-consuming, expensive, and require large sample throughputs (Fellman et al. 2010; Leenheer 2009; Leenheer and Croué 2003). However, recent application of ultra-violet (UV) and visible (Vis) absorption and fluorescence methods allow for rapid characterization of DOM quality using small sample amounts (~ 4 mL) and can be especially useful for characterizing the DOM composition for large numbers of samples generated from watershed studies (Cory et al. 2011; Jaffé et al. 2014; Singh et al. 2014b). Three dimensional excitation-emission matrices (EEMs) of fluorescence measurements provide information about DOM quality and quantity in terms of its source, age, compositional structure and bioavailability and indices derived from these optical methods can also serve as tracers for identifying the sources and flow paths for DOM in watersheds (D'Amore et al. 2010; Fellman et al. 2008; Hood et al. 2006; Singh et al. 2015, 2014a, 2014b). Some of the optical indices that have recently been used include: specific ultra-violet absorbance (SUVA; Weishaar et al. 2003), spectral slope ratio (S_R; Helms et al. 2008), humification index (HIX; Zsolnay et al. 1999), biological index (BIX; Huguet et al. 2009), fluorescence index (FI; McKnight et al. 2001), and %protein-like components (Fellman et al. 2008) derived from fluorescence-based excitation emission matrices.

In addition to absorption and fluorescence measurements, a multivariate statistical technique, parallel factor (PARAFAC) analysis is a unique and emerging technique to decompose three-dimensional EEMs data into underlying meaningful fluorescence components (Murphy et al. 2013; Singh et al. 2015; Stedmon et al. 2003; Stedmon and Bro 2008). These independent fluorescence components reflect various dissolved organic compounds in a given water sample. While the understanding of optical indices for characterizing DOM composition is new and promising, its use is still in its infancy, and much research still needs to be conducted to allow for reliable assessment of DOM. One of the key needs include development of more reliable and site or region-specific multivariate statistical model (i.e., PARAFAC) for extracting biogeochemically meaningful results from fluorescence EEMs. For example, currently there is one PARAFAC model (Cory and McKnight 2005) that is being implemented across various sites, regions and ecosystems in the world to characterize DOM. Ideally, site or region-specific models need to be developed that would account for the variability and uniqueness of DOM for the region or ecosystem under study (Fellman et al. 2009; Larsen et al. 2010; Singh et al. 2013). In addition, it is especially critical that the biogeochemical information derived from optical indices be evaluated or corroborated using independent analytical methods. For example, the bioavailability of DOM derived from optical indices needs to be verified through direct determination of DOM decomposition by photochemical processes or consumption by microbes (Chen and Jaffé, 2014; Fellman et al., 2008). This dissertation addresses these important questions. The EEM-PARAFAC models that were developed in this research are the first attempt for both Mississippi, covering multiple aquatic ecosystems, and for a large river system in India, and will

potentially be applicable to characterize DOM for watersheds in these two distinct eco-regions.

The present study is divided into three main chapters, each dealing with specific objectives as documented in these chapters. Briefly, chapter two focuses on the influence of land use and land cover on the spatial variability in DOM in multiple aquatic ecosystems (e.g., lakes, estuaries, coastal waters). Chapter three is centered on the temporal variability of DOM in the lower Pearl River estuarine region to examine seasonality in the DOM character as the hydrologic discharge conditions and temperature levels change. DOM character changes with the size of the water body as many biogeochemical processes affect the transformations in DOM. In addition, DOM originating from natural or anthropogenic sources also influences its character differently. In chapter four, the spatial and temporal variation in DOM character was compared for a highly urbanized large river system (Ganges River, India) with a small but largely unperturbed river system with minimal human influence in a different geographic regime (Pearl River, USA). The present work is the first study focusing on the characterization of DOM in multiple aquatic environments in varying geographic regimes and examining the spatial and temporal variations in DOM quantity and quality. With the use of such DOM dataset this study provides a comprehensive approach in understanding DOM dynamics, which can be further utilized in order to better understand the DOM exports from variety of watersheds in Mississippi, coastal Louisiana and at a primitive level to the Ganges River, India. This study also serves as a basis for a need of long-term monitoring of DOM exports and its character from such watersheds, especially in the light of predicted climate change and increasing extreme weather events in the 21st century.

CHAPTER II

INFLUENCE OF LAND USE AND LAND COVER ON THE SPATIAL VARIABILITY OF DISSOLVED ORGANIC MATTER IN MULTIPLE AQUATIC ENVIRONMENTS[1]

2.1 Introduction

Dissolved organic matter (DOM) is a ubiquitous and heterogeneous mixture of aliphatic and aromatic organic compounds ranging from simple organic molecules, such as carbohydrates, lipids, and proteins to more complex organic molecules such as humic and fulvic acids (Thurman 1985; McKnight et al. 2001; Qualls 2013). DOM is a general term that is used to describe the dissolved organic substances as the materials that can pass through the 0.45-micron filter paper while dissolved organic carbon (DOC) is a major fraction of the total DOM pool (Aitkenhead-Peterson et al. 2003). DOM originates either by autochthonous (in situ phytoplankton and macrophyte production and cell-lysis) or allochthonous (degradation of terrestrially derived organic matter) sources due to natural biochemical processes in terrestrial and aquatic environments (Hudson et al. 2007). DOM is involved in a variety of biogeochemical processes thereby influencing the budgets of the transport of total carbon, nitrogen, phosphorous etc. from terrestrial ecosystems to the aquatic environments such as lakes, rivers, estuaries, coastal waters and

[1] Singh S, Dash P, Silwal S, et al (2017) Influence of land use and land cover on the spatial variability of dissolved organic matter in multiple aquatic environments. Environ Sci Pollut Res 24(16):14124-14141. doi: 10.1007/s11356-017-8917-5.

open oceans, and hence is an important contributor to the global elemental cycles (Stedmon and Markager 2005; Battin et al. 2008; Tranvik et al. 2009).

Water quality of the lakes and estuaries serve as the indicators of the overall health of not only aquatic ecosystems but also the terrestrial ecosystems those drain to the water body (Yamashita et al. 2008; Adrian et al. 2009; Tranvik et al. 2009). DOM exported to lakes, rivers, and coastal waters from watersheds reflects their characteristics and provide further insights into the origin of DOM (Cawley et al. 2014; Chen and Jaffé 2014). The quality of DOM reflects the biogeochemical processes (e.g., microbial degradation) underway at the source, during transport, and within these aquatic ecosystems, and the additional physicochemical processes such as photo-degradation in the aquatic ecosystems (Bushaw et al. 1996; Moran and Zepp 1997; Maie et al. 2012). For example, Tranvik et al. (2009) examined the mechanisms influencing DOM pools and its transformations in lakes for expected climate change scenarios and have concluded that lakes can serve as a sentinel of climate change especially in response to anthropogenic activities. In addition, estuaries are considered as "hotspots" where DOM plays a major role in influencing food web dynamics and net ecosystem metabolism depending upon the quantity and quality of DOM (Leech et al. 2016). It also plays a key role in transport and transformation of major contaminants and/or pollutants and their reactivity with the environment. For example, DOM interacts with trace metals present in its surrounding environment and affects its solubility and transport (Yamashita and Jaffé 2008). DOM influences the mobilization of heavy metals such as mercury (Schuster et al. 2008), aside from the formation of carcinogenic disinfection byproducts (DBPs) during drinking water treatment (Kraus et al. 2008). Because the chemical character of DOM

(i.e., quantity and quality) influences numerous biogeochemical and physicochemical properties of inland and coastal waters, which depends on the type of DOM in the watershed or on the physicochemical processes it undergoes, it is important to understand the DOM character in accordance with potential watershed sources (e.g., land cover such as wetlands) for explaining and quantifying the DOM exports (Wilson and Xenopoulos 2009; Williams et al. 2010; Yang et al. 2011; Lottig et al. 2012; Kothawala et al. 2014; Singh et al. 2014a). Thus, a clear understanding of the linkages of land use and land cover to the aquatic ecosystems and the ongoing biogeochemical processes affecting the DOM exports is warranted for a comprehensive analysis of the water quality.

Land use and land cover (LULC) plays not only a significant role in controlling the quantity of DOM export, but also influences the quality of DOM via various biogeochemical and degradation processes (e.g., bio- and photo-degradation) that may potentially affect the lakes, rivers, and coastal waters (Bushaw et al. 1996; Bushaw-Newton and Moran 1999; Jaffé et al. 2004; Maie et al. 2012; Chen and Jaffé 2014; Lu et al. 2014; Toosi et al. 2014). Previous studies have shown that the composition of DOM is affected by a range of environmental factors such as quality of soil organic matter, hydrological pathways, temperature, land use and land cover, available light intensity, and microbial metabolic activity within a given watershed (Bertilsson and Tranvik 2000; Post and Kwon 2000; Wilson and Xenopoulos 2009; Cawley et al. 2014; Kothawala et al. 2014). For instance, Bertilsson and Tranvik (2000) have reported the production of low molecular weight DOM with the variation in solar radiation in Swedish lakes. Wilson and Xenopoulos (2009) have found that the land use changes could significantly alter the delivery of DOM to streams in the watersheds of south-central Ontario, Canada region. In

addition, a few studies have observed the spatial variability of DOM in stream networks which has been attributed to varying hydrologic conditions during base flow and storm flow periods (Buffam et al. 2001; Hood et al. 2006; Singh et al. 2015). Landscape characteristics such as specific LULC types (e.g., forest, agriculture or urban) or landscape features (e.g., presence or absence of wetlands) have been found as important factors in influencing DOM quality (Brooks et al. 1999; Ågren et al. 2008; Wilson and Xenopoulos 2009; Williams et al. 2010; Lottig et al. 2012; Toosi et al. 2014).

Previous studies have shown that DOM generated from microbial sources or from in situ production (i.e., autochthonous) are considered as more "labile" while the DOM generated from the degradation of vascular plants or soil materials from terrestrial sources are generally "refractory" in nature (Qualls et al. 2002; Hopkinson and Vallino 2005; Tranvik et al. 2009). Because the quality of DOM determines how it would take part in biogeochemical reactions, for example, whether the DOM will act as a terminal electron acceptor from biogeochemical reactions or as a source of energy to both in situ and ex situ ecosystem metabolism, the biochemical character of DOM quality needs to be examined (Lovley et al. 1996; Mladenov et al. 2010; Cory and Kaplan 2012). Moreover, these two DOM pools differ in their optical and chemical characteristics thereby affecting the decomposition process pathways and rates. The bio-optical character of "labile" DOM is that it absorbs less in the region of visible spectrum due to apparently lower average molecular weight while allochthonous DOM is considered to be more "refractory" and absorbs more ultraviolet (UV) and visible (Vis) light than labile DOM owing to higher average molecular weight (Hopkinson and Vallino 2005; Helms et al. 2008). Therefore, to improve our understanding of the biogeochemical role of DOM in

inland waters and in the receiving coastal waters, it is important to study the DOM composition and its associated environmental factors (e.g., LULC, hydrology etc.) at a watershed scale.

Despite being an important optical constituent in defining overall water quality, DOM has received little attention owing to its complex and heterogeneous structure (Aiken et al. 2011; Qualls 2013). However, optical measurement techniques such as UV-Vis absorption and fluorescence spectroscopy have substantially contributed in gaining important insights about the character and composition of DOM (Coble et al. 1990, 1998; McKnight et al. 2001; Cawley et al. 2014; Chen and Jaffé 2014). Along with the advances in instrumentation and knowledge about known DOM fractions, a multivariate statistical modeling approach, parallel factor (PARAFAC) analysis, have been suggested to augment the rapid identification of fluorescence derived excitation-emission matrices (EEMs) of water samples for characterization of DOM in a range of terrestrial and aquatic ecosystems (Stedmon et al. 2003; Stedmon and Markager 2005; Chen et al. 2010; Singh et al. 2010; Singh et al. 2015). Previously many studies have utilized the EEM-PARAFAC approach for DOM characterization in variety of terrestrial and aquatic ecosystems (Chen et al. 2010; Yang et al. 2012; Toosi et al. 2014). While it has been acknowledged in these previous studies that it is important for estimating the effects of land use and land cover types on the DOM composition, there are limited studies available utilizing a comprehensive approach to characterize and compare DOM quality and quantity in multiple types of water bodies from watersheds with a variety of land use and land covers.

In the present study, the goal is to characterize DOM in multiple water bodies, including inland lakes; an estuary; and coastal waters, located in the state of Mississippi, USA. To my knowledge, this is the first study presenting a synoptic view of DOM composition in Mississippi water bodies covering several types of water bodies and land use and land cover types. The objectives in this study were (i) to develop a site-specific PARAFAC model for characterizing DOM composition, (ii) to assess the spatial variability of DOM in Mississippi's water bodies, and (iii) to evaluate the relationship between LULC and DOM character for addressing the following questions.

1. How do DOM character vary spatially in different types of water bodies?
2. How do nutrients (N and P) vary spatially and how they are correlated with DOM character?
3. What are the major controls or factors (e.g., land use and land cover, photolysis, etc.) that explain the DOM variability?

2.2 Methods

2.2.1 Sample collection and study sites

Surface water samples were collected from five major lakes in Mississippi including Lakes Sardis, Enid, Grenada, Okatibbee, and Ross Barnett reservoir; the Lower Pearl River estuary; and the eastern Mississippi Sound. Lakes Sardis, Enid, and Grenada are located in the northern Mississippi, the Ross Barnett reservoir and the Lake Okatibbee are located in the central Mississippi region while the Lower Pearl River estuary and the Mississippi Sound are located in the southwestern and southeastern region of the Mississippi coast, respectively (Fig. 2.1). Hence, the study areas encompass the major types of aquatic environments ranging from lacustrine, riverine, and estuarine to coastal

waters. More details of the lake study sites and sampling protocols have previously been described in Dash et al. (2015). The water samples from the lakes Sardis (LS), Enid (LE), and Grenada (LG), and the Ross Barnett (RB) reservoir were primarily collected during summers of 2012, 2013, and 2014. Lake Okatibbee (LO) was sampled only once during February of 2015 while eastern Mississippi Sound (MS) was sampled in 2012 and 2013. Lower Pearl (LP) River estuary was sampled during winter (December 2014) and spring (March 2015). The water samples were collected and filtered through a 0.2-micron filter paper (Millipore Inc., Billerica, MA, USA) within 2-3 h of water sample collection and stored in a refrigerator at 4°C in 100 ml amber glass bottles prior to UV-Vis absorption and fluorescence measurements. Dissolved oxygen (DO), pH, temperature, and salinity were measured using a calibrated Hanna multi-parameter probe (HI9828, Hanna Instruments, Woonsocket, RI, USA).

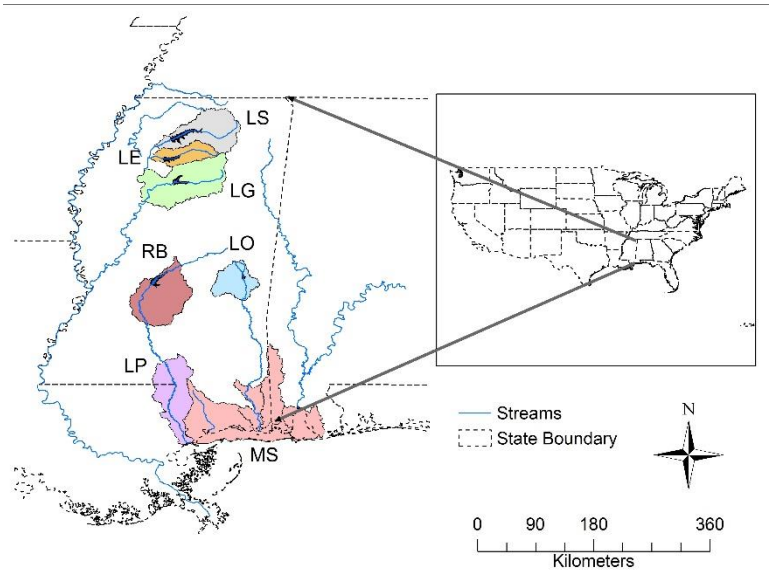

Figure 2.1 The study lakes, estuary, and coastal region along with the watershed boundaries are presented in the map. Main river tributaries are indicated with blue solid lines.

2.2.2 Absorption spectroscopy

On the day of the analysis, water samples were kept outside refrigerator for a period of two hours that allowed the samples to reach ambient room temperature prior to spectroscopic analyses. The instrument was turned on and stabilized for 30 minutes before the samples were analyzed. Absorption spectra were obtained between 200 and 750 nm at 2-nm intervals using the Perkin Elmer Lambda 850 double-beam spectrophotometer (PerkinElmer, Inc., Waltham, MA, USA) equipped with 1 cm path length quartz cuvette (~ 4 ml) and 150 mm spectralon coated integrating sphere. The instrument was set up and calibrated after running particle free Nanopure Milli-Q water as blank, with a purity level of 18.2 MΩ, on daily basis prior to running water samples. The absorption spectra were corrected for scattering and baseline fluctuations by subtracting the average value of absorption between 700 and 750 nm from each spectrum. Blank subtraction of nanopure Milli-Q water was carried out to remove scattering and solvent (water) effects. The absorption coefficients (a) were calculated from the absorbance (A) obtained from the spectrophotometer using:

$$a(\lambda) = \frac{2.303 * A(\lambda)}{L} \qquad 2.1$$

where $A(\lambda)$ is the absorbance measured at a wavelength λ, and L is the path length in meters (Markager and Vincent 2000; Singh et al. 2010; Dash et al. 2011).

2.2.3 Fluorescence spectroscopy

Similar to absorption measurements, water samples were brought to ambient room temperature 2 h prior to spectro-fluorometric analysis. Excitation-emission matrices (EEMs) were generated using the Fluoromax-4 spectrofluorometer (Horiba Jobin Yvon,

Inc., Edison, NJ, USA) equipped with a 150 W ozone-free Xenon arc lamp. The EEM spectra were recorded for excitation from 240 to 450 nm at every 10 nm intervals and emission from 300 to 550 nm at every 2 nm with an integration time of 0.25s. The EEM signals were collected in ratio mode (S/R mode) with dark offsets and a setting of 5 nm bandpass for both the excitation and emission monochromators. Factory supplied correction factors were applied to the scans to correct for instrument configuration. Absorption corrections were applied to account for inner filter effects in "Blank" and sample EEMs. Then corrected Milli-Q water (Blank) EEMs were subtracted from the sample EEMs to eliminate any influence of Raman peaks. Subsequently, EEMs were normalized to daily-determined water Raman integrated area under maximum fluorescence intensity (350 ex/397 em, 5 nm bandpass) as suggested by Lawaetz and Stedmon (2009) to normalize the EEMs data to a comparable Raman Units (R.U.). This approach provided spectrally corrected data, which in turn is quantitatively independent from any instrumental bias. Finally, the corrected EEMs were exported to MATLAB® for further analyses.

2.2.4 Development of PARAFAC Model

EEM dataset of 275 samples with emissions measured at 126 wavelengths and excitations measured at 22 wavelengths were used for modeling. The number of components for model calibration and validation was achieved by split-half analysis and by the visual analysis of residuals and corresponding component loadings (Stedmon et al. 2003; Stedmon and Bro 2008). While modeling, a close inspection of outliers reduced the final EEM dataset to 260 samples for PARAFAC modeling. Prior to final PARAFAC modeling, one emission wavelength (300 nm) was discarded and other emission

wavelengths were interpolated at 4 nm increments, which were originally collected at finer resolution of 2 nm increment. The excitation wavelengths were interpolated at 5 nm increments, which were originally collected at 10 nm increments. Therefore, the final PARAFAC model was developed using the EEM data of 260 samples with 63 emission and 43 excitation wavelengths to derive five split-half validated individual components (Fig. 2.2). PARAFAC component scores were reported as fluorescence intensity, Fmax (R.U.). PARAFAC modeling has been described in more detail in our previous publications (Singh et al. 2014b; Singh et al. 2015).

We calculated several DOM optical indices using absorption and fluorescence measurements to derive relationships between PARAFAC identified components and DOM quality in lakes, estuary, and coastal waters. The absorption coefficient at 254 nm (a_{254}) was calculated using the absorbance measured at 254 nm. a_{254} provides a measure of aromaticity and is directly proportional to the aromatic content in the water samples (Weishaar et al. 2003). Spectral slope ratio, (S_R) was computed using the spectral slopes calculated in two ranges (i.e., S1: 275-295 nm and S2: 350-400 nm). This index serves as a proxy for molecular weight of DOM with low S_R indicating high molecular weight of DOM and high S_R indicating low molecular weight of DOM (Helms et al. 2008). Spectral slope, $S_{254-436}$ was computed for source tracking and for gaining insights about the transformation history of DOM (Jaffé et al. 2004). Humification Index (HIX) was computed as the ratio of the peak integrated area under the emission spectra 435-480 nm and the peak integrated area under the emission spectra 300-345 nm obtained at an excitation wavelength of 254 nm (Zsolnay et al. 1999). An increase in HIX is associated with condensation of fluorescing molecules and a decrease in the H/C ratio, which is

considered to be an indicator of humification (Zsolnay et al. 1999, Zsolnay 2003). Biological Index (BIX) was calculated as the ratio of emission fluorescence intensity at 380 nm and the maximum emission fluorescence intensity observed between 420 and 435 nm at an excitation wavelength of 310 nm. BIX (also referred to as freshness index) provides insights about the proportion of freshly produced DOM versus transported aged DOM (Huguet et al. 2009; Wilson and Xenopoulos 2009). Fluorescence index (FI) was calculated as the ratio of fluorescence emission intensities at 470 and 520 nm with the excitation intensity of 370 nm (Cory and McKnight 2005). This index has been used in several studies to trace DOM from terrestrial and microbial sources based on values between 1.2-1.5 indicating terrestrial origin and 1.6-2.0 indicating microbial origin (McKnight et al. 2001; Cory and McKnight 2005; Singh et al. 2014b; Singh et al. 2015). Finally, another DOM metric, redox index (RI), was computed as the ratio of reduced quinones to total quinones using PARAFAC derived components (Miller et al. 2006). It is a useful index to identify the redox state of humic acids (Miller et al. 2006).

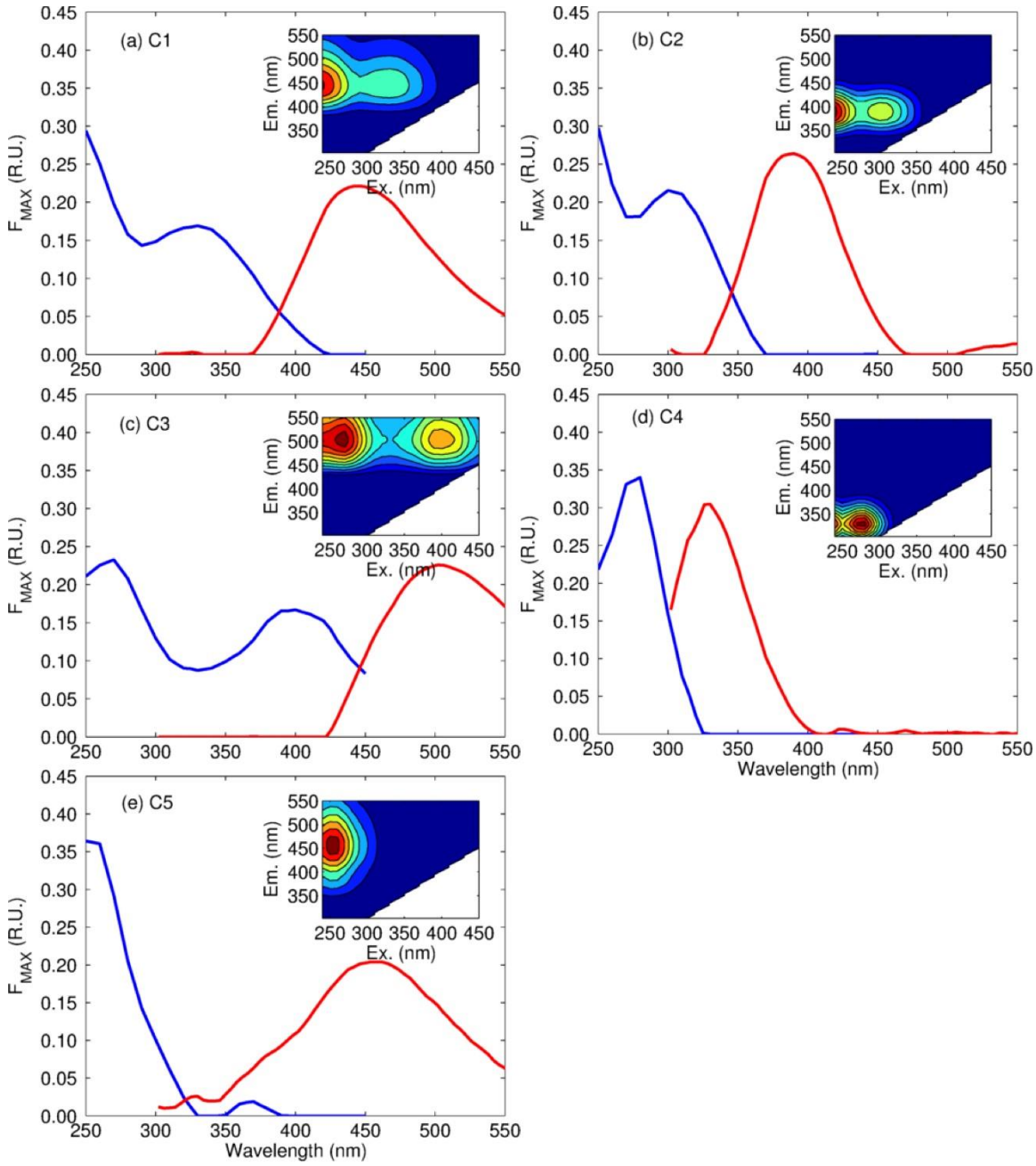

Figure 2.2 The split-half validated results of excitation (blue solid line) and emission (red solid line) loadings for five PARAFAC derived DOM components (C1-C5) are presented. Contour plots of the same five components identified from the PARAFAC model are shown in the insets. F_{MAX} (R.U.) represents the maximum fluorescence intensity in Raman Units.

2.2.5 Nutrient analysis and total chlorophyll-a measurements

Nutrient analyses included measurement of the concentration of total dissolved phosphorous (TDP) and dissolved inorganic nitrogen (DIN) including ammonium nitrogen (NH_4-N) and nitrate nitrogen (NO_3-N). Filtered water samples were transported on ice to Dr. Gary Feng at the USDA ARS located on the Mississippi State University campus. NH_4-N and NO_3-N were measured using 9 mL of filtered water sample on a Lachat QuickChem 8500 Series 2 (Hach Co., Loveland, CO) with a five-point calibration curve (20, 10, 5, 2, and 0 mgL^{-1}). TDP was measured using 8 mL of filtered water sample on an iCAP 6000 ICP Mass Spectrometer (Thermofisher Inc.) fitted with an autosampler using a three-point standard curve. For total chlorophyll-a (Chl-*a*) measurements, 100 ml aliquots of water samples were filtered through 4.7 cm diameter glass fiber (Whatman GF/F) filters and stored in a -80°C freezer. The frozen samples were transported on dry ice to Dr. James L. Pinckney at the Department of Biological Sciences, University of South Carolina, Columbia, SC for total chlorophyll-a analysis using high performance liquid chromatography (HPLC) (Pinckney et al. 2009).

2.2.6 Land use and land cover analyses

The cropland dataset, hydrologic units (8-digit HUC), and hydrography data used for each watershed were ordered from USDA NRCS Geospatial Data Gateway (USDA, 2015) and were processed in. Watershed boundaries were determined for each sampling location from a 30 m digital elevation model (DEM) and ArcGIS version 10.1 (Environmental Systems Research Institute, Inc., Redlands, California, USA). Watershed boundaries were determined using USDA NRCS 8-digit watershed boundary dataset. Percentages of agriculture, aquaculture, barren, forest, rangeland, wetland, urban, and

open water in each watershed were calculated from the 2014 Cropland Data Layer (CDL) from the USDA NRCS Geospatial Data Gateway after re-classification of 255 levels of crop data (Johnson and Mueller 2010; USDA, 2015). The 255 levels of crop data is grouped into eight classes of Level I using classification scheme as suggested by Anderson et al. (1976). The CDL data used in this study had an overall accuracy of 80.7%. The total county population for each watershed was computed using TIGER 2010 for each watershed (Table 2.1 and Fig. 2.3). For each watershed, we calculated the watershed area, lake area, and drainage ratio using layer attribute tables (Table 2.1). Drainage ratio is defined as the ratio of total watershed area to the lake area within the given watershed. This parameter is an important factor in determining the amount and flux of nutrients to a lake related to surface runoff. Drainage ratio is also used as a proxy for water retention time in lakes as higher drainage ratio lakes have shorter retention times (Lottig et al. 2012).

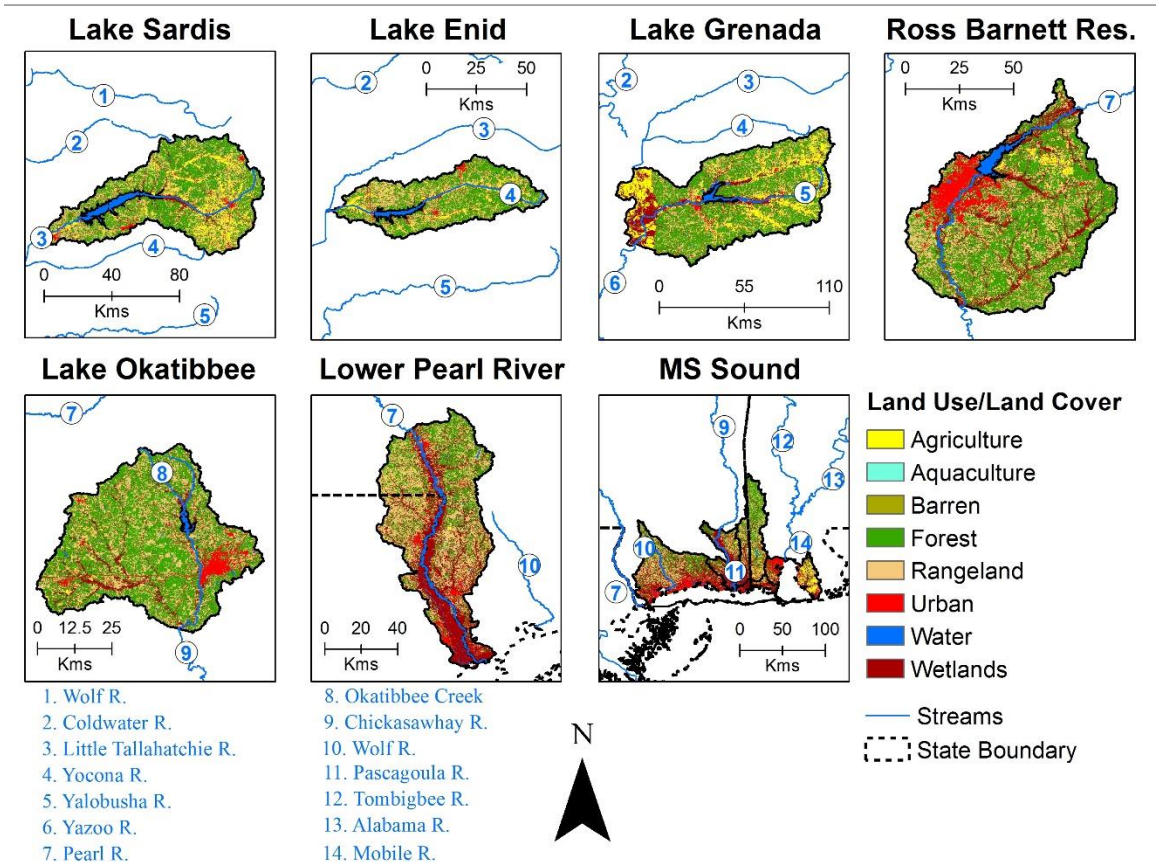

Figure 2.3 Land use and land cover distribution for each watershed is presented here. Main river streams are shown in blue solid lines and numeric markers, and the corresponding names are shown in the figure legend.

2.2.7 Statistical analyses

Statistical differences between sources (observations) and treatments (water bodies) were determined using one-way analysis of variance (ANOVA) with subsequent Tukey-HSD tests for post-hoc analyses and plotted with R software version 3.2.2 (R Core Team, 2015). One-way ANOVA is used here to analyze the differences among group (water bodies) means. It is hypothesized here that each water body type (i.e., lakes, estuary, and coastal region) will show different DOM character. Multivariate Pearson

correlations between PARAFAC components (C1-C5), DOM quality indices (i.e., a_{254}, S_R, HIX, BIX, and FI), and nutrients (NH_4-N, NO_3-N, and TDP), and principal component analysis (PCA) were performed using JMP Pro 11.0 statistical software package (SAS Institute Inc., Cary, NC). Regression analyses were used to examine the relationships between LULC types and DOM compositions using JMP. For the regression analyses, the percent cover of forest, agricultural lands, and wetlands (LULC types) in each watershed were considered as independent variables, two terrestrial humic-like components (C1 and C3) and one microbial humic-like (C2) DOM component were considered as dependent variables. All the statistical analyses were computed at a 95% significance level ($\alpha = 0.05$) unless stated otherwise. For the principal component analysis, the average values of the DOM parameters and nutrients were considered to examine the relationships between DOM parameters, nutrients, and LULC types for each of the watersheds in this study. PCA was performed on correlations of scaled data (Xue et al. 2011)

Table 2.1 Watershed properties of each water body are shown here. The values for each watershed have been extracted from attribute tables using ArcGIS for lakes, estuary, and Mississippi Sound for each parameter in this study.

Water Body	Lake Sardis	Lake Enid	Lake Grenada	Ross Barnett Reservoir	Lake Okatibbee	Lower Pearl River	Mississippi Sound
Watershed area (km^2)	4269.4	1926.4	5917.9	5119.9	2351.4	4717.6	12830.9
Lake area (km^2)	162.2	59.3	79.7	102.5	17.0	—	—
Drainage ratio	26.3	32.4	74.2	49.9	137.7	—	—
Population (X 10^4)	8.9	3.8	7.3	24.9	5.9	15.4	68.3
Proportion of land use and land cover (LULC) of watershed area							
Forest (%)	46.5	47.8	43.2	45.6	52.5	27.0	27.0
Rangeland (%)	26.0	29.1	18.7	24.5	28.7	30.4	23.4
Urban (%)	6.0	6.0	4.6	11.9	8.3	6.8	11.7
Wetlands (%)	5.8	4.0	11.4	12.9	7.9	32.4	30.4
Agriculture (%)	11.1	8.2	17.6	2.2	1.0	0.8	3.7
Aquaculture (%)	0.0	0.0	0.0	0.0	0.0	0.0	0.0
Barren (%)	0.6	0.7	1.3	0.0	0.0	0.4	1.5
Water (%)	4.0	4.2	3.2	2.9	1.7	2.1	2.2

2.3 Results

2.3.1 Spatial patterns of physical and biochemical parameters

For the lakes, estuary, and coastal waters, the average values with standard deviations and the ranges of surface water temperature, salinity, pH, dissolved oxygen (DO), and the concentrations of ammonium-nitrogen (NH_4-N), nitrate-nitrogen (NO_3-N), total dissolved phosphorous (TDP), and total Chl-*a* are given in the appendix (Table A.1). The average surface water temperature (T) ranged between 16.9 and 28.4°C with the lowest value observed in estuarine waters while the highest value observed in coastal waters. Salinity and DO showed an inverse relation across the water bodies with highest average salinity (23.4 psu) and lowest average DO (6.2 mgL^{-1}) observed for the coastal waters while the lowest average salinity (0.0 psu) and highest average DO (7.0 mg L^{-1})

were recorded for the lakes. Estuarine waters had intermediate average values for salinity (2.9 psu) and DO (6.7 mgL^{-1}).

The average concentrations of DIN (NH_4-N+NO_3-N) was highest in the lakes, intermediate in the estuary, and lowest in the coastal waters, however, concentrations of NH_4-N and NO_3-N varied individually for these water bodies (Fig. 2.4). In particular, the average concentration of NH_4-N was highest in coastal waters (0.13 mgL^{-1}) while the lowest average concentration was found in estuarine waters (0.05 mgL^{-1}). The average concentration of NH_4-N for the lake samples (0.08 mgL^{-1}) remained in between the above two extremes. In contrast, the average concentration of NO_3-N was lowest in the coastal waters (0.10 mgL^{-1}) while the average values of the NO_3-N for the lakes and estuarine waters did not vary significantly (0.24 mgL^{-1} and 0.28 mgL^{-1}, respectively). While the average concentration of TDP were found significantly higher in coastal waters (0.032 mgL^{-1}) as compared to the lakes and estuarine waters (0.008 mgL^{-1} and 0.007 mgL^{-1}, respectively; Fig. 2.4 and Table A.1).

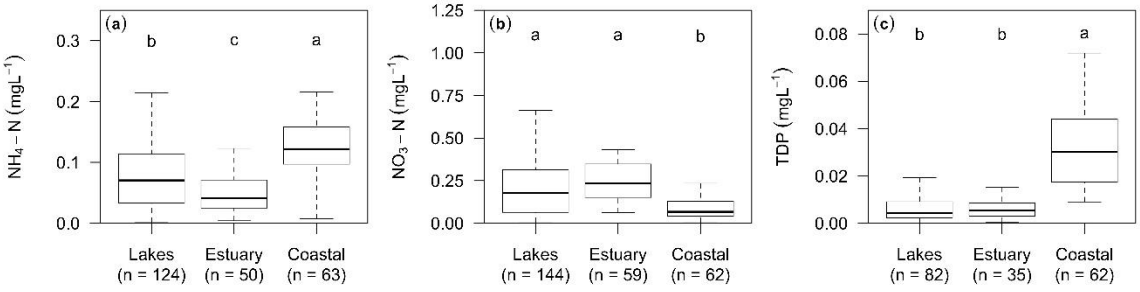

Figure 2.4 Spatial distribution of (a) NH_4-N, (b) NO_3-N, and (c) TDP measured in this study. Same letters in the box plots represent no significant differences (at alpha = 0.05) in variables between the sampling water bodies. Number of samples (n) is shown for each water body.

Similar to the overall trend observed for the average concentration of DIN, the average concentration of Chl-*a* was highest in the lakes (15.5 μgL^{-1}), intermediate in the estuary (8.1 μgL^{-1}), and the lowest in the coastal waters (3.2 μgL^{-1}).

2.3.2 Spatial patterns of PARAFAC components

A total of five different PARAFAC components (C1-C5) representing DOM compositions were determined in this study. These components have previously been identified in the literature (Table 2.2). In this study, the average fluorescence intensities (F_{max}) of the two terrestrially derived humic-like components; C1 and C3 were 0.71 and 0.17 R.U., respectively found in the lakes. The same components were also found in the estuary with F_{max} values of 0.77 and 0.23 R.U., respectively. For the coastal waters, the average F_{max} for C1 and C3 were found to be 0.64 and 0.19 R.U., respectively (Fig. 2.5). Estuarine samples showed significantly higher values of both C1 and C3 than that for lakes and coastal waters, while the coastal waters showed significantly higher average C3 than that of lakes. In contrast to the trends of C3, the average C1 were found to be significantly higher in the lakes in comparison to coastal waters.

The average fluorescence intensities, F_{max} of the two microbially derived humic-like components, C2 and C5 were significantly higher in coastal waters (0.52 R.U. and 0.16 R.U., respectively) while the same components were significantly lower in the estuarine waters (0.45 R.U. and 0.03 R.U., respectively; Fig. 2.5). Lakes showed intermediate average values of C2 and C5 (0.47 R.U. and 0.09 R.U., respectively) but were found significantly different than estuarine and coastal waters. Finally, the average fluorescence intensity of the component, C4, which is similar to protein-like (tryptophan-like) DOM, was significantly lower in lakes (0.16 R.U.) in comparison to estuarine and

coastal waters while no significant difference between estuarine (0.21 R.U.) and coastal waters (0.22 R.U.) was found (Fig. 2.5).

2.3.3 Spatial patterns of DOM indices

The average value of a_{254} was significantly higher in estuarine waters (50.2 m^{-1}) while the lowest average value of the a_{254} was found in coastal waters (18.7 m^{-1}) with an intermediate average value for the lakes (41.4 m^{-1}; Fig. 2.6). In contrast, the average value of S_R was significantly higher in coastal waters (1.8) than that in lakes and estuarine waters (1.0 and 0.8, respectively; Fig. 2.6). No significant difference in the S_R existed between lakes and estuarine waters. The average HIX value for the estuarine waters (5.6) was significantly higher than that of lakes (4.0) while the average HIX value of coastal waters (4.8) did not differ significantly either from the lakes or estuarine waters (Fig. 2.6). The average values of BIX and FI were highest in coastal waters (0.76 and 1.48, respectively) and lowest in estuarine waters (0.62 and 1.44, respectively) while they were in between the coastal and estuarine values for the lakes. Lake samples showed significantly different average values of the BIX and FI (0.66 and 1.46, respectively) than the estuarine and coastal waters (Fig. 2.6).

Table 2.2 Descriptions and the characteristics of the five PARAFAC modeled fluorescence DOM compositions identified in this study and their comparison against those previously reported in the literature.

Components **(Ex / Em)**	**I**	**II**	**III**	**IV**	**V**	**VI**	**VII**	**VIII**	**Description and origin of DOM composition and possible sources**
C1 (< 250-330 / 446)	C4	C3	C1	C4	C2	C4	C1	C1	UVA humic-like; terrestrial origin or allochthonous transport; common to wide range of freshwater aquatic environments.
C2 (< 250-300 / 390)	C6	C2	C2	C2	C4	C2	C2	C3	Microbial humic-like; anthropogenic origin found in agriculturally dominated watersheds; prevalent in wastewater; photo-labile DOM product.
C3 (270-390/ 502)	C2	C6	—	—	C5	C3	—	—	UVA humic-like; terrestrial origin or allochthonous transport; primarily in soil-derived material; reduced terrestrial DOM; common in wide range of freshwater environments such as wetlands and rangelands.
C4 (280 / 330)	C7	C5	C4	C3	C3	C6	C4	C5	Protein-like (Tryptophan-like) DOM; autochthonous production; also commonly found in croplands, wastewater, industrial and livestock wastes.
C5 (< 250 / 458)	C1	C1	—	C1	—	C5	—	C4	UVC humic-like; terrestrial origin; commonly found in wide range of aquatic environments; mainly in high proportion of wetland dominated areas; photo-refractory DOM composition

I: Stedmon and Markager (2005); **II:** Williams et al. (2010); **III:** Zhang et al. (2010); **IV:** Hiriart-Baer et al. (2013); **V:** Meng et al. (2013); **VI:** Kothawala et al. (2014); **VII:** Yang et al. (2014); **VIII:** Harun et al. (2015)

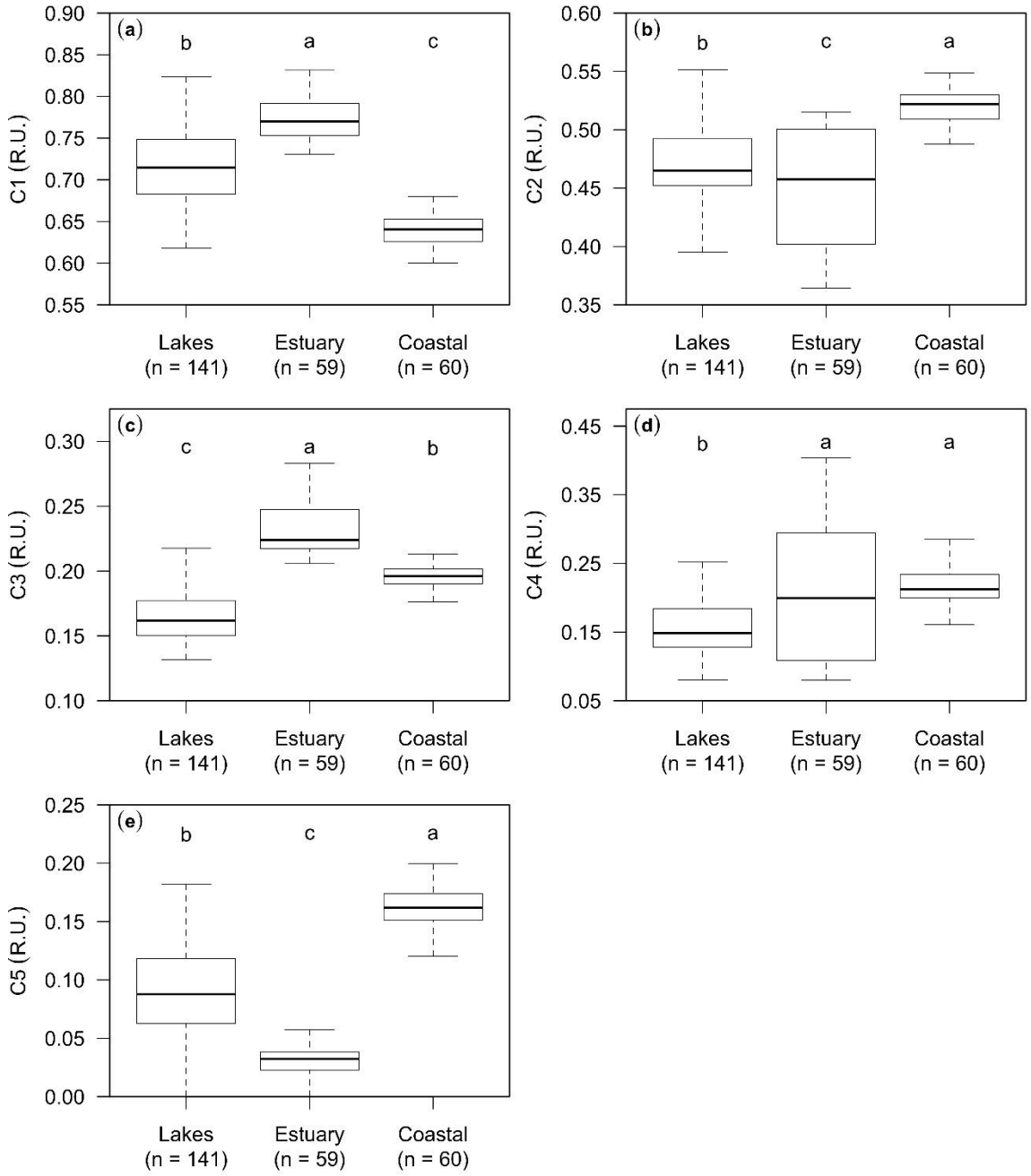

Figure 2.5 Spatial distribution of PARAFAC-modeled components (a) C1, (b) C2, (c) C3, (d) C4, and (e) C5. Same letters in the boxplots represent no significant differences (at alpha = 0.05) in variables between the sampling water bodies. Number of samples (n) is shown for each water body.

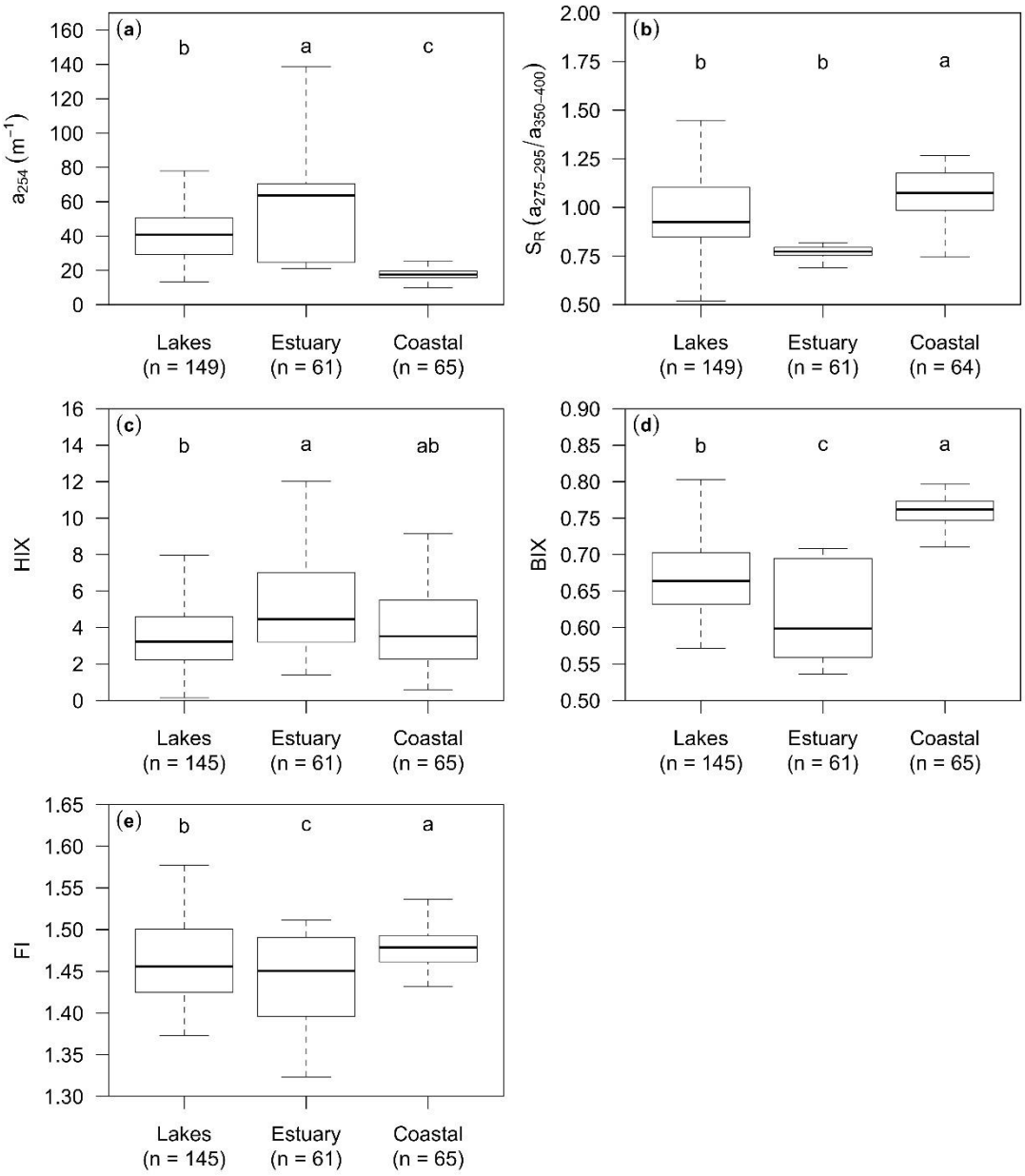

Figure 2.6 Spatial distribution of DOM optical indices (a) a_{254}, (b) S_R, (c) HIX, (d) BIX, and (e) FI. Same letters in the boxplots represent no significant differences (at alpha = 0.05) in variables between the sampling water bodies. Number of samples (n) is shown for each water body.

2.3.4 Land cover types and DOM composition

To investigate the relationships between the DOM compositions in lakes; estuary; and the coastal waters and the influence of land use and land cover types in the respective watersheds, regression analyses were performed using JMP (Fig. 2.7). The results showed that percent forest cover could explain 68% of the variability in terrestrial humic-like DOM (C1) exports in the watersheds while the percent agricultural land use predicted 87% variability in microbially derived humic-like DOM (C2). It was found that percent wetland coverage in studied watersheds serves as a good predictor of soil derived terrestrial humic-like DOM (C3) explaining 82% variability in the data. In general, percent forest cover was higher in the watersheds for the lakes whereas the watersheds for the estuary and coastal waters had increased percentage of wetlands. Percent agricultural land was highest in the watersheds of the northern Mississippi lakes (Lakes – Sardis, Enid, and Grenada; Table 2.1 and Fig. 2.3). Largest proportions of the agricultural lands in the watershed of the Lake Grenada are on the downstream side of the lake, for which a lower contribution of agricultural influence on DOM properties was observed.

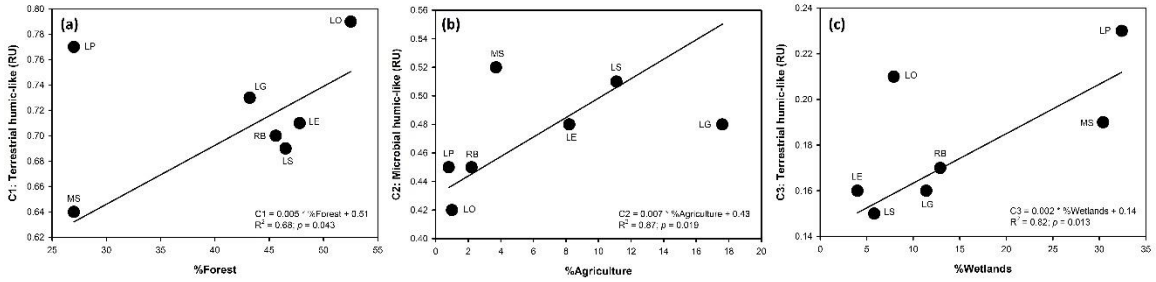

Figure 2.7 The regression analyses between the DOM compositions (C1, C2, and C3) and LULC (percent forests, percent agricultural lands, and percent wetlands) are presented here. LP (in regression between %Forest and C1), MS and LG (in regression between %Agriculture and C2), and LO (in regression between %Wetlands and C3) were identified as outliers and were excluded in the regression analyses.

The first two principal components (PC1 and PC2) together explained roughly 70% of the variation in the dataset in PCA results (Fig. 2.8). PC1 explained 45.6% while PC2 explained 24.1% of the variability. The three northern Mississippi lakes (LS, LE, and LG) with relatively highest proportion of agricultural land use showed positive loadings on PC1 while the other two lakes (LO and RB) and the estuarine samples (LP) were found negative on PC1. Because LO and RB in addition to LP have relatively higher contributions of percent forest, rangeland, and wetland coverage (Table 2.1), negative PC1 loadings for C1, C3, HIX and a_{254} reflects terrestrially derived humic-like DOM exported from forests and wetlands, having structurally complex, refractory, and aromatic DOM. While the components C2, C4, and C5 in addition to BIX, FI, and S_R showed a positive relation with PC1 indicating a more "labile" and relatively simpler DOM exported from watersheds those had relatively higher proportion of agricultural land. Similar to PCA results, the correlations between DOM compositions, optical indices, and nutrients showed strong relationships between microbial humic-like DOM

(C2) and BIX, FI, and a_{254}. Nutrients such as NH_4-N and TDP also showed significantly positive relationships with microbial humic-like DOM (C2) (Table 2.3).

2.4 Discussion

2.4.1 Spatial variability of DOM composition

A total of five different DOM compositions (i.e., PARAFAC components) were identified in lakes; estuary; and coastal waters in this study. The fluorescence signature of the component 1 (C1) showed two excitations (<250 and 330 nm) and one emission (446 nm) peaks (Table 2.2). This component is similar to a mixture of the traditionally defined terrestrial humic-like peaks A and C in seawater, which was first reported by Coble (1996). Since then it has been commonly observed in many freshwater environments. For example, Zhang et al. (2010) found an increase in the terrestrial humic-like component C1 (similar to our C1) because of an increase in terrestrial nutrients from the watershed in lakes of the Yungui Plateau, China. Likewise, the increase of a similar component (C4) has been found in an embayment of western Lake Ontario receiving the largest amount of allochthonous DOM (Hiriart-Baer et al. 2013). Other studies also indicated the ubiquitous character of component C1 and have found in a wide variety of freshwater and marine environments, and attributed to terrestrial and anthropogenic origins (Meng et al. 2013; Kothawala et al. 2014). The component 3 (C3) also exhibited primary and secondary fluorescence peaks, although with a red shift compared to the component 1, occurring at 270 (390) nm/502 nm (Table 2.2). This component can be categorized as a reduced terrestrial DOM originating from soil-derived organic matter (Lochmuller and Saavedra 1986; Singh et al. 2010). The spectral feature of this component is also similar to other reported studies with the widespread presence of allochthonous dissolved organic matter

derived from terrestrial sources and leaching from soil derived fulvic acids in streams, lakes, wastewaters, and wetlands (Stedmon and Markager 2005; Stedmon et al. 2006; Meng et al. 2013; Kothawala et al. 2014). Based on previous research and the results of this study, significantly high terrestrially derived humic-like components (C1 and C3) in estuary waters indicate terrestrial and soil derived organic matter influence on estuarine DOM (Fig. 2.5). It is suggested here that the higher abundance of these terrestrial DOM in estuary were transported from natural forests, rangelands, and in particular, from wetlands (Stedmon and Markager 2005; Graeber et al. 2012; Kothawala et al. 2014).

Table 2.3 Correlation matrix of five PARAFAC components, DOM quality indices, and nutrients measured in distinct water bodies in this study. All the correlations are significant at the alpha = 0.05 level. "Bold" represents "Strong" ($r > 0.70$) correlation. Non-significant correlations at alpha = 0.05 are represented as "N.S.".

Variables	**C1**	**C2**	**C3**	**C4**	**C5**	**HIX**	**BIX**	**FI**	**a_{254}**	**S_R**	**NH_4-N**	**NO_3-N**
C1												
C2	-0.77											
C3	0.55	-0.42										
C4	-0.36	0.68	N.S.									
C5	-0.98	0.68	-0.51	0.25								
HIX	0.17	-0.14	0.25	N.S.	-0.16							
BIX	-0.85	0.97	-0.40	0.63	0.79	-0.15						
FI	-0.43	0.78	-0.40	0.52	0.34	-0.15	0.74					
a_{254}	0.62	-0.90	0.35	-0.65	-0.55	N.S.	-0.87	-0.83				
S_R	-0.25	0.28	N.S.	N.S.	0.28	N.S.	0.27	0.26	-0.27			
NH_4-N	-0.50	0.42	-0.24	0.17	0.50	N.S.	0.49	0.32	-0.38	0.16		
NO_3-N	N.S.	N.S.	N.S.	0.13	N.S.	N.S.	N.S.	N.S.	N.S.	N.S.	N.S.	
TP	-0.49	0.37	0.22	N.S.	0.52	N.S.	0.48	N.S.	-0.33	0.44	0.32	-0.17

While the lakes and coastal waters were significantly higher in microbially generated humic-like DOM (C2 and C5), the lowest abundance of microbial humic-like DOM was found in estuarine waters (Fig. 2.5). The component 2 (C2) exhibited two

excitation (<250 and 300 nm) and one emission (390 nm) peaks while the component 5 displayed (C5) single excitation and emission fluorescence peak (< 250/458 nm; Table 2.2). The results for components C2 and C5 are similar to the components previously identified (Stedmon and Markager 2005; Graeber et al. 2012; Hiriart-Baer et al. 2013; Kothawala et al. 2014). The component 2 (C2) has been either associated with microbial activities in inland waters or with biological production indicating in situ DOM production in aquatic systems (Zhang et al. 2010; Maie et al. 2012). Previous studies have shown that a similar DOM component exported from anthropogenic sources such as wastewater and cropland dominated watersheds (Stedmon and Markager 2005; Graeber et al. 2012). Furthermore, this component has also been characterized as a labile photo-degraded component in groundwater and pore waters in the Everglades ecosystem located in southern Florida (Chen et al. 2010; Cawley et al. 2014). While the component 5 (C5) is typically microbially generated DOM, more recently the presence of similar component has been reported in streams and coastal waters originating from the photo-degradation of terrestrial DOM and reported as a photo-refractory component (Stedmon et al. 2006; Maie et al. 2012; Cawley et al. 2014). Besides, it has also been identified as a photo-resistant and/or photo-degradation product of humic-like DOM components reported only in surface waters but not in ground waters (Chen et al. 2010). While the results here are in agreement with these above-mentioned studies, it is not unexpected that estuary waters exported minimal microbially derived DOM than that in lakes and coastal waters. It could be due to the fact that the lakes and coastal waters provide relatively stagnant water as compared to groundwater fed continuously flowing rivers. The stagnant waters of lakes and coastal margins provide abundant opportunity for

terrestrial DOM to be photo-degraded leaving photo-resistant refractory DOM in lakes and coastal waters.

The component 4 (C4) is commonly found in many studies and has been found spectrally similar to protein-like (tryptophan-like) DOM exhibiting excitation and emission wavelength pair at 280/330 nm (Table 2.2). This component has been attributed to autochthonous production of DOM in many freshwater lakes and coastal waters (Yamashita and Tanoue 2003; Maie et al. 2012; Hiriart-Baer et al. 2013; Singh et al. 2014b). It has also been reported in DOM exported from croplands, wastewater, industrial, and livestock wastes (Baker 2002; Stedmon and Markager 2005; Naden et al. 2010). For instance, Stedmon and Markager (2005) reported a similar component of DOM associated with wastewater. It has been postulated that the decomposition of both allochthonous and autochthonous DOM could generate protein-like DOM owing to autochthonous algal production and/or microbial activity (Yamashita and Tanoue 2003; Maie et al. 2012). Yamashita et al. (2008) have reported the generation of such autochthonous DOM components at higher salinities in estuaries and ascribed such abundance to higher microbial activity. Concurring with these studies, the results here also suggest that protein-like DOM (C4) has been generated both from the microbial activity as well as phytoplankton/macrophyte production. Correlations between C4 against Chl-*a* for each water body indicated both microbial activity and primary production to be the dominant processes in lakes (data not shown). In the estuary, microbial activity dominated mostly, however in the month of March primary production appeared as more dominant process. In the coastal waters both processes were observed. Microbial activity dominated when primary production was not dominant, and primary

production dominated when microbial activity was not dominant. Low Chl-*a* concentrations (Mean = 3.2 μgL^{-1}; Table A.1) suggest the relative dominance of microbial activity and lack of primary production in coastal waters.

Significantly higher a_{254} and HIX for estuarine waters were found here than that for lakes and coastal waters (Fig. 2.6) indicating LP is transporting increased levels of aromatic and humic DOM supplied from the wetlands in its floodplains (Cai et al. 2016). The elevated aromatic and humic DOM indicates allochthonous transport of DOM in estuary. It has been suggested that elevated protein-like fluorescence potentially reduces the sensitivity of HIX values to infer the amount of humified DOM in the total DOM pool (Zsolnay 2003; Singh et al. 2014a). Because the lower region of HIX measurements coincides with the similar spectral region where protein-like DOM fluoresces. Only slight variation in HIX values was noticed across ecosystems in this study that corroborates to the earlier findings. Hence, it is suggested that HIX values may not be as reliable as a_{254} when a comparison between multiple ecosystems is considered. DOM in coastal waters was found with the lowest aromaticity (a_{254}). This could be due to the transformation of refractory to labile fractions via photo-degradation of terrigenous DOM (Moran and Zepp 1997; Maie et al. 2012) or due to mixing of freshwaters with saline waters (Sun et al. 2014; Guéguen et al. 2016). Higher abundance of labile DOM in coastal waters could also be originating from phytoplankton primary production or from increased microbial activity (Milbrandt et al. 2010). Microbes and phytoplankton compete for consumption of available nutrients, especially N species, for primary production or for biomass synthesis (Church et al. 2000). The results of this study are more supportive of increased microbial activity for the production of labile DOM than phytoplankton production of DOM in

coastal waters as indicated by high FI and S_R and low Chl-*a* concentrations. Same phenomenon for coastal waters was also observed here based on the correlations between C4 and Chl-*a* (data not shown), as discussed above. It can be surmised here that the increased production of labile DOM potentially resulted from microbially induced cleavage of refractory DOM with increased solar irradiation levels during summer months (Helms et al. 2008; Santos et al. 2014). Caffrey et al. (2014) found that the waters in the Grand Bay, where majority of our sampling sites are, have a residence time of approximately 11 days. Thus, coastal waters were exposed to sunlight for long period of times, which enhanced the breakdown of higher molecular weight DOM and in turn, bioavailability of DOM increased. This is also reflected in a decrease of the a_{254} values with simultaneous increases in S_R, BIX, and FI values (Huguet et al. 2009; Sun et al. 2014). Contrary to the findings here, an experimental study conducted by Mayer et al. (2011) found less than expected labile DOM produced through photolysis of resuspended coastal sediments in Louisiana, USA. They suggested that the majority of the photo-produced labile DOM might have possibly transported offshore. Nonetheless, results from DOM indices as corroborated by PARAFAC results showed highest labile DOM composition (i.e., photo-produced DOM) in coastal waters.

Previous studies have experimentally evaluated NH_4-N release in coastal waters and attributed such release of nitrogen compounds to photochemical processes in coastal southeastern USA (Bushaw et al. 1996; Moran and Zepp 1997) and more recently in coastal waters of northern Baltic Sea (Vähätalo et al. 2011). Similar conclusions have been drawn in an incubation experiment conducted for Florida and Massachusetts's salt marsh sediments to determine the influence of natural sunlight irradiation on DOM

release (Schiebel et al. 2015). Hence, it is suggested here that high NH_4-N in coastal waters would have generated from the sunlight exposure of terrestrially derived humic-like DOM. Release of sediment bound nitrogen and phosphorus during resuspension of DOM in shallow coastal waters could be another plausible explanation of noted high NH_4-N and TDP values.

Strong inverse correlations of terrestrial humic-like DOM (C1) with both microbially derived humic-like DOM (C2 and C5; -0.77 and -0.98, respectively; Table 2.3) were observed indicating that the source of both C2 and C5 could be the same organic material introduced via allochthonous transport in aquatic systems. While transport, the terrestrial humic-like DOM (C1) may have undergone digenetic changes and transformations and modified by factors such as photochemical process. Hence, labile microbial DOM compositions (C2 and C5 – photo-labile and photo-refractory components, respectively) can be considered as photoproducts resulting from the degradation of terrestrial humic-like DOM (C1 in this study; Chen et al. 2010; Cawley et al. 2014). In addition, the DOM indices such as BIX and FI were found highly correlated with DOM photoproducts (C2 and C5; Table 2.3). In contrast, a_{254} showed a very strong negative correlation (-0.90) with C2 and a moderate negative correlation (-0.55) with C5. This further emphasizes that when aromatic and humic DOM of terrestrial origin was subjected to photo- and microbial degradation, diagenetically modified labile DOM could enhance further breakdown of available refractory DOM, a phenomena known as "priming effect" (Bianchi 2011). A weak but significant correlation between TDP and C3 (0.22) further highlighted that TDP may have originated from coastal sediments. Further, microbial DOM compositions (C2 and C5) showed moderate positive correlations with

both NH4-N and TDP (Table 2.3). This relationship indicates that photochemical processes are an important control for DOM and nutrient dynamics in coastal waters in Mississippi (Shiller et al. 2006).

2.4.2 Land use and land cover types influence DOM properties

The quality of DOM in terrestrial and aquatic ecosystems differs depending upon land use and land cover in the watersheds. Percent forest cover was found as a strong predictor for terrestrially derived humic-like DOM (C1; Fig. 2.7). A study in several sub-watersheds of Horsens estuary, Denmark noticed a spectrally similar fluorescence DOM signature dominated by humic-like organic material associated with highest percent of forest cover (Stedmon and Markager 2005). In another study, while evaluating the effects of changing land use on DOM properties in a subtropical Jiulong River watershed in southeast China, Yang et al. (2011) found a similar component that showed the highest average values when the forest cover ranged from 52 to 77%. Humic-like DOM fluorescence signature, as represented by C1, has been correlated with terrestrially derived organic material with a high aromatic carbon content possibly from lignin breakdown products (Cory and Kaplan 2012). Recently, Singh et al. (2015) also noticed the similar component in a sub-watershed (0.62 ha) of a mid-Atlantic forested watershed with 100% forest cover. They stated that runoff from surficial flow during storms, and over leaf litter on the forest floor and organic-rich soil horizons generated this type of fluorescence DOM signature. The results here concur with these studies and indicate that streams draining in natural forest and grassland covers have significantly different terrestrially derived DOM character than other land use and land cover types.

In the present study, percent agricultural land use predicted 87% variability in microbially derived humic-like DOM (C2, Fig. 2.7). This DOM component showed a labile character representing simpler DOM structure compared to the two terrestrially derived DOM components (C1 and C3). Stedmon and Markager (2005) attributed anthropogenic origin to a spectrally similar humic DOM fluorescence exported from agricultural sub-catchments possibly due to the use of manure in agricultural fields. It is widely known that the agricultural runoff is often high in nutrients (e.g., nitrogen and phosphorous) that may be bioavailable to microbes as a nutrient source. Wilson and Xenopoulos (2009) in a study examining a land use gradient of increasing agricultural fields showed that the DOM exported from croplands were structurally simpler. Further they found an increase in BIX ratio with an increase in percent agricultural fields with a corresponding increase in total dissolved nitrogen (TDN), a nutrient responsible for increased biological activity. While TDN was not measured directly in this study, the higher levels of C2 showed strong positive correlations with BIX and FI, (0.97 and 0.78, respectively) which can be attributed to increased microbial activity due to nutrient inputs from agricultural runoff. Moreover, moderate but significant positive correlations of C2 with NH_4-N, and TDP (0.42 and 0.37, respectively) also indicate the origin of microbially derived humic-like DOM due to nutrient inputs from agricultural runoff (Table 2.3). Williams et al. (2010) found a similar component in agricultural streams, and related it to increased bacterial decomposition making a more labile DOM accessible to the microbial community. They also highlighted that besides microbial activity, sunlight can cause reductions in the molecular weight of DOM via direct photo-degradation as agricultural streams with reduced tree canopy is expected to receive increased levels of solar

radiation. Contrary to these studies, Graeber et al. (2012) and Stedmon and Markager (2005) found that agriculturally dominated streams drained structurally complex DOM in central European headwater streams and in an estuarine region in Denmark. However, more recently, Singh et al. (2014a) noticed spectrally similar DOM component in a mid-Atlantic agricultural field and attributed the origin of this component to poultry manure application. Hence, in the light of results from the above mentioned studies and in this study, it is suggested that microbial humic-like DOM (C2), which is labile in character, was generated from photo-degradation (Maie et al. 2012; Cawley et al. 2014) of nutrient rich allochthonous organic materials exported to the lakes (Stedmon and Markager 2005; Singh et al. 2014a).

Wetlands appear to be a significant source of aromatic or refractory DOM with an average high molecular weight originating from allochthonous transport (Mulholland 2003). The results of this study are consistent with those of previous studies that have shown that percent wetland coverage have a strong influence on DOM properties. Similar to the results presented here, Wilson and Xenopoulos (2009) observed greater contributions of soil derived humic-like DOM as the proportion of wetlands increased. They also noticed negative correlations of BIX and FI with increasing proportion of wetlands and positive correlations of a_{280} and HIX with increasing percent of wetlands. The correlations between C3 and these DOM indices and regression between C3 and percent wetland coverage reflected similar characteristics (Table 2.3 and Fig. 2.7). DOM has been found to be refractory and less accessible for microbial utilization in wetland streams (Williams et al. 2010). Additionally, Williams et al. (2010) also found decreasing FI and BIX ratios in streams with an increasing proportion of riparian wetland area.

Contrasting results have been reported in a study by Graeber et al. (2012) in the North German plains where headwater streams with increasing proportion of wetland coverage showed structurally simpler DOM. They suggested this simpler DOM could have resulted from high variability in water table depth, evaporation, and photo-degradation processes. A strong flood plain connection of LP with its riparian zone may have induced DOM with higher NH_4-N levels to oxidize into significantly higher NO_3-N concentrations in estuarine waters (Cai et al. 2016). The highest NO_3-N concentrations in estuarine waters was observed here possibly due to the rapid oxidation of proximal wetlands sourced NH_4-N to NO_3-N. Thus, the findings of this study are in coherence with the previously reported results where terrestrially derived aromatic and humic DOM with more reduced character is directly related to increasing proportion of wetland coverage.

The principal component analysis helped in separating watersheds based on the distributions of DOM composition and nutrients influenced by dominant land use and land cover types for each watershed (Fig. 2.8). The percent of total variance explained by PC1 may be controlled by the DOM sources where positive PC1 loading can be due to DOM from "anthropogenic" sources (e.g., agriculture) and the negative PC1 loading can be due to DOM derived from "natural" sources or land cover types (e.g., forest and rangeland). Similar statistical approach by Kalscheur et al. (2012) has been employed while evaluating the effects of anthropogenic inputs from wastewater treatment plants on DOM quality in urbanized streams of Illinois, USA. The second principal component (PC2) in this study showed a gradient from inland water bodies to coastal margins with positive loadings for coastal waters. It suggests that the biogeochemical transformation and removal processes influencing the DOM composition could be represented on PC2

depending on the type of aquatic ecosystem (i.e., lakes to coastal water gradient). This further highlighted the importance of photo-degradation processes acting on DOM exported from adjacent terrestrial areas into relatively stagnant and shallow waters of lakes and coastal margins. Positive PC2 loadings for TDP and wetlands further support the assumption that wetland sediment bound phosphorous was released to the coastal waters. Based on the principal component and correlation analyses, it is suggested that biochemical properties of DOM and its transformations in quality (i.e., composition) can be highly influenced by watershed characteristics and can be linked to different land use and land cover types in watersheds.

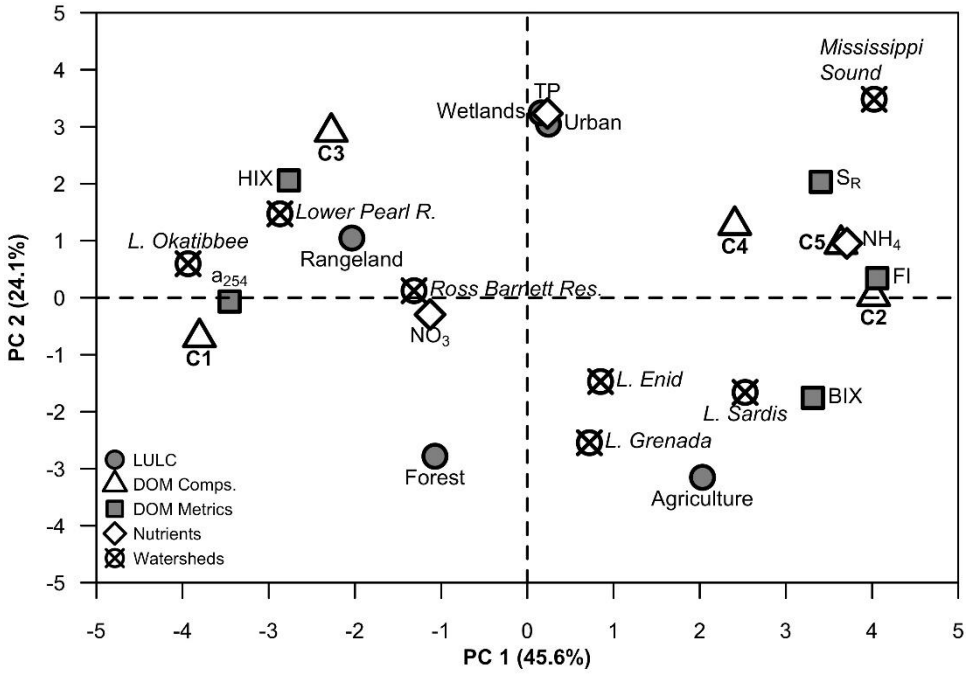

Figure 2.8 PCA plot of loadings and scores determined using the average values for each of the computed or measured parameter (PARAFAC components, optical indices, and nutrients) for each water body.

2.5 Conclusions

DOM compositions and nutrient variations were investigated in multiple water bodies in the Mississippi ranging from inland lakes, estuarine to coastal waters influenced by varying proportions of forest, agriculture, and wetlands. While evaluating DOM compositions, approaches of absorbance and fluorescence spectroscopic techniques in conjunction with multivariate analysis tools such as PARAFAC and PCA were utilized. Combining EEM-PARAFAC for optical properties of DOM and statistical analyses using correlations, regressions and principal components, important insights were derived into the role of land use and land cover types in the resulting DOM compositions. Variability in DOM character due to both biotic (e.g. microbial degradation of refractory DOM to labile DOM in river water) and abiotic processes (e.g., photo-degradation) was deciphered, especially in shallow and stagnant lake and coastal waters. Release of sediment bound nutrients such as NH_4-N and TDP during resuspension can have further implications on DOM character and its microbial utilization in coastal waters. Abiotic factors such as temperature, precipitation amount and intensity, and photo-degradation processes can substantially impact DOM character depending on the source material. In addition, in situ microbial activities can further transform the DOM character. The findings here suggest that for characterizing spatial variations in DOM properties, studies need to pay greater attention to land use and land cover types, as well as physicochemical processes affecting its transformation in watersheds.

As future climate change scenarios predict a greater variation in temperature and precipitation patterns globally, it is important to understand the source, transport, and fate of DOM in a variety of aquatic ecosystems and their relationship to the land use and land

cover in the watershed. More “labile” DOM may not only support increased heterotrophic activity but also contribute to the cleaving of “more” refractory DOM known as “priming effect” (Bianchi 2011) thereby influencing microbial processes (Tank et al. 2011) and nutrient and carbon cycling (Toosi et al. 2014; Yang et al. 2016). Hence, monitoring DOM exports on a watershed scale is important especially where fertilizers and organic wastes are used on agricultural fields. The efficacy of monitoring these changes in DOM export and properties from such watersheds is imperative for regulators and resource managers accountable for estimating the total maximum daily load (TMDL) required for water quality protection (Molinero and Burke 2009; Dash et al. 2015) and for understanding the role of land use and land cover in global carbon cycling through the export of organic matter to the aquatic ecosystems.

CHAPTER III

SEASONALITY IN DISSOLVED ORGANIC MATTER DELIVERY TO THE LOWER PEARL RIVER ESTUARINE WATERS

3.1 Introduction

Dissolved organic matter (DOM) is a heterogeneous mixture of soluble molecules supplied to aquatic ecosystems from the decomposition of living plants and organisms (McKnight et al. 2001; Aiken et al. 2011; Miller et al. 2016; Singh et al. 2017). It is often regarded as one of the largest organic carbon pool in rivers, which plays a central role in altering the biogeochemistry of various elements (e.g., C, N, P, and S) in estuarine, coastal, and oceanic environments (Aitkenhead-Peterson et al. 2003; Yamashita et al. 2008; Battin et al. 2008; Cawley et al. 2014). Recently, riverine and estuarine dissolved organic carbon (DOC) flux has been estimated to be 260 $TgCyr^{-1}$ globally delivered to coastal oceans and comprises a major part of the oceanic carbon cycle (Bianchi 2011; Raymond and Spencer 2014; Osburn et al. 2015). DOM is key to metabolic processes in rivers and estuaries as it regulates carbon and nitrogen supply, which serves as the building blocks for microbes, zooplankton, and phytoplankton (Wiegner and Seitzinger 2004; Blanchet et al. 2017). In addition, biotic and abiotic breakdown of terrestrially derived organic matter transported via river discharge in coastal margins can potentially contribute to environmental problems such as coastal eutrophication causing phytoplankton blooms and hypoxia (Wiegner and Seitzinger 2004; Duan and Bianchi

2006; DeVilbiss et al. 2016). Thus, it is clear that the rivers and streams are not simply a conduit for the transport of water and materials but also serve as a reactor for material transformation as opined by the river continuum concept (Vannote et al. 1980; Cole et al. 2007; Spencer et al. 2013; Raymond and Spencer 2014; Leech et al. 2016).

High discharge in streams and rivers contribute to higher DOM concentrations especially during local rainstorm events within the watershed (Duan and Bianchi 2007; Duan et al. 2007b; Catalan et al. 2013; Osburn et al. 2015; Leech et al. 2016). Additionally anthropogenic activities (e.g., modifications to natural land cover within watersheds) and natural in-situ DOM processing influence the spatial and temporal changes in riverine DOM abundance and its composition (McKnight et al. 2002; Duan et al. 2007b; Molinero and Burke 2009; Shank et al. 2009; Singh et al. 2017). Further, hydrological, photochemical, and biogeochemical processes in the river and in the watershed play a vital role in the seasonal expressions of DOM (Moran and Zepp 1997; Duan et al. 2007b; Chen and Jaffé 2014; Graeber et al. 2015; Singh et al. 2015; von Schiller et al. 2015). Hydrologic conditions define the flow path and control the rate of transport of DOM within a watershed. This further implies that DOM export can be directly linked to the amount of runoff and the variation in discharge conditions during different periods of the year in a watershed (Eimers et al. 2008; Fellman et al. 2011; Butturini et al. 2016). While high runoff produces high DOM exports during surficial flow paths with shorter travel times when surface runoff intersect carbon-rich soil horizons (Hood et al. 2006; O'Donnell et al. 2010; Butturini et al. 2016). DOM in deeper flow path via groundwater travels through mineral soil horizons resulting in decreased amounts due to sorption losses (Marschner and Kalbitz 2003; Banaitis et al. 2006; Kaiser

and Kalbitz 2012). Numerous other studies have also reported seasonal changes in DOM especially during episodic events such as snowmelt (Sebestyen et al. 2008; Balcarczyk et al. 2009; Pellerin et al. 2011) and rainstorm events (Duan and Bianchi 2006; Fellman et al. 2009; Singh et al. 2014), particularly the rainstorms that follow drought periods (Duan et al. 2007b; Vazquez et al. 2010; Catalan et al. 2013; Leech et al. 2016). Therefore, it is clear those seasonal changes in watershed characteristics (e.g., land use and land cover change, hydrologic conditions) would influence the seasonal variation of organic matter concentration and composition in aquatic environments.

Processes such as photochemical reduction and microbial degradation are important pathways for the removal of labile DOM or alteration of refractory DOM in aquatic ecosystems (Amon and Benner 1996; Obernosterer and Benner 2004; Wiegner and Seitzinger 2004; Chen and Jaffé 2014). Both these processes influence the rates and transformations of DOM facilitating its integration into the microbial loop (Coleman 1994; Moran and Zepp 1997; Bushaw-Newton and Moran 1999; Maie et al. 2012; Cawley et al. 2014; Chen and Jaffé 2014; Nelson and Wear 2014). Sunlight enhances the breakdown of higher molecular weight DOM molecules into smaller and more labile compounds (Opsahl and Benner 1998; Wiegner and Seitzinger 2004; Cory et al. 2007; Meng et al. 2013; Yang et al. 2014). For example, Opsahl and Benner (1998) demonstrated the evidence of photo-induced changes in the molecular size distribution of terrigenous DOM in the Mississippi River. Thus, photochemical processes can modify DOM pool by facilitating numerous chemical reactions through production of biologically labile compounds and dissolved inorganic carbon species or such as ammonia and phosphate (Moran and Zepp 1997; Bushaw-Newton and Moran 1999;

Shank et al. 2009; Maie et al. 2012; Schiebel et al. 2015). In addition to these products, photo-oxidation of low molecular weight DOM may release other reactive free radical species such as the organically bound iron (Fe) and hydroxyl (OH) radicals (Moran and Zepp 1997; Schiebel et al. 2015; Sun and Mopper 2016). The resulting DOM and its photoproducts are utilized by microbes and phytoplankton and incorporated into the microbial loop (Wiegner and Seitzinger 2004; Bracchini et al. 2006; Boyer et al. 2006; Stedmon et al. 2007). While microbes and phytoplankton can consume DOM directly through the extracellular enzymatic hydrolysis and surface cell oxidation (Mulholland et al. 1998; Wiegner and Seitzinger 2001), microbially mediated remineralization of DOM produces refractory DOM and releases ammonia and phosphate back into the water column (Wiegner and Seitzinger 2001; Keller and Hood 2011). Although it is clear from these studies that many photo-induced chemical reactions involving different DOM constituents have been examined, the extent of in-situ riverine processing and alterations in its compositions are still unclear. Because the origin and chemical composition of DOM has a large impact on its photo-reactivity and bio-reactivity, seasonal changes in the quantity and quality of riverine DOM are of great environmental and ecological significance (Bertilsson and Tranvik 2000). However, the difficulties in the characterization of this organic matter present a major challenge for its use in biogeochemical studies.

Characterizing DOM composition and its amount has been challenging since the traditional analytical methods are laborious, time-consuming, expensive, and require large sample throughputs. However, recent availability of increasingly rapid optical analyses of the chromophoric (CDOM) and fluorescent (FDOM) fractions of the DOM

pool allow rapid characterization of DOM quality using small sample amounts (~ 4 mL). CDOM and FDOM also serve as optical proxies for DOM source and relative lability (Cory et al. 2010; Cory and Kaplan 2012). Recently there has been increasing use of optical measurements to gain insights into dissolved organic matter (DOM) composition in aquatic ecosystems, and more precisely to identify DOM source in watersheds (Cory et al. 2010; Miller and McKnight 2010; Singh et al. 2010a; 2015; 2017). Many of these studies have also focused on obtaining biogeochemically meaningful results by utilizing spectrofluorometric techniques such as absorption and fluorescence excitation-emission matrix (EEM) measurements in conjunction with statistical tools, such as a multivariate analysis technique named parallel factor analysis – PARAFAC (Stedmon et al. 2003; Cory and McKnight 2005; Miller and McKnight 2010; Singh et al. 2015; Singh et al. 2017). The introduction of EEM-PARAFAC approach in watershed studies have helped researchers to characterize DOM quality and quantity in number of research sites with different environment ranging from oceanic to terrestrial regions (Balcarczyk et al. 2009; Singh et al. 2010a; Graeber et al. 2012; Catalán et al. 2013; Singh et al. 2014). Despite an increasing number of studies on DOM using EEM-PARAFAC in estuarine environments (Yamashita et al. 2008; Santín et al. 2009; Hong et al. 2011; Cawley et al. 2012; Leech et al. 2016; Osburn et al. 2016), the dynamics of DOM and its distribution in an estuary-coastal interface remain elusive.

The aim in the present study is to examine the seasonal variability of DOM amount and quality in the lower Pearl River estuary located in southeastern Louisiana using EEM-PARAFAC approach. This is the first study to my knowledge showing seasonal distribution of DOM composition while utilizing EEM-PARAFAC techniques.

It was hypothesized that hydrologic discharge would regulate riverine DOM properties. The seasonal variability of dissolved organic carbon (DOC) and total dissolved nitrogen (TDN) concentrations and DOM optical proxies representing quality descriptors with respect to discharge were explored. It was further hypothesized that photochemical processes distinctively affect DOM composition, especially during summer periods. In particular, the objectives in this study were (i) to develop a site-specific PARAFAC model for characterizing DOM composition, (ii) to assess the seasonal variability of DOM in the lower Pearl River estuary, and (iii) to assess the relationship between transport (e.g., discharge) and transformation (e.g., photochemical degradation) processes on DOM characteristics for addressing the following questions:

1. What are the DOM characteristics that determine seasonality in a small black water river system?
2. What are the drivers (hydrologic conditions *versus* photochemical process) of the seasonal variability in DOM properties?

3.2 Methods

3.2.1 Study Area

The Pearl River is a small black water river lies within the Gulf-Atlantic Coastal Plain Physiographic Region (Fig. 3.1). It drains an area of approximately 22,500 km^2 constituting 24 counties of Mississippi and 3 counties of Louisiana. It has a meander length of approximately 790 km and it empties into the Gulf of Mexico through Lake Borgne Lagoon and the western Mississippi Sound (Duan et al. 2007; Duan and Bianchi 2007). The Pearl River drains five HUC8 watersheds namely Upper Pearl, Middle Pearl-Strong, Middle Pearl-Silver, Bogue Chitto, and the Lower Pearl River watersheds. This

study was conducted in the Lower Pearl River watershed. The Bogue Chitto River is a tributary of the Pearl River, but flows in the Lower Pearl River watershed also. DOM originating from distant sources or upper reaches of the watershed may not reflect the characteristics of DOM found in the water body and is less likely to affect the DOM composition in the estuary given the distance from the estuary to the upper reaches of the watershed. Hence, following a practical approach, two HUC8 watersheds, the Lower Pearl River watershed and the Bogue Chitto River watershed have been considered as the determinant of DOM composition in the Lower Pearl River Estuary. These two watersheds combined cover an area of approximately 7,848 km^2.

Productive Oyster reefs in the western Mississippi sound are dependent on the salinity moderation that the Pearl River provides. However, with freshwater, the river brings in high amount of suspended sediments, pathogens, nutrients, and organic matter that result in a myriad of water quality issues. Additionally, the marshes and oyster reefs in these areas take a direct hit from the frequent hurricanes in this area, for example, by Hurricane Katrina in 2005, and then Hurricanes Gustav in 2008, Isaac in 2012 etc. The Deepwater Horizon Oil Spill further compounded hurricanes Katrina and Gustav's damage in 2010. Many poor fishermen depend on these oyster reefs for their livelihood. Additionally, the Lower Pearl River estuary is home to two federally threatened species such as the Gulf Sturgeon and the endemic Ringed Sawback turtle.

The climate in the study area is humid subtropical (type Cfa according to Köppen classification system) characterized by a long, hot summer period and mild winters (Kottek et al. 2006). The average temperatures range from 11 ºC in January to 28 ºC in July (www.ncdc.noaa.gov). Precipitation is evenly distributed throughout the year with a

mean annual precipitation of 1524 mm. During winter and spring, cold fronts typically characterize precipitation patterns while summer and fall precipitation occurs mostly due to convective activities with periodical cyclones and hurricanes reaching to the northern Gulf shores.

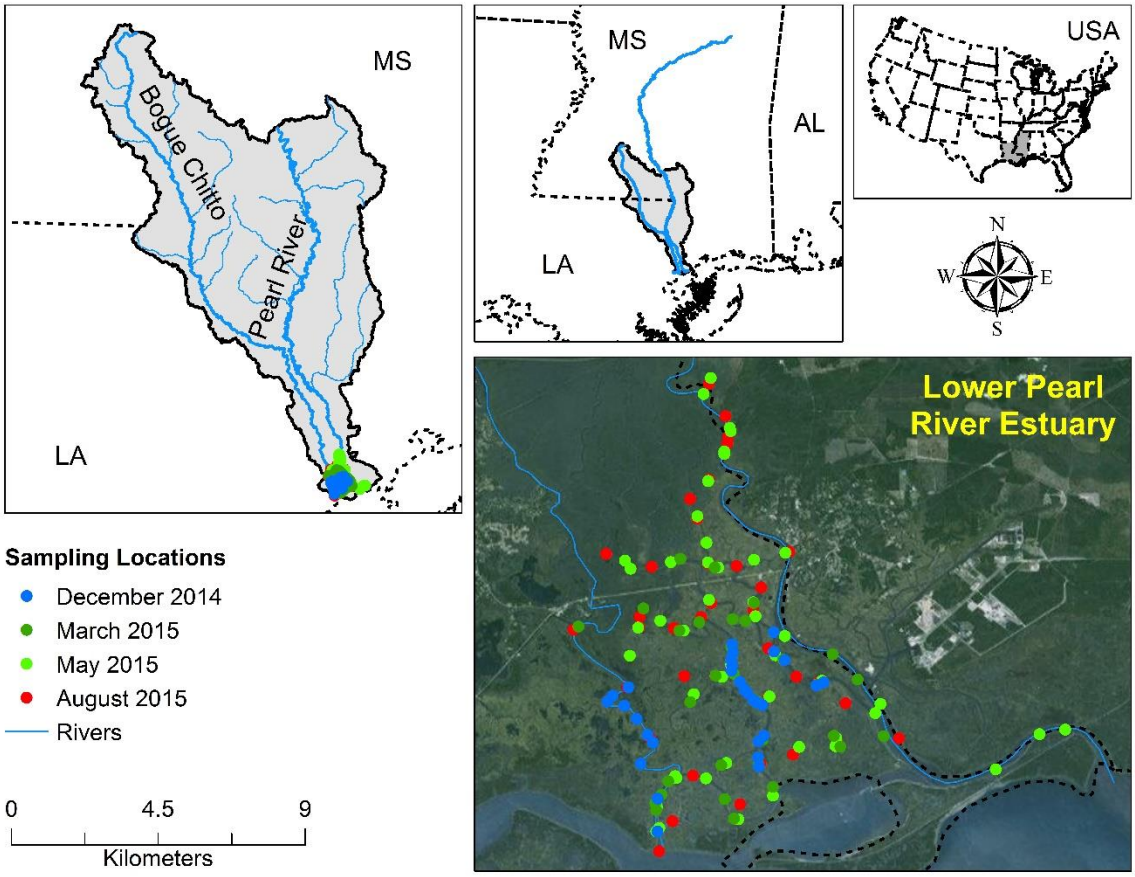

Figure 3.1 Location of the study area with 148 data collection sites indicated.

3.2.2 Water sample and ancillary data collection

Surface water samples were collected during four field campaigns each spanning a week period. The field campaigns were conducted in December (winter) 2014, March

and May (spring), and August (summer) 2015 in the lower Pearl River. Water samples were collected from a total of 148 sampling sites in the estuarine region of lower Pearl River located in the southeastern Louisiana (Fig. 3.1). Temperature, salinity, pH, and dissolved oxygen (DO) were also measured at each site using a calibrated Hanna multi-parameter probe (HI9828, Hanna Instruments, Woonsocket, RI, USA). After collection, the water samples were brought to the laboratory on ice and filtered through 0.2-μm filter papers (Millipore Inc., Billerica, MA, USA) at the end of the day of water sample collection. After filtration the water samples were stored in a refrigerator at 4 °C in 100 mL amber glass bottles for UV absorbance and fluorescence measurements and the determination of dissolved organic carbon (DOC) and total dissolved nitrogen (TDN) concentrations.

3.2.3 DOM concentration and quality measurements

DOC concentrations were measured using high-temperature catalytic oxidation (HTCO) and TDN concentrations by oxidative combustion chemiluminiscence, respectively, on a Shimadzu TOC-VCSN (Shimadzu Scientific Instruments, Columbia, MD) coupled with a TN analyzer unit. The coupled system allowed simultaneous determination of DOC and TDN in the same sample using a single injection and provided low detection limits and appreciable linear ranges for both DOC and TDN. Measurements were determined with a precision of < 5% for both analytes (Lu et al. 2013; Lu et al. 2014). In this study, four qualitative DOM descriptors were used: ratio of DOM absorbance at 250 nm and 365 nm, a_{250}:a_{365} absorbance ratio (also called E2:E3; Peuravuori and Pihlaja 1997; von Schiller et al. 2015; Santos et al. 2016), specific UV absorbance at 254 nm ($SUVA_{254}$; Weishaar et al. 2003), fluorescence index (FI;

McKnight et al. 2001; Cory and McKnight 2005), and biological index (BIX; Huguet et al. 2009; Wilson and Xenopoulos 2009). Two more DOM quality descriptors: humification index (HIX; Ohno 2002) and spectral slope ratio (S_R; Helms et al. 2008; Helms et al. 2013) were also calculated. E2:E3 ratio is reported to be an optical measure of changes in relative size of DOM molecules and inversely proportional to molecular weight (MW) in addition to showing the photo-degradability and photo-reactivity of DOM (Dalrymple et al. 2010; Chow et al. 2012). Specific ultraviolet absorbance (SUVA) was calculated as the ratio of the decadic absorption coefficient at 254 nm to the DOC concentration, with measurement units as $Lmg^{-1}m^{-1}$ (Miller et al. 2016). SUVA has been widely recognized as a surrogate of aromatic carbon content of DOM (Weishaar et al. 2003; Chow et al. 2012). While $SUVA_{254}$ is also an indicator of DOM bioavailability and biodegradability (Marschner and Kalbitz 2003), which provides a more qualitative indication of aromaticity, fluorescence may be a more reliable tool when attempting to discriminate between aquatic and terrestrial DOM source pools (Hood et al. 2006; Jaffé et al. 2008; Cory et al. 2011). McKnight et al. (2001) developed a fluorescence index (FI) to differentiate precursor DOM sources (i.e., aquatic versus terrestrial). This index is calculated as the ratio of fluorescence emission intensity at 470 and 520 nm with an excitation at 370 nm, which provides a measure of the steepness and shape of the emission intensity peak (Cory and McKnight 2005). Larger rivers predominately exporting terrestrially derived DOM across the U.S. reported FI values 1.4 to 1.5. In contrast, lakes within the U.S. had higher FI values ranging from 1.6 to 1.9 (McKnight et al. 2001). While FI is extremely useful in discriminating between aquatic and terrestrial organic matter source material (McKnight et al. 2001; Korak et al. 2014), weak responses

to changes in FI among terrestrial source pools have also been reported (Hood et al. 2006; Roelke et al. 2006). The biological index (BIX) was measured as the ratio of fluorescence emission intensity at 380 nm divided by the emission intensity maximum observed between 420 and 440 nm, obtained at excitation 310 nm (Huguet et al. 2009; Wilson and Xenopoulos 2009). This index, also known as freshness index, is an indicator of the contribution of fresh DOM originating from autochthonous production or biological activity (Wilson and Xenopoulos 2008; Wilson and Xenopoulos 2009; Singh et al. 2015) and has been determined for various ecosystems (Huguet et al. 2009; Singh et al. 2010b; Duan et al. 2015; Singh et al. 2017). High BIX values (>1) suggest a predominantly autochthonous origin of DOM relating to the presence of freshly released DOM in aquatic systems, whereas lower BIX values of 0.6-0.7 indicate lower DOM production in these systems (Huguet et al. 2009).

3.2.4 Absorption and fluorescence EEM measurements

UV-Vis absorption and fluorescence measurements were performed using the PerkinElmer Lambda 850 double-beam spectrophotometer (PerkinElmer, Inc., Waltham, MA, USA) and Fluoromax-4 fluorometer (Horiba Jobin Yvon, Inc., Edison, NJ, USA), respectively. Detailed information on sample processing protocols are discussed by Singh et al. (2017) and Dash et al. (2015). Briefly, the absorption spectra of the water samples were obtained between 200 and 750 nm at 2-nm intervals. Absorbance values at wavelength, λ, corrected for particle-free Nanopure Milli-Q water blanks (at purity level of 18.2 MΩ) were converted to Napierian absorption coefficients (a in units m-1) using the following equation:

$$\frac{a(\lambda)= 2.303*A(\lambda)}{L} \quad 3.1$$

where $A(\lambda)$ is the absorbance measured at a wavelength λ and L is the path length in meters (Singh et al. 2010; Dash et al. 2010; Singh et al. 2017).

Fluorescence EEMs were recorded for excitation in the range 240 to 450 nm at every 10-nm intervals and emission in the range 300 to 550 nm at every 2-nm. The EEM scans were collected in ratio mode (S/R mode) with dark offset and a bandwidth setting of 5-nm for both the excitation and emission. To correct for instrument bias, factory-supplied correction factors were applied to the scans. A daily lamp scan, cuvette check, and water Raman scan were collected to ensure instrument stability. EEM processing for the corrections and blank subtractions were carried out in MATLAB 7.12 (MathWorks Inc., Natick, MA, USA) following the recommendations of Cory et al. (2010). Absorption spectra were applied to correct for inner filter effects (IFE) in blank and sample EEM scans. Following IFE correction, EEM scans were normalized to daily analyzed water Raman integrated area under maximum fluorescence intensity (Ex-350/Em-397, 5-nm bandwidth) as suggested by Lawaetz and Stedmon (2009) to normalize the EEM data to a comparable Raman units (R.U.; nm-1). Finally, corrected Milli-Q water (blank) EEMs were subtracted from the sample EEMs to eliminate any influence of Raman peaks. EEM scans were normalized by the maximum-recorded fluorescence intensity for each sample. This processing step ensured that all the samples had equal weightage in PARAFAC modeling procedure (Westerhoff et al. 2001; Singh et al. 2013).

3.2.5 EEM-PARAFAC analysis

A total of 148 EEM scans were used to develop a site-specific parallel factor analysis (PARAFAC) model using MATLAB 7.12 and DOMFluor toolbox (ver., 1.7; Feb., 2009) (Stedmon and Bro 2008; Singh et al. 2010b; Singh et al. 2017). In this study, a EEM-PARAFAC model of four distinct fluorescence components (C1-C4) was validated by split-half analysis and random initialization explaining more than 99% of variation in the EEM dataset. Details of steps for performing PARAFAC modeling using EEMs are discussed by Singh et al. (2010a; 2010b; 2013; 2014a; 2014b; 2015; 2017). The relative abundance of each of these four fluorescent components (*Cn*, *n* = 1 to 4) was calculated as the % contributions of the individual fluorescence components by dividing each component F_{max} score by the sum of the total fluorescence intensity (sum of F_{max} scores of all four components) as discussed by Fellman et al. (2009) and Lu et al. (2013).

$$\%Cn = \frac{F_{Cn}*100}{TF} = \frac{F_{Cn}*100}{\sum_{n=1}^{4} F_{Cn}} \quad 3.2$$

where F_{Cn} represented fluorescence intensity of each specific fluorescent component and TF was total fluorescence intensity.

3.2.6 Photochemical degradation experiment

For the photochemical degradation experiment, 3L of water sample was collected on September 13, 2016 from the lower Pearl River estuary near NASA's John C. Stennis Space Center, Mississippi. The water sample was brought to the laboratory on ice and 2L of water sample was filtered using 0.2 µm filter papers. 180 mL of this bacteria-free filtrate and 20 mL of unfiltered water sample (as inoculum) was dispensed each to a total of six 250 mL French square clear glass bottles and six 250 mL amber glass bottles

maintaining a headspace of 50 mL. Six of the French square clear glass bottles are labeled as sunlight samples while the other six amber glass bottles were wrapped with aluminum foil and labeled as dark controls. The subsamples were shaken well to mix thoroughly prior to starting the experiment. The bottle heads were covered with parafilm to allow gas exchange (e.g., oxygen) while protecting the samples from any outside contamination that may occur while the subsamples were left outside in the natural sunlight. The subsamples (both dark and sunlight) were exposed to natural sunlight for 6-8 hours each day for 10 consecutive days. During 10-day experiment, subsamples were collected after 1, 3, 5, 7, and 10 days. Immediately, after the end of each day collection, samples were re-filtered through the 0.2 μm filter paper to reduce any masking effects of flocculation that may have occurred while incubation and storage to photochemical degradation (Shank et al. 2009; Shank et al. 2011). Theses re-filtered subsamples were kept refrigerated until spectroscopic (absorption and fluorescence) measurements. Fluorescence intensity values for the PARAFAC modeled components (C1-C4) were identified from the excitation-emission peak positions in EEMs measured for photochemical degradation experiment.

3.2.7 Statistical analysis

Statistical differences between sources (observations) and groups (seasons) were determined using one-way analysis of variance (ANOVA) with subsequent Tukey-HSD pairwise multiple comparison post-hoc analyses and plotted with R software version 3.3.3 (R Core Team, 2017). One-way ANOVA offers a statistical method to compare differences across multiple group means. The null hypothesis was that the seasonal means for each parameter (e.g., DOC) are not different. One-way ANOVA is more

appropriate method choice here for comparing group means over t-tests because three seasons were compared. Multivariate Pearson correlations between PARAFAC components (C1-C4), DOM concentrations (DOC and TDN) and quality descriptors (i.e., $SUVA_{254}$, E2:E3, BIX, and FI) were performed using JMP Pro 13.1.0 statistical software package (SAS Institute Inc., Cary, NC). All the statistical analyses were computed at a 95% significance level ($\alpha = 0.05$) unless stated otherwise. Non-metric multidimensional scaling (NMDS) was performed using R software version 3.3.3 (R Core Team, 2017) and applied to the data set to ordinate the samples by DOM properties (DOC, TDN, PARAFAC components (C1-C4), $SUVA_{254}$, E2:E3, BIX, and FI) and hydrographic parameters (temperature, salinity, pH, and DO) using the matrix imputation by Bray-Curtis dissimilarity calculation. NMDS ordination technique uses rank orders and has been shown to be efficient in grouping samples in many DOM studies (Vazquez et al. 2010; Catalan et al. 2013; Kellerman et al. 2014).

3.2.8 Delineation of Land use and land cover of the watershed

Watershed boundaries for the lower Pearl River and the adjacent Bogue-Chitto River were determined using USDA NRCS eight-digit watershed boundary dataset and merged into a single watershed. The land use and land cover dataset in the merged watershed were calculated from the Cropland Data Layer (CDL) from the USDA NRCS Geospatial Data Gateway by combining the original 255 classes to output eight major land use and land cover classes including agriculture, aquaculture, barren, forest, rangeland, wetland, urban, and open water (Johnson and Mueller 2010; USDA 2017). The grouping of 255 classes into eight classes was achieved by following the Level I

classification scheme of Anderson et al. (1976) for land use and land cover. The CDL data used in this study had an overall accuracy of 80.7%.

3.2.9 Collection of hydrographic parameters

Water discharge data for the Pearl River were obtained from U.S. Geological Survey site at Bogalusa, Louisiana. The multi-sensor precipitation estimates (MSPE) derived from hourly Weather Surveillance Radar – 1988 Doppler (WSR-88D) data were used in this study. From the hourly precipitation estimates, daily totals were calculated for the study period. The MSPE data is used here because of its high spatial resolution (4km x 4km). The data is generated for a 15-month period over the study area centered at Bogalusa, Louisiana with a 0.5º x 0.5º grid (roughly 50km x 50km in all directions from Bogalusa). Detailed information about estimating the MSPE data is given by Dyer and Mercer (2013).

3.3 Results

3.3.1 Land use and land cover in the watershed

The land cover in the watershed is dominated by rangeland (37%) that includes shrubland and grassland/pasture followed by natural forest (30%), which includes evergreen, deciduous and mixed-forests (Fig. 3.2). Herbacious and woody wetland areas make up 23% of the land cover and are distributed mainly along the river channel while the urban areas and croplands make upto 7 and 1% of the land cover, respectively in the watershed.

3.3.2 Seasonal patterns of hydrographic parameters

Salinity ranges in the surface water samples were 0.0-3.6, 0.1-14.3, and 0.3-12.6 (psu) during spring, summer, and winter, respectively. Surface water temperature varied from 16.7 to 28.0 °C, 30.0 to 34.0 °C, and 13.8 to 15.8 °C, respectively during spring, summer, and winter seasons. DO was between 0.4 and 8.6 mgL^{-1}, 0.8 and 2.7 mgL^{-1}, and 5.2 and 10.5 mgL^{-1}, respectively during spring, summer, and winter seasons, respectively, whereas the pH was between 7.9 and 10.3, 7.0 and 9.1, and 9.1 and 11.3, respectively during spring, summer, and winter seasons (Table 3.1). Both DO and pH followed an inverse pattern to temperature values during seasons. Water discharge in the Pearl River was characterized by a high frequency seasonal variability with highest flow observed during spring (March and April) 2015 following precipitation events (Fig. 3.3). In addition, a long low-flow period occurred during summer 2015 from July to October. Water discharge in the lower Pearl River at Bogalusa averaged 7430 ft^3s^{-1} (range: 1360 – 31800 ft^3s^{-1}) from November 2014 to December 2015 (Fig. 3.3). In general, high discharge occurred between late fall and early summer followed by a prolonged dry period of low discharge from mid-summer to early fall. Average discharge during spring 2015 was 13914 ft^3s^{-1}, followed by an average lowest discharge (3207 ft^3s^{-1}) during summer 2015. The four sampling dates are shown during representative stages of the hydrograph (Fig. 3.3).

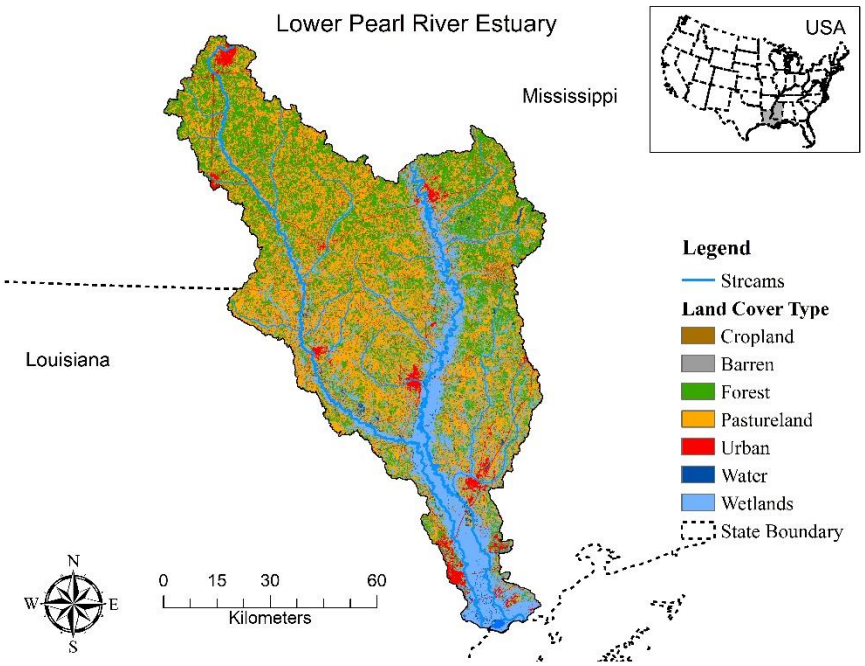

Figure 3.2 Land use and land cover in the lower Pearl and Bogue-Chitto river watershed.

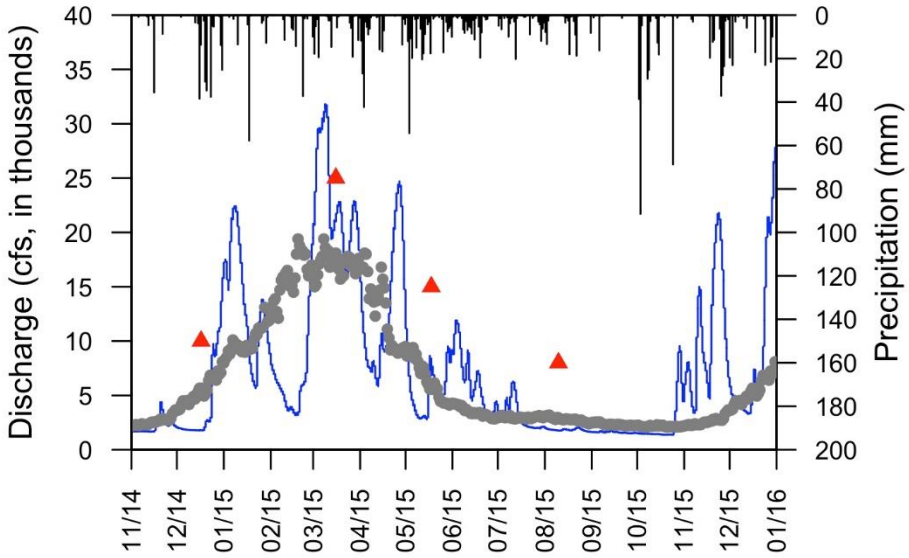

Figure 3.3 Discharge and precipitation data for USGS measuring station located at Bogalusa, LA is presented here along with a long-term median (~ 77 years) discharge (shown with grey circles). Discharge is given by blue solid line while the precipitation is shown with inverted bar plots from secondary x-axis. Solid red triangles correspond to the weeks of water sampling.

Table 3.1 Seasonal distribution of PARAFAC modeled fluorescence components, DOM concentrations (DOC and TDN) and quality descriptors, and hydrographic parameters are shown for the lower Pearl River estuary.

Variables	Spring	Summer	Winter
C1 (%)	30.59 ± 1.71 (77)	26.24 ± 0.92 (35)	26.08 ± 0.48 (29)
	27.08 − 34.29	23.96 − 28.93	25.28 − 27.07
C2 (%)	32.82 ± 0.74 (77)	31.92 ± 0.80 (35)	31.71 ± 0.38 (29)
	30.68 − 34.65	30.20 − 33.87	30.83 − 32.20
C3 (%)	19.83 ± 0.84 (77)	24.36 ± 0.45 (35)	23.67 ± 0.25 (29)
	18.36 − 23.45	22.77 − 25.10	23.03 − 24.16
C4 (%)	6.73 ± 1.37 (77)	14.98 ± 1.66 (35)	18.45 ± 2.57 (29)
	4.59 − 10.98	10.04 − 17.74	14.32 − 24.88
DOC (mgL^{-1})	6.73 ± 1.58 (76)	3.95 ± 0.71 (36)	2.33 ± 0.30 (29)
	0.68 − 11.37	2.73 − 5.83	1.55 − 3.09
TDN (mgL^{-1})	0.29 ± 0.08 (76)	0.11 ± 0.03 (36)	0.18 ± 0.04 (29)
	0.01 − 0.50	0.04 − 0.17	0.11 − 0.28
$SUVA_{254}$ ($Lmg^{-1}m^{-1}$)	4.68 ± 0.80 (75)	2.81 ± 0.40 (36)	4.69 ± 0.90 (29)
	2.95 − 7.38	1.73 − 3.56	3.31 − 6.90
Fluorescence Index, FI	1.39 ± 0.02 (77)	1.48 ± 0.01 (36)	1.49 ± 0.01 (29)
	1.32 − 1.45	1.44 − 1.50	1.46 − 1.51
Biological Index, BIX	0.56 ± 0.02 (77)	0.69 ± 0.02 (36)	0.69 ± 0.01 (29)
	0.52 − 0.62	0.64 − 0.77	0.67 − 0.71
E2:E3 (a_{250}:a_{365})	4.73 ± 0.35 (78)	5.93 ± 0.53 (36)	5.14 ± 0.34 (30)
	4.14 − 5.52	4.93 − 6.97	4.31 − 5.82
Humification Index, HIX	0.76 ± 0.07 (77)	0.66 ± 0.08 (36)	0.60 ± 0.12 (29)
	0.54 − 0.88	0.40 − 0.81	0.38 − 0.81
Spectral Slope ratio, S_R	0.80 ± 0.04 (78)	1.04 ± 0.08 (36)	0.81 ± 0.13 (30)
	0.72 − 0.96	0.89 − 1.31	0.69 − 1.03
Temperature (°C)	23.01 ± 3.67 (79)	31.65 ± 0.73 (38)	14.82 ± 0.61 (29)
	16.66 – 28.02	29.97 – 33.91	13.75 − 15.73
Salinity (psu)	0.39 ± 0.64 (79)	7.99 ± 4.16 (38)	5.72 ± 3.79 (29)
	0.02 – 3.61	0.06 – 14.33	0.25 − 12.56
DO (mgL^{-1})	3.34 ± 2.27 (79)	1.82 ± 0.46 (38)	7.52 ± 1.70 (29)
	0.43 – 8.55	0.75 – 2.68	5.24 – 10.53
pH	9.01 ± 0.51 (79)	8.08 ± 0.36 (38)	10.08 ± 0.69 (29)
	7.94 – 10.34	7.02 – 9.07	9.09 − 11.26

Values of the parameters are represented as Mean ± Std. Dev. Sample size is represented within brackets (N). Minimum and maximum of the values are shown as Min − Max.

3.3.3 Seasonal patterns of DOM descriptors

DOC and TDN concentrations were highest during high flow periods during spring with average concentrations of 6.73 (±1.58) and 0.29 (±0.08) mgL^{-1}, respectively (Table 3.1 and Fig. 3.4). The DOC and TDN concentrations during summer were 3.95 (±0.71) and 0.11 (±0.03) mgL^{-1}, respectively. DOC concentration was lowest during winter season with an average value of 2.33 (±0.30) mgL^{-1}. Significantly higher TDN concentration of 0.18 (±0.04) mgL^{-1} was observed during winter season, while the lowest concentration was observed during the summer season. The highest average $SUVA_{254}$ was observed during winter season (4.69 ± 0.90 $Lmg^{-1}m^{-1}$) and lowest was recorded during the summer season (2.81 ± 0.40 $Lmg^{-1}m^{-1}$). However, $SUVA_{254}$ values were not significantly different between spring (4.68 ± 0.80 L $mg^{-1}m^{-1}$) and winter seasons indicating similar DOM sources during these periods. Average values of an absorbance derived DOM descriptor, E2:E3 showed highest values during summer (5.93 ± 0.53) while the lowest E2:E3 values were observed during the spring season (5.14 ± 0.34) with an intermediate value observed during the winter season (4.73 ± 0.35). Both FI and BIX showed the highest average values during winter (1.49 ± 0.01 and 0.69 ± 0.01, respectively), medium values during the summer (1.48 ± 0.01 and 0.69 ± 0.02, respectively), and low values during spring season (1.39 ± 0.02 and 0.56 ± 0.02, respectively) (Table 3.1 and Fig. 3.4).

3.3.4 Seasonal patterns of PARAFAC components

PARAFAC analyses of fluorescence EEMs provided the dominant fluorescing components within the total DOM pool and determined distinct seasonal shifts in the proportion of individual DOM components. Both the components C1 and C2 are

indicative of the presence of terrestrially derived humic-like organic matter (Fig. 3.5 and Table 3.2). Component C1 has been previously defined as soil-derived organic matter while the abundance of C2 has been commonly observed in various aquatic environments as a result of degrading plant and animal detritus (Singh et al. 2010b; Osburn et al. 2016; Singh et al. 2017). Component C3 has operationally been attributable to microbial humic-like DOM and has been found both in terrestrial and marine environments (Liu et al. 2009; Romera-Castillo et al. 2011; Singh et al. 2017). This component also has similar spectral features to a component found in a previous study by Stedmon and Markager (2005), where the authors attributed its origin to microbially processed phytoplankton degradation products. While the fluorescence characteristics of component C4 reflect the organic matter similar to free tryptophan or protein-like DOM, autochthonous production of DOM in addition to microbial degradation can also generate similar fluorescence features in many terrestrial and oceanic environments (Lapierre and Frenette 2009; Para et al. 2010; Zhang et al. 2010; Tedetti et al. 2011). In addition, this component is also similar to microbially deduced DOM in multiple environments ranging from agricultural runoff inputs in streams, wastewater-impacted streams, and in natural streams due to in situ biological processing (Table 3.2).

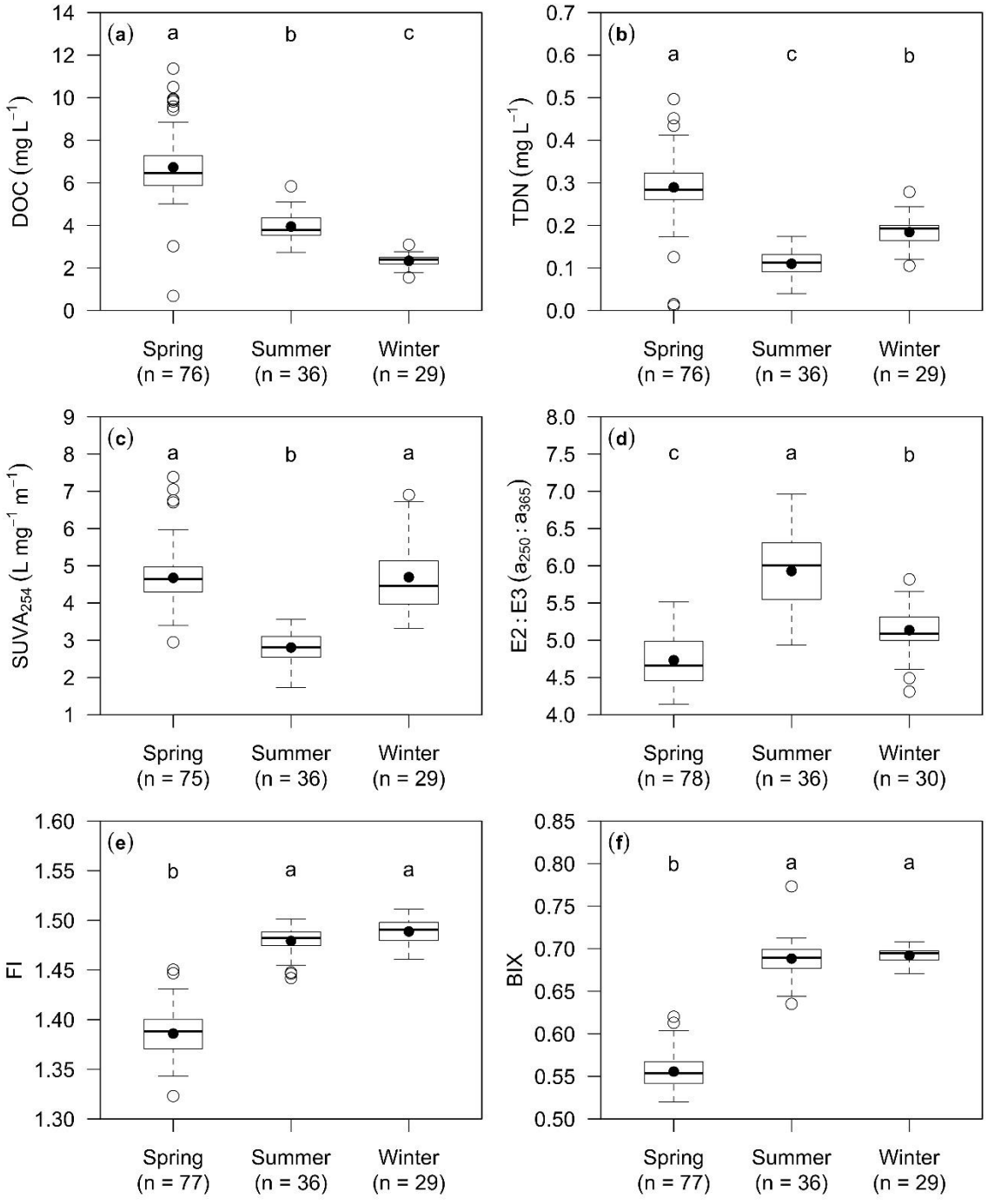

Figure 3.4 Seasonal distributions of (a) DOC, (b) TDN, (c) $SUVA_{254}$, (d) E2:E3, (e) FI, and (f) BIX for the lower Pearl River estuary.

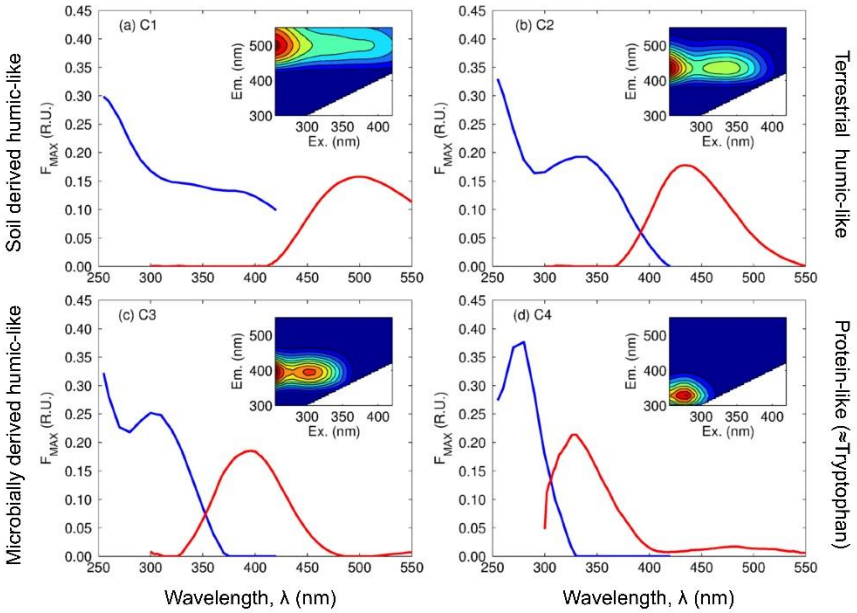

Figure 3.5 Four PARAFAC modeled components (C1-C4) identified in this study are shown here.

Table 3.2 Descriptions and the characteristics of the four PARAFAC modeled fluorescence DOM compositions identified in this study and their comparison against those previously reported in the literature.

Components (Ex/Em)	**I**	**II**	**III**	**IV**	**V**	**VI**	**VII**	**VIII**	**Description and origin of DOM composition and possible sources**
C1 (< 250-380/500)	C2	C3	C2	C4	C3	C4	C2	C3	UVA humic-like; terrestrial origin or allochthonous transport; primarily in soil-derived material; reduced terrestrial DOM; common in wide range of freshwater environments such as wetlands and rangelands.
C2 (< 250-335/434)	C4	C2	C1	C2	C1	C2	C1	C1	UVA humic-like; terrestrial origin or allochthonous transport; common to wide range of freshwater, estuarine and oceanic aquatic environments.
C3 (<250-300/396)	C6	C6	C3	C3	C2	C8	C4	C2	Microbial humic-like; component similar to polyaromatic hydrocarbons (PAHs); biological and/or microbial origin; photo-labile DOM product.
C4 (280/330)	C7	C4	C5	—	C4	C7	C5	C4	Protein-like (Tryptophan-like) DOM; autochthonous production; similar to N-containing fluorophores such as indoles; also commonly found in agriculture and wastewaters.

I: (Stedmon and Markager 2005); **II:** (Yamashita et al. 2008); **III:** (Santín et al. 2009); **IV:** (Singh et al. 2010); **V:** (Guo et al. 2011); **VI:** (Osburn et al. 2015); **VII:** (Arellano and Coble 2015); **VIII:** (Singh et al. 2017)

The percent contribution of components C1 (soil-derived humic-like DOM) and C2 (terrestrially originated humic-like DOM) composed the majority of the fluorescence signal for all samples, averaging 30.59 ± 1.71% and 32.82 ± 0.74%, respectively during spring (Fig. 3.6 and Table 3.1). Both these DOM components (i.e., C1 and C2) were found to have much lower concentrations during summer (26.24 ± 0.92% and 31.92 ± 0.80%, respectively) and winter (26.08 ± 0.48% and 31.71 ± 0.38%, respectively). The proportion of component C3, which has fluorescence characteristics resembling microbially derived humic-like DOM, was highest during summer (24.36 ± 0.45%), whereas the lowest values were observed during spring (19.83 ± 0.84%). During winter season, the proportion of the component C3 (23.67 ± 0.25%) was found to be intermediate during summer and spring seasons. The proportion of the component C4, which has fluorescence characteristics that resemble protein-like DOM (e.g., amino acids tryptophan), was composed of a smaller proportion of fluorescence in total DOM pool. The proportion of C4 varied seasonally in the lower Pearl River estuary, accounting for the highest value during winter (18.45 ± 2.57%), followed by an intermediate value during summer (14.98 ± 1.66%), and very low value during the spring (6.73 ± 1.37%) season (Fig. 3.6 and Table 3.1).

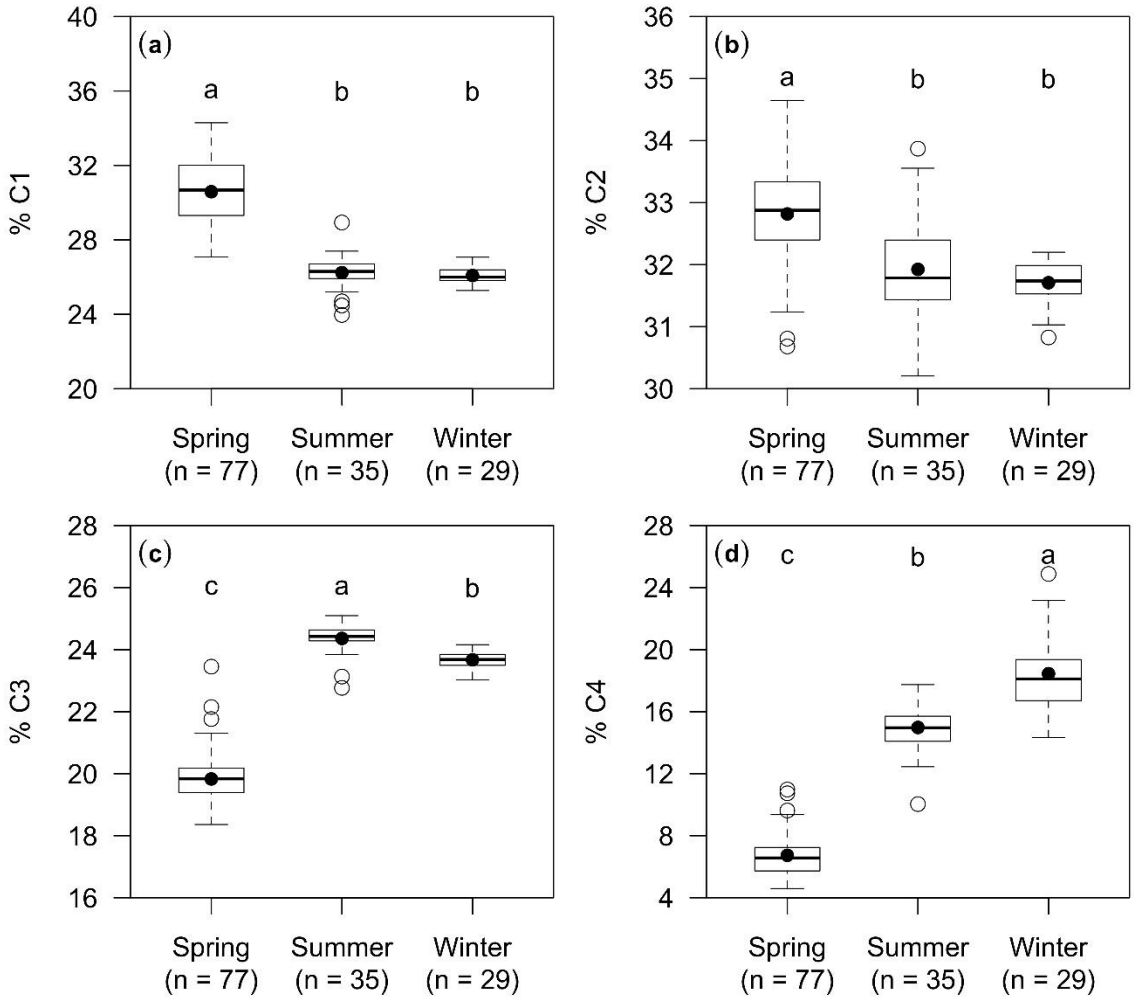

Figure 3.6 Seasonal distributions of the PARAFAC modeled components (a) C1, (b) C2, (c) C3, and (d) C4 in the lower Pearl River estuary.

3.3.5 DOM components relationships with salinity

The relationships between salinity and fluorescence intensity of individual fluorescent components, DOC, and FI in lower Pearl River estuary is shown in the Fig. 3.7. The fluorescence DOM components showed non-conservative relationships with salinity. The non-conservative relationships are indicative of non-linear variations in DOM properties with salinity suggesting biogeochemical processes are in action during

DOM transport. The terrestrially derived humic-like fluorescence components, C1 and C2, generally showed decreasing trend with increasing salinity. However, it is to be noted that the component C2, which is common in many terrestrial environments, showed a relative conservative mixing as compared against the soil-derived humic-like DOM (C1). The microbial humic-like DOM (C3), in fact, showed a substantially increasing trend with increasing salinity and this relationship could not be explained by conservative mixing. This indicates that the presence of this fluorescence component could have originated from microbially mediated photo- or biodegradation of terrestrially derived organic matter inputs into the estuary (Yamashita et al. 2008). Component C4, which represents a protein-like or tryptophan-like amino acid DOM also showed an increasing trend with increasing salinity. High abundance of protein-like DOM, which has been considered to be a labile DOM in high salinity waters, could have resulted from biological production in estuarine environments (Yamashita et al. 2008; Cawley et al. 2012; Cawley et al. 2014). After the microbial processing of autochthonous DOM within the water column, the remains of the degraded organic material could also produce biologically labile component such as protein-like DOM, C4, in estuarine waters (Yamashita et al. 2008). In addition, DOC concentration also followed a similar pattern to terrestrial humic-like fluorescence components, C1 and C2, and decreased with increasing salinity. However, FI at higher values (> 1.4), suggestive of microbial origin of DOM showed an increasing pattern with increasing salinity indicating higher biological activity in estuarine waters on DOM transported from terrestrial landscapes.

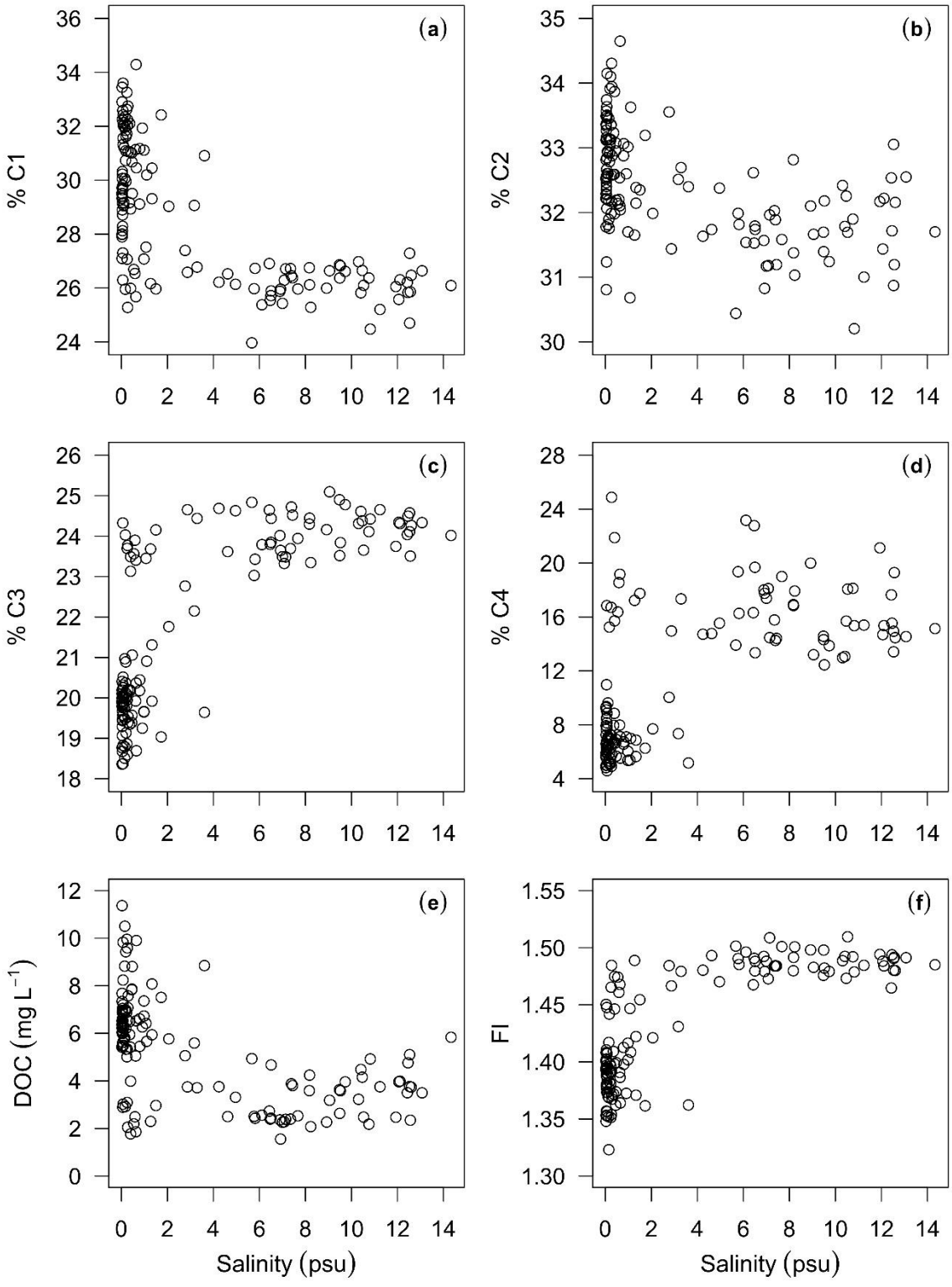

Figure 3.7 Relationships between PARAFAC modeled components (a) C1, (b) C2, (c) C3, (d) C4, (e) DOC, and (f) FI with salinity for lower Pearl River estuary.

3.3.6 DOM photochemical experiments

Photochemical degradation causes bleaching and alters the chemical composition of total DOM pool. In particular, photo bleaching causes specific fluorescence to decrease (Mopper et al. 1991; Vodacek et al. 1995; Mopper et al. 2015). Thus, to better understand the role of photochemical degradation on the fate of DOM during their transport in the lower Pearl River estuary, the photo-degradation potential of the DOM sample was investigated using natural sunlight exposure (McCallister et al. 2005; Shank et al. 2009; Meng et al. 2013). The photo-degradation caused considerable changes in the bulk concentration of DOM as indicated by absorbance values shown in Table 3.3, with a decrease of 30 to 40%. Although all the fluorescence components (C1-C4) declined gradually over the 70-hr period of sunlight exposure, the terrestrially derived humic-like DOM, both C1 and C2, had the largest rates of decline ranging between 70 to 75%. In comparison, the loss in C4 was lowest at 25% and the microbial humic-like DOM (C3) declined to 50% of its pre-irradiation values (Figs. 3.8 and 3.9; Table 3.3). These results suggest that terrestrial humic-like organic materials are more vulnerable to photochemical degradation during summer. Half-lives of photo-bleached DOM composition (C1-C4) were computed using exponential decay equation (Table 3.3), which showed a range of 37 to 201 h for lower Pearl River estuary sample of summer 2016. The shortest half-lives for components C1 and C2 were 37 to 39 h, respectively indicating that terrestrial derived organics were highly susceptible to photo-induced alterations. This is comparable to the findings of Caffrey et al. (2014), who suggested a 11-day residence time of waters in Grand Bay, a bay close to the Pearl River mouth. Hence, it appears that the terrestrial

DOM from lower Pearl River may disappear rapidly along its transport under higher rates of photochemical reactions.

Table 3.3 Initial (pre-irradiation), Final (post-irradiation), Percent Remaining and three-parameter exponential decay/growth model [$y = y_0 + a*e^{(-kt)}$ or $y = y_0 + a*(1-e^{(-kt)})$] with rate of decay/growth k (hr^{-1}) for PARAFAC components and DOM descriptors, after 10-day photochemical degradation experiment for the lower Pearl River estuary for a water sample collected on September 13, 2016.

	a_{254} (m^{-1})	a_{350} (m^{-1})	$S_{275-295}$ (μm^{-1})	C1	C2	C3	C4
Initial (Pre-irradiation)	55.37	15.31	14	0.44	0.79	0.71	0.28
Final (Post-irradiation)	39.96	8.73	18	0.12	0.23	0.34	0.22
Percent Remaining	72.18	57.00	–	26.77	29.45	47.32	77.13
y_0	23.50	6.77	0.01	13.88	22.93	31.81	14.24
a	32.31	8.70	0.01	5.80	11.93	5.62	20.03
k **(hr^{-1})**	0.0097	0.0215	0.0287	0.1168	0.0201	0.0850	0.0091
half-life (h)	≈ 149	≈ 86	–	≈ 37	≈ 39	≈ 66	≈ 201
R^2	0.97	0.97	0.98	0.95	0.98	0.97	0.89
***p*-value**	0.0053	0.0054	0.0021	0.0118	0.0026	0.0045	0.0390

In this study, a clear distribution in NMDS space and clusters were observed for spring, summer, and winter seasons (Fig. 3.10). The first axis (dimension 1) was related to DOM concentration and lability. Spring samples were grouped in positive side of dimension 1 and were linked to highly colored aromatic DOM as indicated by high SUVA and high DOM concentrations as indicated by high DOC and TDN. In addition, both the terrestrial derived DOM components, C1 and C2, were located in the same direction as of both DOC and TDN concentrations. The negative side on dimension 2 depicts microbially generated DOM (high FI and BIX) indicating labile DOM. High humic-like DOM was observed during spring while summer and winter samples showed

labile DOM character of microbial origin. Hydrographic variables (temperature, salinity, pH, and DO) showed the dispersion of samples along the second axis (dimension 2). Temperature was plotted on the positive side of dimension 2, which showed higher influence of temperature during summer while pH and DO were plotted on the negative side of dimension 2 showing pH and DO controlled the DOM character during winter (Fig. 3.10). Similar to NMDS ordination results, the correlations between DOM concentrations (DOC and TDN), compositions (C1-C4), and quality descriptors (optical indices), and hydrographic parameters showed strong relationships between terrestrial humic-like DOM (both C1 and C2) and DOC, FI, BIX, and E2:E3. Microbial humic-like DOM (C3) also depicted strong relationships with DOC, FI, BIX, E2:E3, and salinity (Table 3.4).

3.4 Discussion

Estuaries are highly dynamic and complex ecosystems with highly variable autotrophic and heterotrophic bacterial activities primarily depending on seasonal hydrologic and climatic conditions (Caffrey et al. 2014; Oestreich et al. 2016). Seasonal changes in flow conditions may influence DOM quantity and quality thereby shaping estuarine microbial loop dynamics and net ecosystem metabolism while transporting riverine organic material (Leech et al. 2016). Because DOM transport by black water rivers may play an important role in biogeochemistry of coastal waters, therefore examining amount and quality of organic solutes from such rivers during varying hydrologic and climatic conditions need careful consideration.

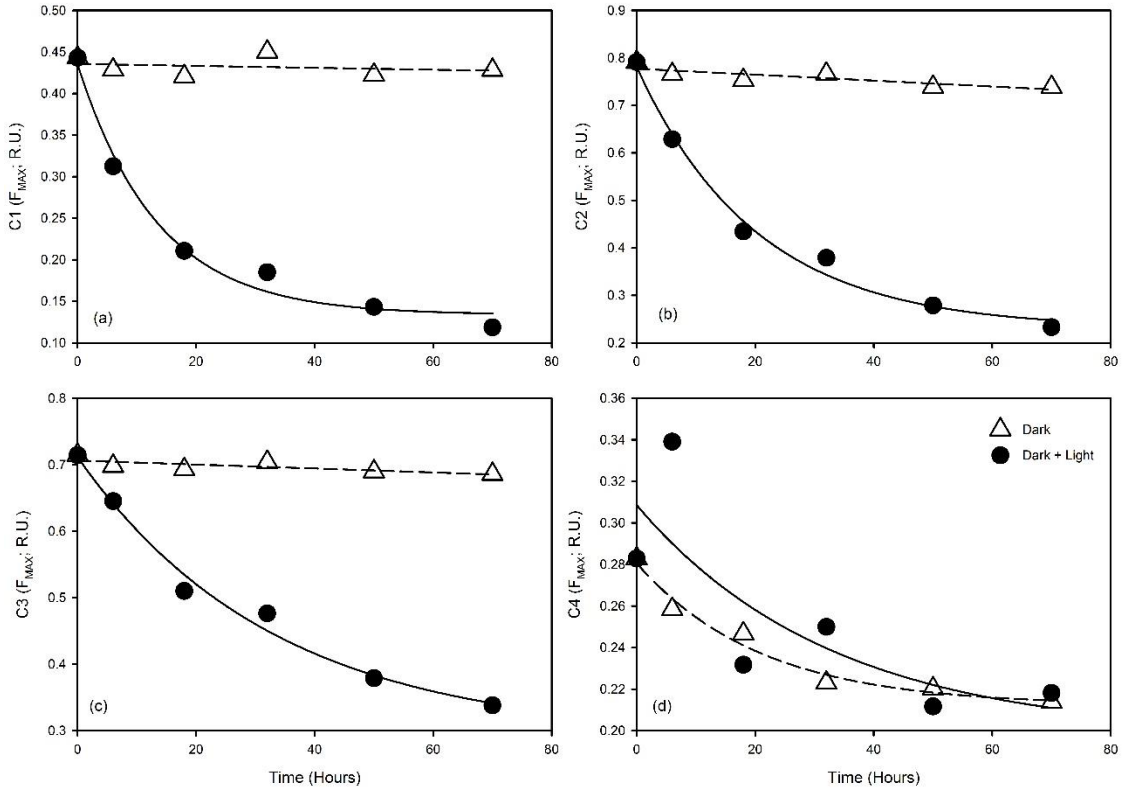

Figure 3.8 Results of photochemical degradation experiment for PARAFAC modeled components for the lower Pearl River estuary.

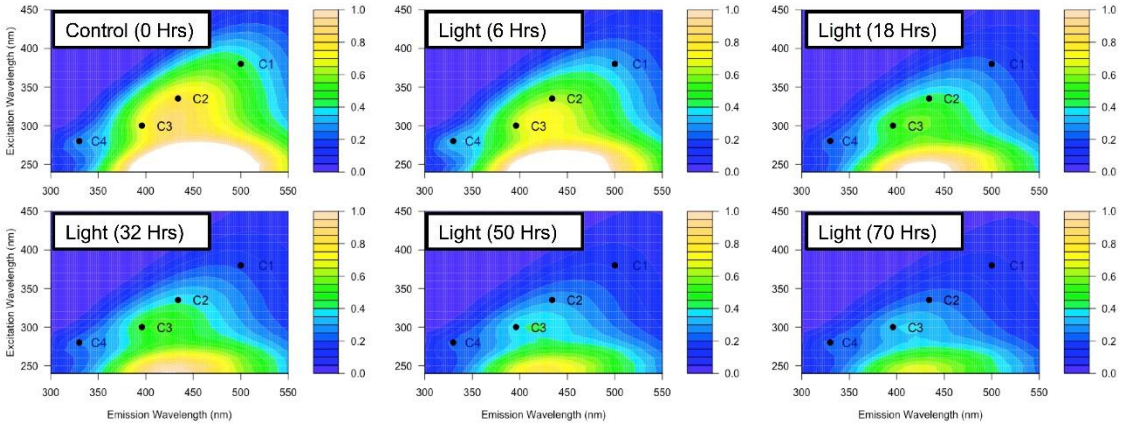

Figure 3.9 Photo bleaching of DOM is observed in EEMs after 70-hrs of natural sunlight exposure.

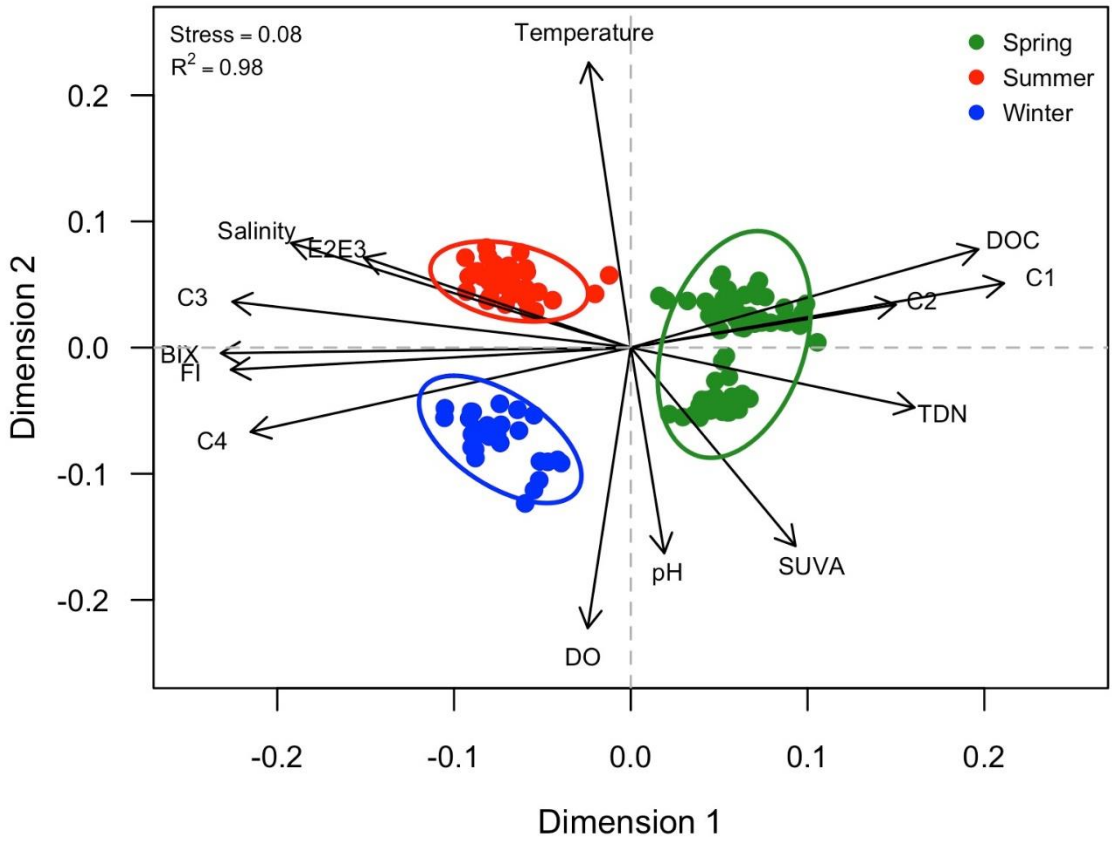

Figure 3.10 Non-metric dimensional scaling (NMDS) ordination of DOM concentration (DOC and TDN), PARAFAC modeled composition (C1-C4), DOM metrics (optical indices), and hydrographic parameters.

Table 3.4 Correlation analysis of four PARAFAC components, DOM concentration (DOC and TDN) and quality descriptors, and hydrographic parameters measured in lower Pearl River estuary.

Variables	C1	C2	C3	C4	DOC	TDN	SUVA	FI	BIX	E2:E3	Temp	Salinity	DO	pH
C2	**0.73**													
C3	**-0.88**	-0.58												
C4	**-0.83**	-0.57	**0.87**											
DOC	**0.76**	0.43	**-0.82**	**-0.87**										
TDN	0.63	0.36	-0.69	-0.65	0.60									
SUVA	0.37	—	-0.53	-0.25	—	0.37								
FI	**-0.91**	-0.58	**0.95**	**0.88**	**-0.86**	-0.64	-0.46							
BIX	**-0.90**	-0.66	**0.98**	**0.92**	**-0.84**	-0.67	-0.45	**0.96**						
E2:E3	-0.69	-0.42	**0.71**	0.50	-0.43	-0.62	-0.64	0.67	0.66					
Temp	—	—	**0.18**	—	0.18	-0.26	-0.64	—	—	0.31				
Salinity	-0.68	-0.52	**0.77**	0.65	-0.55	-0.56	-0.58	**0.78**	**0.79**	0.64	0.26			
DO	-0.39	-0.27	—	0.38	-0.41	—	0.48	0.28	0.20	—	**-0.85**	—		
pH	—	—	—	0.17	-0.21	—	0.49	—	—	-0.41	-0.71	-0.30	0.59	
Discharge	0.31	0.26	-0.61	-0.58	0.48	0.47	0.45	-0.52	-0.62	-0.26	-0.36	-0.54	0.28	—

All the correlations are significant at the alpha = 0.05 level. "Bold" represents "Strong" ($r \geq 0.70$) correlation. Non-significant correlations at alpha = 0.05 are represented as "—".

3.4.2 Seasonal distributions of DOM concentration and composition

DOC and TDN concentrations and optical proxies measured for lower Pearl River estuarine waters during spring, summer, and winter seasons are summarized in Table 3.1. Increases in discharge and faster runoff with shorter flushing times have resulted in increases in DOM concentrations in various estuarine waters (Duan et al. 2007a; Petrone et al. 2011; Bittar et al. 2016). The same phenomenon, freshwater discharge and flushing time influencing DOM concentration and composition were also observed in this study throughout the sampling period (Fig. 3.3). DOC and TDN concentrations were highest during spring high discharge periods. Following the patterns of DOC concentration, the concentrations of two humic-like DOM components, C1 and C2, were also highest during spring and showed highly humic and aromatic character marked by higher HIX and $SUVA_{254}$ values that was presented in Table 3.1. Previous studies associated high DOM concentrations and humic and aromatic character to high discharge (Duan et al. 2007a; Duan and Bianchi 2007; Bittar et al. 2016; Leech et al. 2016). During high discharge following precipitation events, terrestrial organic materials flush out from near-stream or riparian zones that could potentially contribute to high DOM levels in streams (Buffam et al. 2007; Singh et al. 2014; Osburn et al. 2015). Condensed, high molecular weight humic-rich organic materials from riparian soils with strong light absorption characteristics usually dominate this DOM in streams. Significantly high levels of this type of DOM were observed in spring, which corresponded with high discharge in spring (Fig 3.3). DOM from riparian soils and sediments were attributed to the occurrence of high concentration in component C1. Component C2 has been found to have spectral signatures similar to fluorescence organic matter derived from terrestrial landscape

potentially from the degradation of vascular plants detritus and dead animal tissues. High concentrations of component C2 in spring are again attributable to runoff post precipitation events. Additionally, the optical proxies FI, BIX, and E2:E3 that are indicative of autochthonous DOM of microbial origin were low in spring. Additionally, reduced levels of components C3 and C4 also indicate lower concentration of microbial and/or autochthonous DOM during the spring season in this study. Numerous studies have found high levels of DOM of terrestrial inputs to be associated with DOM of high humic and aromatic character (Duan et al. 2007a; Mann et al. 2012; Bittar et al. 2016; Leech et al. 2016). Results from this study are consistent with these previous studies in estuarine waters and suggest that the shorter flushing times in spring after precipitation events reduced the time for biogeochemical processing of DOM. This significantly affected the allochthonous DOM pool allowing unaltered allochthonous organic materials to be flushed and transported through the Pearl River estuary (Duan and Bianchi 2006; Paerl et al. 2006; Duan et al. 2007a; Cai et al. 2016).

Shifts in DOM concentration and quality (i.e., optical properties) and lower concentrations in DOC and TDN were observed in the low discharge periods in summer and winter, which suggest that DOM character changed from terrestrial to microbial and/or autochthonous origin. In addition to being lower in concentrations than the spring, during summer and winter the DOC and TDN concentrations showed an inverse pattern. DOC levels were higher during summer than winter while TDN levels were higher during winter than summer. Microbial humic-like DOM (C3) was high during low discharge indicating high microbial activity during summer. Additionally, both FI and BIX showed similar high levels during low discharge periods (both summer and winter)

indicating higher microbial and/or autochthonous origin of DOM (Fig. 3.4). During summer, high temperatures promote increased microbial activity and autochthonous production in streams, therefore, the shift from more allochthonous DOM during spring to more microbial and/or autochthonous DOM during summer was observed in this study. It is attributable to summer temperatures and lack of much precipitation causing low discharge. Lack of precipitation during summer increases residence time of water in stream channels and allows for substantial autochthonous production and degradation of DOM either by heterotrophic activity or by photochemical processes (Stedmon et al. 2007; Vazquez et al. 2010; Chen et al. 2013b). Increases in FI, BIX, and SR values with corresponding decrease in HIX and $SUVA_{254}$ values along with DO (< 2 mgL^{-1}) suggest the occurrence of low molecular weight autochthonous DOM and increased microbial activity during summer (Table 3.1). Other studies have reported that phytoplankton primary production and exudation in addition to Spartina leachates contribute to the autochthonous sources of DOM within the marshy estuarine systems (Maie et al. 2006a; Maie et al. 2006b; Singh et al. 2010a; Wang et al. 2014; Ya et al. 2015; Bittar et al. 2016). For example, Wang et al. (2014) showed greatest leaching of Spartina derived DOM during summer. According to these authors Spartina leachates are an important source of organic materials that promote secondary productivity in estuaries dominated by saltmarsh systems. Thus, high average salinity during summer may suggest DOM import from coastal waters. Additionally, benthic algae covering the marsh sediments also contribute to algal DOM via leaching into the water column (Roelke et al. 2006; Petrone et al. 2011). Results of this study are in line with previous studies that suggest

elevated primary production during the summer dry season in the lower Pearl River estuary (Duan and Bianchi 2006; Duan et al. 2007a; Duan and Bianchi 2007).

Photochemical processes play an important role in modifying DOM character during summer periods. However, photochemically induced break-up of DOM molecules depends on its composition or photo-reactivity and on its exposure to ultraviolet (UV) radiations (Helms et al. 2008; Vähätalo et al. 2011; Helms et al. 2013; Yamashita et al. 2013). For instance, Helms et al. (2008) reported an increase in S_R values within the Delaware estuary ranged from a terrestrial value of 0.88 in the river to a near-shore estuarine value of 1.32 at the bay mouth of the river due to photo bleaching of natural water. A higher S_R value during summer (1.04 ± 0.08) dry period compared to lower S_R value in spring (0.80 ± 0.04) suggested high rates of photo bleaching of DOM during summer in the lower Pearl River estuary. However, to confirm this, a mesocosm experiment was conducted, which is discussed in detail in the next section (section 3.4.2).

Protein-like DOM (C4) showed highest levels during winter indicating increased nitrogen constituents in the DOM pool. Numerous studies have reported high levels of nitrogen-rich DOM and reduced microbial activities during winter as a result of decline in nutrient uptake due to decreased temperatures, which inhibits microbial activity (Mulholland and Hill 1997; Cronan 2012). Unlike these studies, Duan and Bianchi (2007) observed an increased concentration of amino acids in the eastern branch of Pearl River during the summer dry period. Increased protein-like DOM increases amino acid concentrations and microbes mediate both the both production and consumption processes of protein-like materials (Maie et al. 2012; Yang et al. 2016). For example, Maie et al. (2012) in a study in Florida Bay found the production of protein-like

component at higher salinities that could be ascribed to increased microbial activity. Moreover, the protein-like component was as ascribed to biologically derived labile organic materials (Yamashita and Tanoue 2003; Kowalczuk et al. 2010) that could be degraded primarily through microbial processes (Cawley et al. 2014; Hansen et al. 2016). Particularly, the protein-like fluorescence signature was associated with undegraded polyphenols known to be present in vascular plants (Beggs and Summers 2011; Hansen et al. 2016). Therefore, high levels of protein-like DOM during winter are observed from two possible explanations in this study. Firstly, by release of nitrogen-rich organic matter from riparian soils when microbial activity is dormant and nutrient uptake is reduced. The other plausible explanation of high levels of protein-like fluorescence during winter could be attributed to flushing of undegraded vascular plant detritus into the stream channels. While DOM descriptor (e.g., BIX) supported the evidence of import of fresh organic materials to show seasonality during winter, elevated levels of DO and pH were also observed as prominent features during winter, which is suggestive of increased autochthonous production and contribution from Spartina leachates contributed increasingly to the DOM pool during summer.

Two terrestrial humic like components, C1 and C2, and DOC concentration showed a non-conservative relationship with salinity (Fig. 3.7). As salinity increased, the abundance of these DOM components along with DOC concentration declined sharply but non-linearly. The non-conservative relationship between humic-like DOM and salinity could be in part due to mixing of freshwater with saline coastal waters (Milbrandt et al. 2010; Guéguen et al. 2016). Settling of DOM molecules due to flocculation and adsorption in saline waters during summer could also substantially decrease the amount

of humic-like DOM in water column (Uher et al. 2001; Wachenfeldt et al. 2008; Cai et al. 2013). Also, microbial decomposition of refractory DOM in aquatic ecosystems owing to priming effect may cause degradation of humic-rich riverine organic material in coastal waters. This process supports the hypothesis that the supply of labile organics facilitates microbial degradation of refractory DOM (Guenet et al. 2010; Bianchi 2011; Catalán et al. 2015). Under experimental conditions, Blanchet et al. (2017) observed contrasting effects of adding labile substrates to fuel microbial decomposition of riverine DOM. The authors did not notice any occurrence of priming effect on riverine DOM exported from Rhone River into the Mediterranean Sea via Gulf of Lion. Opposite to the fate of humic-rich organic material, microbial DOM character increased with increasing salinity indicating enhanced microbial activity on DOM during summer and winter. Yamashita et al. (2008) reported high concentration of a similar DOM component at the low-salinity range in a study in Ise Bay, Japan. The fluorescence level of microbial DOM component steadily increased along the salinity gradient and a maximum value was observed at middle medium salinity range (salinity < 20) in their study. This is also evidenced from the relationship of increased FI levels with increasing salinity (Fig. 3.7). Therefore, it can be concluded that increased microbial activity during summer may have reduced the humic-like materials stimulated by high temperature in this study when more labile substrates were available either from primary production or from bacterial activity.

DOM concentration, composition, and quality indices exhibited a consistent temporal pattern in the lower Pearl River estuary in this study as expected. NMDS analysis clearly showed the temporal variability in DOM properties and hydrographic parameters (Fig. 3.10). Using a similar technique, Catalan et al. (2013) separated the

winter-spring and fall samples in Mediterranean ephemeral washes. Although the results in this study are in line with the findings of Catalan et al. (2013) as the occurrence of humic-rich high molecular weight DOM followed the precipitation and runoff patterns during fall. The authors observed more labile and recently produced DOM during winter and spring periods as opposite to the occurrence of humic-rich aromatic DOM in spring found in this study. This further suggests that hydrologic conditions in the watersheds are primary controls of DOM characteristics (Vazquez et al. 2010; Catalán et al. 2016). Strong positive correlations between the components C1, C2, and DOC concentrations were observed in spring (Table 3.4). While summer and winter DOM concentrations and compositions were controlled by hydrographic parameters, high temperature levels influenced DOM properties during summer and increasing DO and pH influenced DOM properties during winter. Based on this, it can be concluded that more bioavailable DOM was present during summer and winter in the lower Pearl River estuary during low discharge periods in the study region (Duan et al. 2007a; Duan and Bianchi 2007). Moreover, DOM descriptors (e.g., FI and BIX) displayed the increasing influence of microbial activity on DOM properties during low discharge conditions. However, high negative correlations between BIX and FI with C1 suggest that DOM originated from riparian soils was more susceptible to microbial breakdown in the river. This finding contrasts with traditional understanding where terrestrial organic matter is supposedly highly refractory and may not be suitable for microbial processing (Wehr et al. 1997; Stubbins et al. 2010). However, results of this study suggests otherwise and in line with some recent studies those have suggested high photochemical and biochemical transformation of terrestrial DOM with high bio-reactivity depending upon the quality of

DOM (Bushaw-Newton and Moran 1999; Milbrandt et al. 2010; Bianchi 2011; Catalán et al. 2013). Furthermore, high discharge periods showing positive correlations with humic-rich DOM compositions in this study suggests that this DOM was transported following precipitation events and could be available for rapid biochemical changes during low flow conditions. In contrast, negative correlations shown between discharge and microbial humic-like DOM further suggested that during low discharge periods, microbes get sufficient time to breakdown the terrestrial inputs (Table 3.4). Photochemical breakdown of these high molecular weight DOM molecules also contributed in addition to cleaving mediated by microbes (Spencer et al. 2009; Shank et al. 2011; Meng et al. 2013). Interestingly, the strong negative correlations between component C1 and C3 showed that the source material of C3 is perhaps the same as that of C1 (e.g., riparian soils), which is highly susceptible to photochemical and microbial degradation and hence an increase in microbial humic DOM was observed with concurrent decrease in C1 component.

3.4.3 Photo-reactive DOM compositions during summer

The primary constituents of DOM in black water streams are terrestrial humic-rich and aromatic organic materials that are generally considered as refractory, aged, diagenetically modified and resistant to further microbial degradation (Hernes et al. 2008; O'Donnell et al. 2010; Leech et al. 2016). However, photolysis can degrade such DOM molecules where chromophoric fractions of DOM are destroyed upon absorption of ultraviolet (UV) radiation, which results in decreased light absorption capabilities of DOM molecules. Indeed, carbon mineralization via photochemical degradation of DOM is considered as a significant mechanism. However, the rate of mineralization of carbon

generally depends on its composition or photo-reactivity (Obernosterer and Benner 2004; Yang et al. 2014). For example, Obernosterer and Benner (2004) in an experimental study showed that photo- and bio-mineralization accounted for the removal of 46 and 27% of terrestrial DOM from a black water river system in South Carolina. In comparison, results from this study suggest that terrestrial fluorescence signatures declined to 70-75% (C1 and C2) of its pre-irradiation values (Table 3.3; Figs. 3.8 and 3.9). Nevertheless, the photo-bleaching rates computed in this study were very similar to DOM photo-bleaching rates reported in other estuarine and coastal environments (Shank et al. 2005; Shank et al. 2009; Spencer et al. 2009; Shank et al. 2010; Chen and Jaffé 2014).

The component C3 decreased to roughly 50% of its pre-irradiation levels, which suggests that this type of DOM is both being produced and also consumed during the course of the experiment. Furthermore, a strong inverse correlation between C1 and C3 suggests that C3 may have been produced by the decomposition of C1 (Table 3.3). This finding is consistent with Chen et al. (2013a), where the authors have noticed the production of a microbial-humic like DOM at the expense of a terrestrial DOM from diffuse soil sources in a photo-bleaching experiment with samples from Yangtze River, China. Similar to the findings of this study, Chen and Jaffé (2014) observed the production of a fluorescence component similar to microbial humic-like component (C3) while assessing the effects of photo- and bio-reactivity of DOM from biomass, soil leachates and surface waters in a subtropical wetland. Contrasting to these results, Lønborg et al. (2010) reported the production of microbial humic-like substances as a by-product of the microbial metabolism in the coastal upwelling system of the Ría de Vigo,

Spain. The authors attributed the production of this type of DOM to the degradation of protein-like labile DOM from the observation of inverse relationships of DOC and protein-like DOM with this component. In another study, a comparison of the rates of photo bleaching, it was found that relative amounts of fresh DOM from mangrove leaves and Sargassum declined faster in comparison to other terrestrial or marine DOM (Shank et al. 2010). These studies suggest that the production of microbial humic-like DOM can occur from both the terrestrial and autochthonous sources. However, results from this study supports the findings of Chen et al. (2013a), as the lower Pearl River system transports increased levels of terrestrial material after precipitation events than the contributions from autochthonous material.

It is well recognized that the photo bleaching of DOM in natural waters lead to increased absorption spectral slope ($S_{275-295}$), spectral slope ratio (S_R) and E2:E3 ratio (Helms et al. 2008; Zhang et al. 2009; Helms et al. 2013; Chen et al. 2013a; Santos et al. 2014). For instance, Helms et al. (2013) reported increases in spectral slope ratio (S_R) and spectral slope ($S_{275-295}$) values from 2.14 to 8.92 and 19 to 39 (μm^{-1}), respectively in a 68-day photo bleaching experiment of Hawaiian Pacific Ocean samples. Additionally, Santos et al. (2014) observed increases in S_R, $S_{275-295}$, and E2:E3 from 0.80 to 1.01, 7.21 to 8.23 (μm^{-1}), and 6.51 to 7.60, respectively in samples from the estuary Ria de Aveiro in Portugal while conducting the 12-h photo bleaching mesocosm experiment on the rooftop of their laboratory. While values for these parameters for the lower Pearl River estuary were not as high as the values of the above two studies, these parameters showed a similar pattern of increases in S_R, $S_{275-295}$, and E2:E3 values from 0.90 to 1.45, 14 to 18 (μm^{-1}), and 4.40 to 5.37, respectively (Table 3.3). Thus, it is evident from these results

that photo bleaching of DOM caused by UV radiation in natural waters can occur to a considerable degree and could decrease the molecular weight of DOM molecules at least during summer as found in this study (Fig. 3.9). Considering the important role of photochemical degradation process during summer in lower Pearl River estuary, cautious approach in budgeting DOM flux and loads from this system to receiving coastal margins is suggested.

3.4.4 Conceptual DOM model for the lower Pearl River estuary

A conceptual DOM model that integrates the observations of DOM concentration and composition for varying hydrologic conditions and processes that regulate the supply and/or inputs of DOM in the lower Pearl River estuary is presented (Fig. 3.11). In spring, surficial flow paths during high discharge conditions following precipitation events mobilize and transport relatively higher amounts of DOM from carbon rich riparian soils. During summer, elevated temperatures facilitate higher autochthonous production of DOM with simultaneous photochemical and biogeochemical degradation processes for DOM breakdown. The dominant high discharge conditions during spring yield elevated DOC concentrations and the DOM character is highly humic and aromatic. Contrary to this pattern, low discharge conditions during summer and winter yield more microbially generated DOM. Additionally, photo bleaching of DOM during summer plays an important role in breaking down the large molecules and reducing the overall molecular weight of DOM. This also suggested a preferential removal of DOM of terrestrial origin by photochemical processes. The concentration and composition of DOM for spring precipitation events was the highest while the concentration and composition for winter had values between the seasonal extremities of summer and spring. Seasonal patterns of

DOM with hydrologic conditions suggest the occurrence of more labile DOM during summer and winter in contrast to increased levels of refractory DOM in spring. While the lability of DOM during summer is associated with photolysis, higher marine influence facilitates the lability during winter.

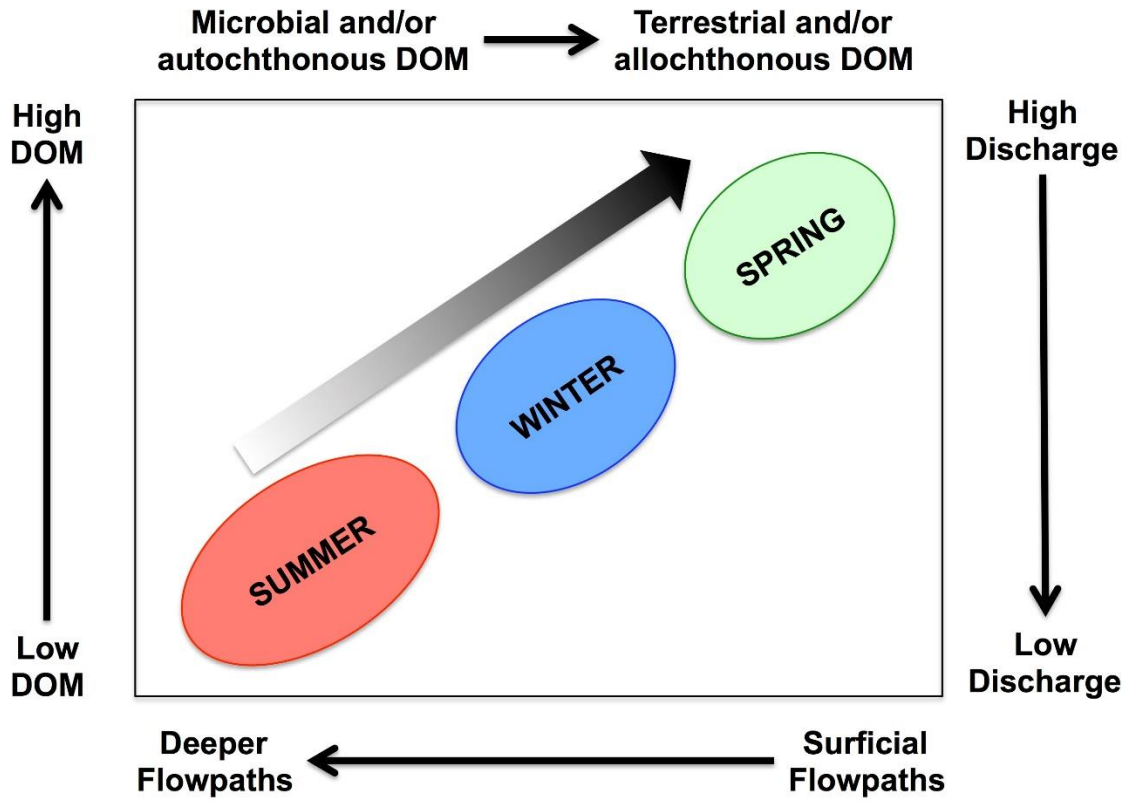

Figure 3.11 A conceptual model for DOM dynamics with varying hydrologic and climatic conditions in the lower Pearl River estuary.

3.5 Conclusions

This study examined the seasonal distribution of DOM concentration and composition in the lower Pearl River estuary while utilizing the EEM-PARAFAC modeling approach. The EEM-PARAFAC model identified four unique DOM

components from 148 EEM scan measured for water samples collected during the winter 2015, and spring and summer of 2016. These four distinct fluorescence groups of DOM consisted of two terrestrial humic-like components, C1 and C2, one microbial-humic like, C3, and one protein-like (tryptophan-like) component, C4. Considering the significant negative relationships between the components, C1 and C2, with salinity, this study showed that the two humic-like components were originated from terrestrial sources such as riparian soils and vascular plant detritus. The significant positive relationship between the components, C3 and C4, with salinity indicated the DOM generation by primary production and microbial activity. However, the most dominant control of seasonal DOM character in the lower Pearl River estuary was the hydrologic condition, especially in spring. DOM destruction via photolysis played an important role in controlling DOM concentration and composition during summer. These findings helped in understanding the DOM dynamics in the lower Pearl River estuarine system, where short precipitation pulses and photochemical reactions control the biogeochemistry of DOM. This in turn, controls the supply and fate of important chemical constituents such as carbon and nitrogen (e.g., C and N fractions of DOM) from terrestrial origin to the receiving coastal waters.

This study further implies that understanding the role of DOM biogeochemistry is imperative for future climate change scenario. Increased levels of terrestrial DOM is expected to leach in river systems and mix with microbial DOM with increasing global temperatures and increasing extreme weather events (Bittar et al. 2016). This may in turn alter the DOM concentrations and compositions substantially and may significantly impact the DOM biogeochemistry in coastal waters. Expected precipitation patterns

associated with future climate change for the southeast US for the next century may also shift the regime for saline water intrusions in the coastal areas (Seager et al. 2009). Additionally, increased drought severity and/or precipitation (both intensity and duration) patterns in addition to hydrological discharge are expected to change for the southeast US (Ingram et al. 2013; Walsh et al. 2014). Therefore, interactions between hydrologic discharge from coastal rivers and carbon and nutrient biogeochemistry is important to understand in estuarine systems for improved prediction and management of aquatic systems in response to climate-induced changes in the southeast US.

CHAPTER IV

COMPARISON OF THE SPATIAL AND TEMPORAL DISTRIBUTIONS OF DOM IN THE GANGES RIVER, INDIA AND THE PEARL RIVER, USA

4.1 Introduction

Rivers are the major transporter of dissolved organic matter (DOM) from terrestrial landscapes to the oceanic environments. In fact, DOM is the largest reactive reservoir of reduced carbon on the Earth surface and an integral component of riverine material transport (Cole et al. 2007; Battin et al. 2008; Para et al. 2010). Since rivers are the main conduits of DOM transport, their role in modulating the characteristics of DOM is receiving wide attention globally. The DOM composition in rivers flowing through forested watersheds or through watersheds having natural landscapes as the dominant land cover would be different than the rivers flowing through a watershed that dominantly contributes pollutants from anthropogenic sources such as sewage effluents from municipalities, industrial, and agricultural wastes (Paerl et al. 2006; Jaffé et al. 2008; Naden et al. 2010; Baghoth et al. 2011; Jaffé et al. 2012; Meng et al. 2013; Chen and Jaffé 2014). All these organic material once enter the river system are further transformed in varying degrees depending on their reactivity levels. For instance, microbial metabolic activities transform organic carbon to carbon dioxide via respiration that is then either stays dissolved in the water or released from the rivers to the atmosphere (McKnight et al. 2002; McKnight et al. 2003; Battin et al. 2008; Butman and

Raymond 2011). Globally, it has been estimated that world's major rivers transport 0.25 $PgCyr^{-1}$ terrestrial dissolved organic carbon to coastal oceans, which is comparable to CO_2 emissions, ranging from 0.7 to 3.3 $PgCyr^{-1}$ from freshwater systems to the atmosphere (Hedges et al. 1997; Battin et al. 2008; Osburn et al. 2016).

While an array of biogeochemical and physicochemical processes control DOM cycling in rivers, its composition or quality actually determine the fate of DOM in aquatic ecosystems. Many biogeochemical and ecological functions of DOM depend on its quantity and quality (Engelhaupt et al. 2003; Battin et al. 2008; Bianchi 2011; Cory et al. 2011; Jaffé et al. 2014). For example, DOM in aquatic systems provides carbon and energy sources for the microbial growth and reproduction (Coble 2007; Coble 2008). DOM also attenuates damaging UV radiations thereby protects phytoplankton and other organism (Del Vecchio and Blough 2004; Del Vecchio and Blough 2006; Coble 2008). Sometimes DOM forms complexes with toxic elements and heavy metals (Brooks et al. 1999; Bolan et al. 2004; Yates et al. 2016). DOM is an ecologically important chemical component that plays a vital role in many physical, chemical and biological processes in aquatic ecosystems, thus it is important to understand its reactivity and distribution within a given system.

As it is clear that reactivity of DOM depends on its composition, it is important to determine the composition at the molecular level. However, due to the complexity of analytical techniques and heterogeneity of the DOM pool, at this point only a small fraction (roughly 20%) of the total DOM can be identified at the molecular level (Gremm and Kaplan 1998; Bolan et al. 2011; Cory et al. 2011). Therefore, earlier studies have operationally divided the DOM pool into two major fractions, humic and non-humic (or

labile) fractions of DOM (Gremm and Kaplan 1998; Wang et al. 2009; Watanabe et al. 2012). Determining these fractions using biochemical methods is expensive and time-consuming, hence optical analysis serves as an excellent alternative to determine these fractions cheaply and in a rapid manner. These optical techniques do not require any chemical treatments and offers the best solution for quick determination of DOM properties in many aquatic ecosystems. Small amounts of samples are generally required for optical determination of water sample constituents (Cory et al. 2011; Chen et al. 2013b; Jaffé et al. 2014). Because of these advantages, recent absorption and fluorescence measurement techniques have received wide attention and have been used in a variety of aquatic systems (Coble et al. 1990; Coble 2007; Cory et al. 2010; Fellman et al. 2010a). Furthermore, the combination of UV-Vis absorption and fluorescence excitation-emission matrices (EEMs) in conjunction with multivariate statistical techniques such as parallel factor analysis (PARAFAC) offers a reliable tool for tracking sources of dissolved organic materials from terrestrial and/or aquatic systems (Stedmon et al. 2003; Stedmon and Bro 2008; Jaffé et al. 2014). These techniques help in tracking biogeochemically and ecologically important processes such as microbial and photochemical degradation of DOM in many aquatic ecosystems (Fellman et al. 2010b; Chen and Jaffé 2014; Schiebel et al. 2015). Despite being limited in classifying the fluorophore groups to molecular levels in greater detail at the moment, these techniques are developing very fast and being employed by researchers in wide environments. Nonetheless, as stated above, classification of DOM molecules in two broad categories of humic and non-humic groups are clearly separable using these techniques and hence

allow researchers to quickly determine the concentration and composition of DOM in a variety of aquatic environments.

The character and abundance of DOM in large river systems warrant greater attention, especially where anthropogenic processes are contributing to a greater amount of DOM (Dalzell et al. 2007; Hanley et al. 2013). The Ganges River basin is one of the most densely populated river basins in the world. The population in the Ganges River basin is roughly 500 million when the population of both India and Bangladesh in the basin is considered (Sharma 1997; Singh and Singh 2007; Das and Tamminga 2012). Also, the Ganges River basin is home to more than 25,000 wildlife species. The river has experienced severe degradation in its water quality over the years as a result of human activities such as construction of dams, industries, and domestic, municipal and industrial waste discharges (Singh and Singh 2007; Sharma et al. 2016). For the improvement of the water quality of this large river, the Ministry of Environment and Forest, Government of India, initiated a comprehensive project, the Ganga Action Plan (GAP), in 1985 (Singh and Singh 2007; Das and Tamminga 2012). Unfortunately due to poor environmental planning and too much bureaucracy, the GAP has achieved little success in accomplishing the planned goals of prevention of pollution and improvement of water quality (Das and Tamminga 2012; Pandey 2013; Sharma et al. 2016).

The present study aims to evaluate the characteristics of DOM in the highly urbanized section of the Ganges River (in Varanasi, India) and compare those with a relatively pristine small river (Pearl River located in the Mississippi, USA) in similar climatic regime (i.e., subtropical). In addition, the temporal patterns of DOM distribution are also investigated in both the rivers. Particularly, the objectives of this study were (i)

to develop EEM-PARAFAC model for characterizing DOM composition, (ii) to assess the temporal variability of DOM in the Ganges and Pearl Rivers, and (iii) to compare the DOM abundance and distribution in these two distinctly different water bodies

The following questions were posed to answer the above stated objectives.

1. What are the temporal patterns of the DOM characteristics in a large river system?
2. How do DOM characteristics in a large river system compare against those in a small river in a different geographic regime?

4.2 Methods

4.2.1 Sampling sites and water sampling

Surface water samples were collected from multiple sample points along a highly urbanized 9-km stretch of the Ganges River adjacent to the City of Varanasi during two field-campaigns, one in the month of July 2015 and another in the month of January 2016 (Fig. 4.1). The samples were immediately frozen and kept in the cooler before they were shipped to the laboratory located at the Mississippi State University. In the Pearl River, surface water samples were collected from multiple sample points located in lower reaches of the river close to the city of Slidell, LA (Fig. 4.2). Subsequently, the water samples were filtered through a 0.2-μm filter paper (Millipore Inc., Billerica, MA, USA) and stored in a refrigerator at 4 °C in 100-mL amber glass bottles for UV absorbance and fluorescence measurements, and the determination of dissolved organic carbon (DOC) and total dissolved nitrogen (TDN) concentrations.

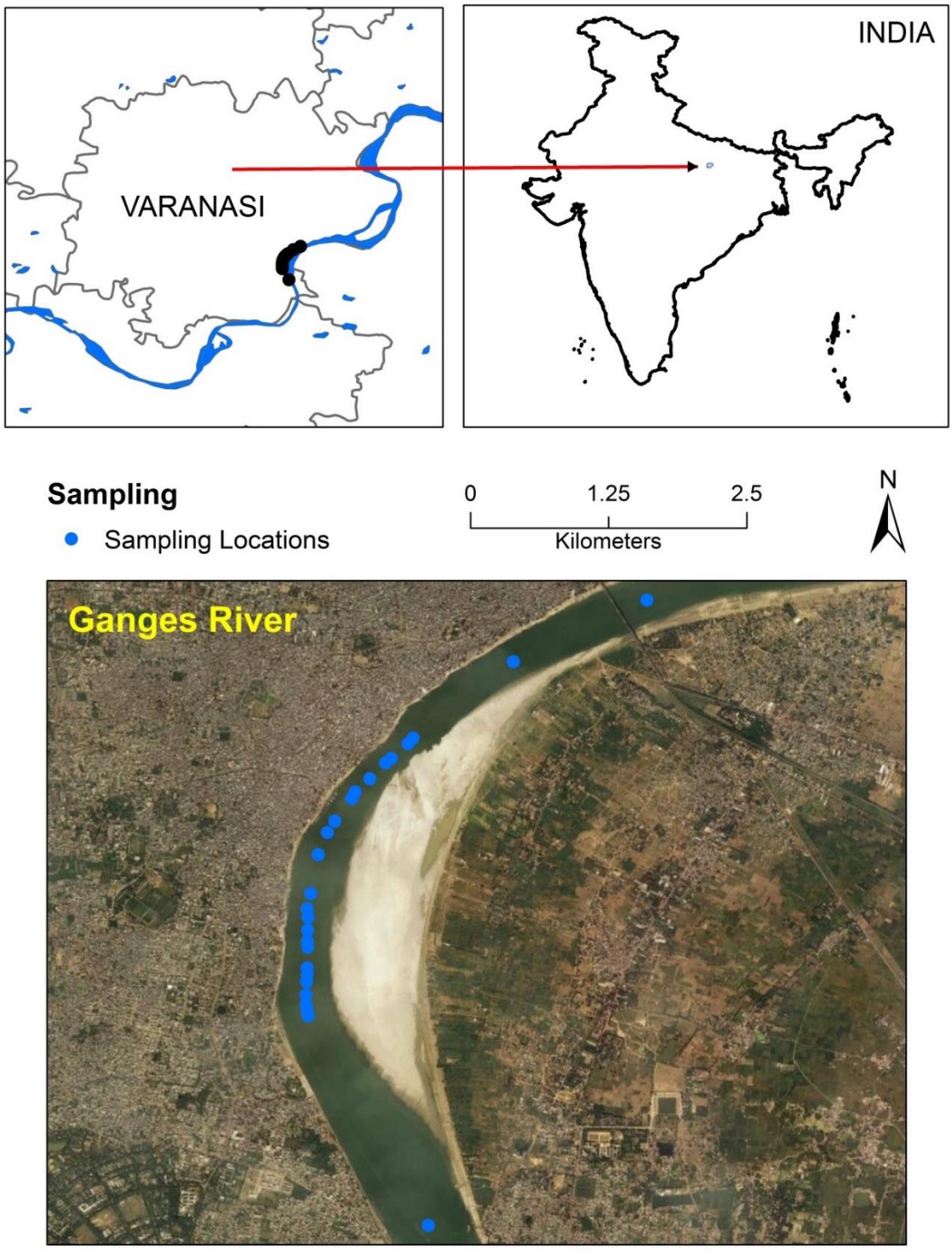

Figure 4.1 Sampling along a 9-km transect in the Ganges River at Varanasi, India. Surface water samples were collected in two field campaigns (July 2015 and January 2016).

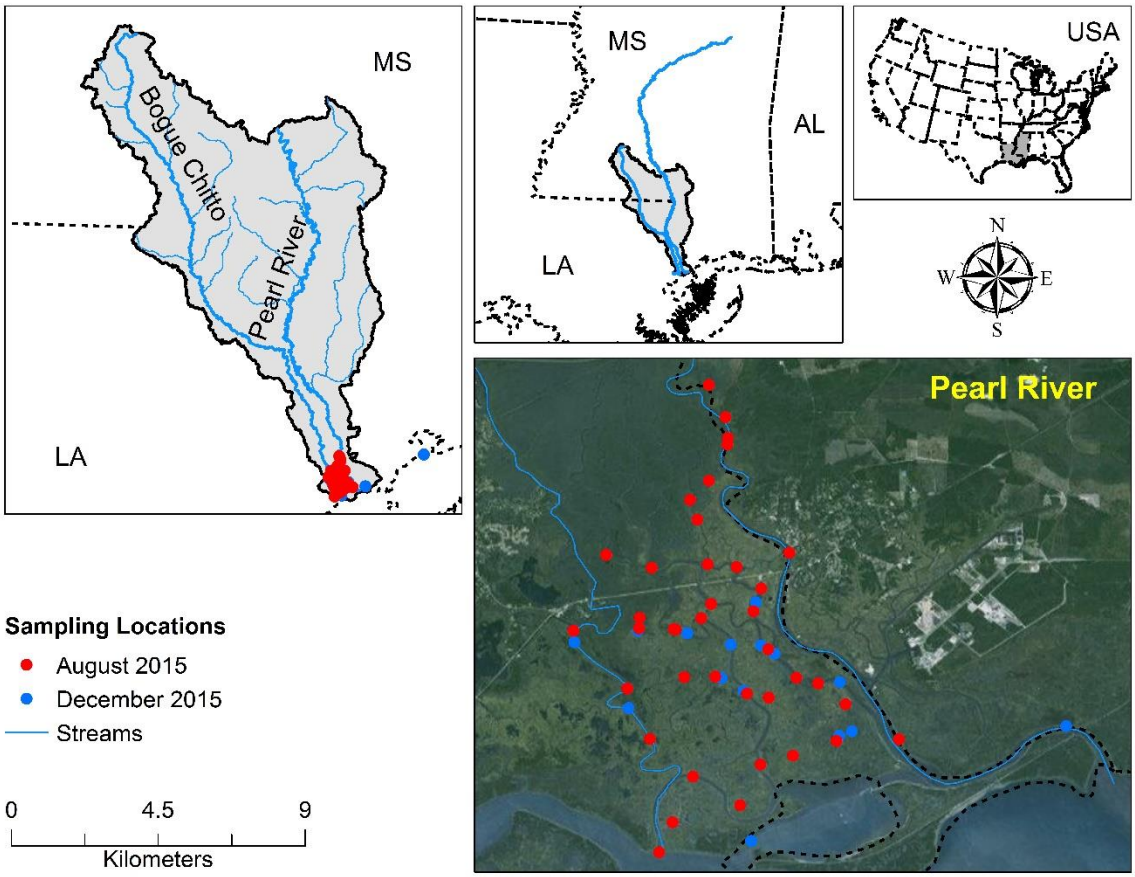

Figure 4.2 Sampling locations in the Pearl River close to the city of Slidell, LA during two-weekly field campaigns (August 2015 and December 2015).

4.2.2 DOC and TDN measurements

DOC concentrations were measured using high-temperature catalytic oxidation (HTCO) and TDN concentrations by oxidative combustion chemiluminiscence, respectively, on a Shimadzu TOC-VCSN (Shimadzu Scientific Instruments, Columbia, MD) coupled with a TN analyzer unit. The coupled system allowed simultaneous determination of DOC and TDN in the same sample using a single injection and provided low detection limits and appreciable linear ranges for both DOC and TDN. Measurements were determined with a precision of < 2% for both DOC and TDN (Lu et

al. 2013; Lu et al. 2014a). DOC and TDN concentrations were not measured on the July samples collected from the Ganges River due to lack of enough sample volumes.

4.2.3 Absorption and EEM-PARAFAC analyses

DOM absorption spectra were determined with a PerkinElmer Lambda 850 double-beam UV-Vis spectrophotometer (PerkinElmer, Inc., Waltham, MA, USA), with a 1cm quartz cuvette. Particle-free Nanopure Milli-Q water was used as the blank. The scanning wavelength range was 200-750 nm with a spectral resolution of 2 nm. Absorbance (A) was converted into absorption coefficient (a in m^{-1}) using the following expression:

$$a(\lambda) = \frac{2.303 * A(\lambda)}{L} \quad 4.1$$

where λ is the wavelength and L is the path-length in meters (Dash et al. 2015; Singh et al. 2017).

EEM scans were obtained using a Fluoromax-4 spectrofluorometer (Horiba Jobin Yvon, Inc., Edison, NJ, USA) and fluorescence emission spectra from 300-550 nm at every 2 nm intervals were recorded for excitation wavelengths ranging from 240-450 nm with increments of 10 nm. The EEM scans were collected in ratio mode (S/R mode) with dark offset and a bandwidth setting of 5-nm for both the excitation and emission. The EEMs were corrected for all biases including instrument bias, inner filter effects, and blank subtraction as suggested by previous studies (Cory et al. 2010; Miller et al. 2016; Singh et al. 2017). Subsequently, the EEM scans were normalized to daily-analyzed water Raman integrated area under maximum fluorescence intensity (Ex-350/Em-397, 5-

nm bandwidth) as proposed by Lawaetz and Stedmon (2009) to normalize the EEM data to comparable Raman units (R.U.; nm^{-1}).

A total of six DOM indices were calculated, three indices were computed using absorption measurements (i.e., a_{254}, S_R, and E2:E3) while the other three were computed using fluorescence measurements (BIX, FI, and HIX). The absorption coefficients (a_{254}) were measured using absorbance (*A*) at wavelength 254 nm from the absorption spectra. This index was used to estimate aromatic content of total DOM (Weishaar et al. 2003). Spectral slope ratio, S_R was calculated as a ratio between two spectral slope regions: S1 (275-295 nm) and S2 (350-400 nm) according to Helms et al. (2008). The E2:E3 ratios were calculated as the absorbance measured at two wavelengths, 250 and 365 nm, respectively (Santos et al. 2016). These two indices were calculated to estimate the relative molecular weight of DOM. McKnight et al. (2001) developed a fluorescence index (FI) to differentiate precursor DOM sources (i.e., aquatic versus terrestrial). This index is calculated as the ratio of fluorescence emission intensity at 470 and 520 nm with an excitation at 370 nm, which provides a measure of the steepness and shape of the emission intensity peak (Cory and McKnight 2005). The biological index (BIX) was measured as the ratio of fluorescence emission intensity at 380 nm divided by the emission intensity maximum observed between 420 and 440 nm, obtained at excitation 310 nm (Huguet et al. 2009; Wilson and Xenopoulos 2009). This index, also known as freshness index, is an indicator of the contribution of fresh DOM originating from autochthonous production or biological activity (Wilson and Xenopoulos 2008; Wilson and Xenopoulos 2009; Singh et al. 2015) and has been determined for many ecosystems (Huguet et al. 2009; Singh et al. 2010; Duan et al. 2015; Singh et al. 2017). Humification

index (HIX) was computed as the ratio of the peak integrated area under the emission spectra 435-480 nm and the total sum of peak integrated area under the emission spectra 300-345 nm and 435-480 nm obtained at an excitation wavelength of 254 nm (Ohno 2002). An increase in HIX is associated with condensation of fluorescing molecules and a decrease in the H/C ratio is considered to be an indicator of humification (Zsolnay et al. 1999; Zsolnay 2003).

A total of 85 EEMs were modeled using PARAFAC with MATLAB 7.12 and DOMFluor toolbox (ver., 1.7; Feb., 2009) (Stedmon and Bro 2008; Singh et al. 2010; 2017). EEM spectra were decomposed into five individual fluorescent components (C1-C5) by PARAFAC and the number of components were determined and validated by split-half analysis and random initialization (Stedmon and Bro, 2008). The proportional contribution of each fluorescence component was calculated by dividing its fluorescence intensity, F_{max} (R.U.) to the sum of fluorescence intensities (total fluorescence) of all components. Hence, the components are reported here in $\%F_{max}$ values (Lu et al. 2013; Lu et al. 2014b). Detail information on modeling EEM scans using PARAFAC technique is discussed by Singh et al. (2010; 2014b; 2017).

All the statistical analyses were conducted and plotted with R software version 3.3.3 (R Core Team, 2017). Two-way analysis of variance (ANOVA) was used to determine the effects of sampling locations (Ganges River vs. Pearl River) and months on DOM parameters along with factor (locations and months) interactions. For sampling locations, months, and their interactions comparisons, the Tukey-HSD tests for post-hoc comparison of means procedure was performed at $\alpha = 0.05$. The null hypothesis for two-way ANOVA was that there are no significant differences in DOM properties with

sampling locations, months, and their interactions. All the correlation analyses were also conducted at $\alpha = 0.05$, and the Pearson correlation coefficients were calculated. Moreover, principal component analysis (PCA) was conducted on DOM optical data including EEM-PARAFAC model DOM components (C1-C5) and absorption and fluorescence derived DOM indices. DOM concentration (i.e., DOC and TDN) data was not included in the PCA, because of unavailability of DOC and TDN measurements for July 2015 samples in the Ganges River. Only complete cases for the optical measurements were considered for PCA in this study.

4.3 Results and Discussion

4.3.1 DOM concentrations in the Ganges and the Pearl Rivers

Spatial and temporal variations in DOC concentrations were observed in both the Ganges and Pearl Rivers. DOC ranged from 2.04-2.96 mgL^{-1} in the Ganges River and from 1.39 to 6.13 mgL^{-1} in the Pearl River (Table 4.1). The average DOC (4.06) in the Pearl River was significantly high compared to the average DOC (2.46) in the Ganges River. Additionally, the DOC concentrations were not significantly different across months in the Pearl River indicating that the source of DOC may be similar during August and December. When the DOC concentrations in the Ganges River from this study were compared with other large rivers, it was found that they were similar to that of the Mississippi River (2.67-4.56 mgL^{-1}; Duan et al. 2007) and Yangtze River in China (2.60-5.20 mgL^{-1}; Chen et al. 2013). In another study, Pandey (2013) found much higher DOC concentrations (4 to 19 mgL^{-1}) in the Ganges River along the same transect as this study but in that study the DOC concentrations were measured during the summer seasons over three year period (2009-2011). Since our summer samples could not be

processed for DOC we were not able to compare our DOC concentrations with that of Pandey (2013). In general, high DOC is expected during summer as Indo-Gangetic plain receives maximum precipitation (90%) during the monsoonal rainfall in the summer months (June-September) (Krishna et al. 2015). In comparison to the Ganges River, the average DOC value in the Pearl River (4.06 ± 0.87 mgL^{-1}) was high (Table 4.1). Similarly high DOC concentrations were reported by Duan et al. (2007a) ranging from 4.03-16.44 mgL^{-1} and by Cai et al. (2016) ranging from 3.05-12.77 mgL^{-1}. The larger variability in DOC concentration in the Pearl River is linked with hydrologic conditions in the watershed. River discharge increases in response to precipitation in the watershed, which establishes a hydrologic connection between the river channel and the flood plain facilitating DOC contribution from riparian soils and sediments to the river (Duan et al. 2007a; Duan et al. 2007b; Cai et al. 2016).

In contrast to DOC concentrations, TDN concentrations were very high in the Ganges River in comparison to the Pearl River. In the Ganges River, the average TDN concentration was 1.19 ± 0.41 mgL^{-1} while it was 0.13 ± 0.05 mgL^{-1} in the Pearl River. Similar to DOC patterns, no significant difference was observed in TDN concentrations between August and December in the Pearl River (Fig. 4.4). The average TDN concentration in this study was consistent with the relatively low concentrations reported in previous studies. For example, Cai et al. (2016) reported a TDN range between 0.19-0.68 mgL^{-1} in the lower reaches of the Pearl river and suggested that most of the nitrogen were dissolved organic nitrogen (DON) as the inorganic nitrogen may have been reduced to DON. TDN values in the present study are also comparable to TDN in the highly eutrophic coastal waters of the Maryland, USA (0.17-0.77 mgL^{-1}) (Duan et al. 2015).

TDN values in the present study are also comparable to TDN in the highly eutrophic coastal waters of Maryland, USA (0.17-0.77 mgL^{-1}) (Duan et al. 2015). On the other hand, the high TDN in the Ganges River indicated influence of anthropogenic activities, such as untreated sewage effluents or municipal wastes discharged into the Ganges River (Rai et al. 2010; Sharma et al. 2016). In a previous study, Singh (2010) reported highest TDN as 0.985 mgL^{-1} in the month of June and the lowest as 0.015 mgL^{-1} in the month of January in the Ganges River in Varanasi. In another study, Tiwari et al. (2016) reported that the nitrate value varies from 2.1 mgL^{-1} during the winter to a moderate increased value of 2.6 mgL^{-1} during the summer season. These previous studies corroborate with the TDN values of this study.

Table 4.1 Descriptive statistics for PARAFAC modeled components (C1-C5), DOC and TDN concentrations, and a suite of DOM indices measured for the Ganges and the Pearl River samples. Values are represented as Mean ± SD (N = Number of samples) and Min – Max.

	Total		Summer (July and August)		Winter (January and December)	
	Ganges River	**Pearl River**	**Ganges River**	**Pearl River**	**Ganges River**	**Pearl River**
C1	35.54 ± 3.51 (31)	45.87 ± 0.93 (51)	32.90 ± 3.42 (15)	45.84 ± 0.92 (35)	38.02 ± 0.34 (16)	45.94 ± 0.96 (16)
	28.64 – 38.86	43.59 – 47.91	28.64 – 38.86	43.59 – 47.91	37.09 – 38.58	44.83 – 47.75
C2	16.87 ± 1.33 (31)	26.59 ± 1.40 (51)	16.16 ± 1.64 (15)	25.83 ± 0.77 (35)	17.54 ± 0.26 (16)	28.23 ± 0.98 (16)
	12.66 – 18.58	24.23 – 29.71	12.66 – 18.58	24.23 – 28.04	16.64 – 17.95	25.60 – 29.71
C3	17.74 ± 5.59 (31)	5.40 ± 0.76 (51)	23.14 ± 2.51 (15)	5.87 ± 0.27 (35)	12.68 ± 0.12 (16)	4.37 ± 0.33 (16)
	12.45 – 28.09	3.73 – 6.19	19.33 – 28.09	4.84 – 6.19	12.45 – 12.82	3.73 – 4.89
C4	18.72 ± 2.88 (31)	11.45 ± 1.62 (51)	18.62 ± 4.19 (15)	12.16 ± 1.16 (35)	18.81 ± 0.41 (16)	9.91 ± 1.39 (16)
	14.26 – 26.45	8.05 – 14.34	14.26 – 26.45	8.44 – 14.34	17.66 – 19.73	8.05 – 13.21
C5	11.13 ± 2.01 (31)	10.69 ± 0.84 (51)	9.18 ± 0.83 (15)	10.30 ± 0.59 (35)	12.96 ± 0.30 (16)	11.55 ± 0.65 (16)
	7.40 – 13.90	9.20 – 12.38	7.40 – 9.95	9.20 – 12.38	12.58 – 13.90	9.40 – 12.22
DOC	2.46 ± 0.23 (16)	4.06 ± 0.87 (52)	–	3.95 ± 0.71 (36)	2.46 ± 0.23 (16)	4.32 ± 1.13 (16)
(mgL^{-1})	2.04 – 2.96	1.39 – 6.13	–	2.73 – 5.83	2.04 – 2.96	1.39 – 6.13
TDN	1.19 ± 0.41 (16)	0.13 ± 0.05 (52)	–	0.11 ± 0.03 (36)	1.19 ± 0.41 (16)	0.18 ± 0.06 (16)
(mgL^{-1})	0.79 – 2.03	0.02 – 0.29	–	0.04 – 0.17	0.79 – 2.03	0.02 – 0.29
a_{254}	15.92 ± 4.33 (33)	30.07 ± 8.50 (52)	19.20 ± 3.57 (17)	24.97 ± 2.66 (36)	12.43 ± 1.14 (16)	41.53 ± 5.15 (16)
(m^{-1})	11.55 – 31.62	21.60 – 48.59	15.47 – 31.62	21.60 – 35.85	11.55 – 15.07	33.52 – 48.59
SUVA	2.21 ± 0.21 (16)	3.39 ± 1.71 (52)	–	2.81 ± 0.40 (36)	2.21 ± 0.21 (16)	4.70 ± 2.62 (16)
($Lmg^{-1}m^{-1}$)	1.91 – 2.60	1.73 – 14.13	–	1.73 – 3.56	1.91 – 2.60	3.02 – 14.13
HIX	0.50 ± 0.19 (33)	0.71 ± 0.11 (52)	0.41 ± 0.23 (17)	0.72 ± 0.12 (36)	0.59 ± 0.06 (16)	0.68 ± 0.08 (16)
	0.05 – 0.77	0.43 – 0.89	0.05 – 0.77	0.43 – 0.89	0.50 – 0.74	0.45 – 0.82

Table 4.1 (Continued)

FI	1.70 ± 0.06 (33)	1.47 ± 0.02 (52)	1.69 ± 0.08 (17)	1.48 ± 0.01 (36)	1.71 ± 0.01 (16)	1.46 ± 0.01 (16)
	1.64 − 1.99	1.43 − 1.50	1.64 − 1.99	1.44 − 1.50	1.69 − 1.76	1.43 − 1.49
BIX	1.02 ± 0.18 (33)	0.67 ± 0.04 (52)	1.15 ± 0.15 (17)	0.69 ± 0.02 (36)	0.87 ± 0.01 (16)	0.63 ± 0.02 (16)
	0.66 − 1.32	0.61 − 0.77	0.66 − 1.32	0.64 − 0.77	0.85 − 0.88	0.61 − 0.68
$S_{275-295}$	16 ± 3 (33)	17 ± 2 (52)	17 ± 4 (17)	18 ± 1 (36)	15 ± 1 (16)	15 ± 1 (16)
(μm^{-1})	4 − 22	13 − 22	4 − 22	15 − 22	12 − 17	13 − 17
S_R	1.41 ± 0.42 (33)	1.00 ± 0.09 (52)	1.62 ± 0.46 (17)	1.04 ± 0.08 (36)	1.19 ± 0.21 (16)	0.92 ± 0.06 (16)
	0.34 − 2.32	0.83 − 1.31	0.34 − 2.32	0.89 − 1.31	1.03 − 1.80	0.83 − 1.06
E2:E3	5.20 ± 0.93 (33)	5.63 ± 0.71 (52)	5.04 ± 1.03 (17)	5.93 ± 0.53 (36)	5.37 ± 0.82 (16)	4.97 ± 0.62 (16)
	3.31 − 7.09	4.22 − 6.97	3.31 − 7.09	4.93 − 6.97	3.34 − 6.09	4.22 − 6.02

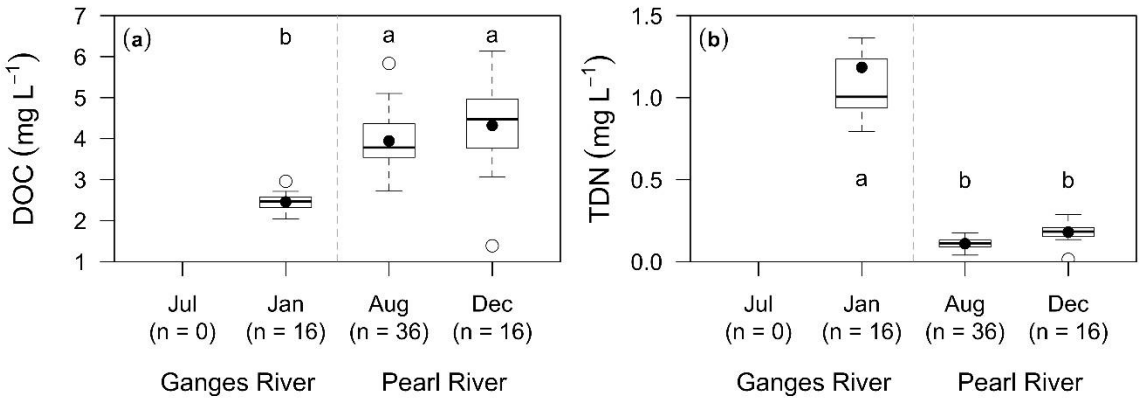

Figure 4.3 Distributions of (a) DOC and (b) TDN concentrations during July 2015 and January 2016 in the Ganges River. Same parameters during August 2015 and December 2015 are shown for the Pearl River. Same letters represent no significant difference at alpha = 0.05.

4.3.2 DOM compositions in the Ganges and the Pearl Rivers

DOM compositions in this study were assessed together for the Ganges and Pearl Rivers using PARAFAC analysis of EEM fluorescence, which resulted a five-component model. The DOM components identified were spectrally similar to previously reported DOM constituents (Table 4.2 and Fig. 4.4). Components C1 and C2 together contributed to 50 and 70% of the total fluorescence of DOM in the Ganges River and the Pearl River, respectively. While component C1 did not differ in the Pearl River between the months of August and December, it was different in the month of July than in January in the Ganges River with higher values in January. This component is spectrally similar to microbial humic-like component reported in previous studies (Table 4.2). Relatively lower values of C1 in July in the Ganges River could be attributed to dilution effects caused by high discharge during monsoon season. This fluorescence peak has previously

been thought of as marine humic-like organic matter while many studies have identified this peak in samples from terrestrial environments and have associated its presence to high biological or microbial activity in water bodies receiving agricultural, industrial and sewage wastes (Baker 2002; Coble 2007; Meng et al. 2013). Photochemical degradation of terrestrial organic matter can also show a similar fluorescence peak by blue shift of the peak position of the terrestrial fluorescence signatures (Coble 2007).

Component C2 had the highest contribution to the total fluorescence of DOM in the Pearl River (26.59 ± 1.40%) than the Ganges River (16.87 ± 1.37%) (Fig. 4.5 and Table 4.1). This fluorescence peak (C2) is reported as the most abundant DOM component in fulvic and humic acid fractions extracted from sediments and soils (Santín et al. 2009). Additionally, the presence of this peak has been identified in the tropical rivers (Yamashita et al. 2010) and in the recycled wastewaters (Murphy et al. 2010). Thus, source of the component C2 can be ascribed to wetland soils and sediments in the Pearl River, while the abundance of the C2 component in the Ganges River could be attributed to the sewage effluent from treatment plants located along the banks of the Ganges River. The lower values of C2, 16.16 ± 1.64% and 25.83 ± 0.77% in the months of July in the Ganges River and in August in the Pearl River, respectively, as compared to higher values 17.54 ± 0.26% and 28.23 ± 0.98% in the months of January in the Ganges River and in December in the Pearl River, respectively, are indicative of mixing and photochemical processes acting on DOM molecules during summer season (Fig. 4.5 and Table 4.1). Further, mixing because of high water discharge in the month of July in the Ganges River during monsoon may have diluted this signal, while photochemical degradation under strong UV radiations during summer may have broken up large

molecules reducing them to smaller molecular size of DOM (Wiegner and Seitzinger 2001; Lu et al. 2013; Guéguen et al. 2016). These processes could have contributed to the temporal variability of C2 observed for both the Ganges River and the Pearl River.

Table 4.2 Description of EEM-PARAFAC modeled DOM components identified in this study and compared against those reported in the literature.

Comp.	Ex/Em (nm)	Description	Peaks in Coble (2007)	Possible Sources	Reference – Comp.
C1	< 250-305/416	Marine humic-like; biological and/or microbial origin	A, M	Terr., Auto., Micr.	Hong et al. (2012) - C2; Hiriart-Baer et al. (2013) - C4; Olefeldt et al. (2013) - CM/CA; Chen et al. (2015) - C4
C2	< 250-370/498	Terrestrial humic-like; Soil derived humic acids	–	Terr., Anth.	Guo et al. (2011) - C3; Hong et al. (2012) - C3; Hiriart-Baer et al. (2013) - C1; Olefeldt et al. (2013) - Cx; Chen et al. (2015) - C3
C3	< 300/374	Marine humic-like; biological and/or microbial origin	N	Terr., Auto., Micr.	Guo et al. (2011) - C2; Hong et al. (2012) - C5; Hiriart-Baer et al. (2013) - C5; Olefeldt et al. (2013) - CM
C4	280/336	Protein-like (Tryptophan like)	T	Terr., Auto., Micr.	Guo et al. (2011) - C4; Hong et al. (2012) - C4; Hiriart-Baer et al. (2013) - C3; Olefeldt et al. (2013) - CT; Chen et al. (2015) - C2
C5	360/430	Terrestrial humic-like	C	Terr., Anth.	Guo et al. (2011) - C1; Hong et al. (2012) - C1; Olefeldt et al. (2013) - CC/CA; Chen et al. (2015) - C1

Terr. - Terrestrial plant/animal detritus or soil organic matter, Auto. - Autochthonous production, Anth. - Anthropogenic inputs, Micr. - Microbial processing.

The most prominent distributional pattern was observed for the component C3. The average proportional contribution of C3 was three fold more in the Ganges River (17.74 ± 5.59%) than the Pearl River (5.40 ± 0.76%). While the proportional contribution of C3 in the Ganges River in the month of July was approximately four times higher of the Pearl River in the month of August, C3 in the Ganges River in the month of January was nearly three times higher in the Pearl River in the month of December (Table 4.1).

This component is similar to previously identified N-peak (Coble 2007). This fluorescence peak was used as a tracer for wastewater impacts (Hiriart-Baer et al. 2013). While evaluating the anthropogenic effects of industrial effluent discharge in Kishon River, Israel, the same fluorescence component was reported by Borisover et al. (2011). The authors however claimed this component to be a mixture of both proteinaceous and non-proteinaceous components. Occurrence of this component in the water samples was attributed to selective preservation of the proteinaceous constituents by interactions with other DOM components, which protect this component from microbial degradation (Borisover et al. 2011). Numerous other studies reported this component as the result of anthropogenic activities in the watershed, especially from agricultural fields, urban runoff, and drinking water and wastewater treatment plants (Baker 2002; Baker et al. 2003; Spencer et al. 2007; Singh et al. 2014a). Significantly high value of C3 in the Ganges River in the month of July could be attributed to runoff from industrial and urban areas in addition to local wastes and residual matter from biomass burning, especially burnt dead bodies on the river bank followed by monsoonal rains (Prasad et al. 2007; Singh and Singh 2007; Chauhan et al. 2015; Pandey et al. 2015; Sharma et al. 2016). Previous studies have also suggested that DOM in agricultural runoff is generally different than DOM in natural stream systems, and may be more bioavailable to microbes as a nutrient source (Gao et al. 2004; Dalzell et al. 2007). It is well known that the runoff from agricultural fields is often high in nutrients such as nitrogen, phosphorus, and potassium that are common constituents in inorganic fertilizer. Because there are large agricultural fields located at the upstream end of the sampling area in the Ganges River,

an expected source of C3 could be agricultural runoff in July during monsoonal rains that may generate larger surface runoff from these fields (Pandey et al. 2015).

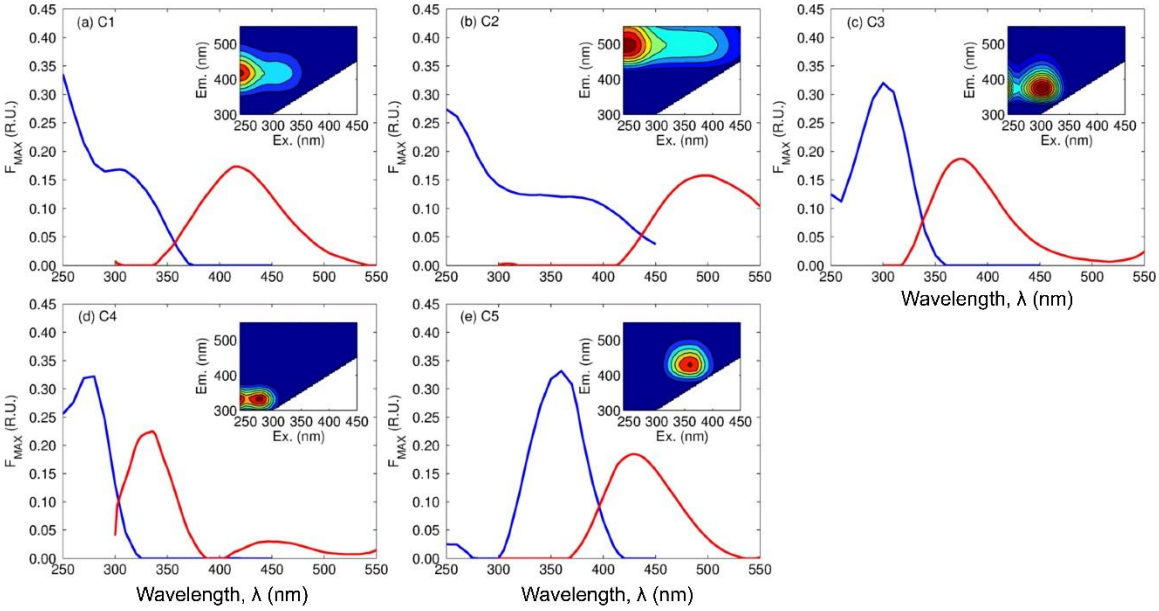

Figure 4.4 The five EEM-PARAFAC modeled DOM compositions for the Ganges and Pearl River samples.

Component C4 typically resembled a protein-like (tryptophan-like) DOM indicating autochthonous production of biological origin as reported in previous studies (Table 4.2). This component was significantly higher in the Ganges River than the Pearl River (Fig. 4.5). The average proportions of C2 for the Ganges River in the months of July and January was 18.62 ± 4.19% and 18.81 ± 0.41%, respectively and was not very much different across months. While the Pearl River samples showed lower average contributions from C4 in the total DOM pool, significant difference in C4 was observed in the months of August (12.16 ± 1.16%) and December (9.91 ± 1.39%). The higher value in the month of August could be due to high autochthonous production as indicated by macrophyte and periphyton production in the Pearl River. A study in the Ganges River

during summer examined the production of algal periphyton in relation to dissolved organic carbon and has linked light attenuation to lower benthic production due to increased turbidity in the Ganges River at Varanasi, India (Pandey 2013). On the other hand, protein-like DOM is used as a tracer in tracking anthropogenic inputs in many ecosystems ranging from lakes to rivers (Baker and Inverarity 2004; Stedmon and Markager 2005; Borisover et al. 2011; Meng et al. 2013). For example, Hosen et al. (2014) have observed that runoff from an impervious surface had enhanced amounts of anthropogenic protein-like DOM in the urbanized streams of Maryland, USA. The authors suggested that the higher proportion of protein-like DOM was because of increased levels of bioavailable DOM in these urbanized streams, especially during spring and summer. Thus, increased runoff because of impervious surfaces (e.g., concrete banks on the Ganges River) may have contributed to this DOM signal. Further, C4 did not differ temporally in the Ganges River because these constructions have been there for many years.

Traditionally, the component C5 resembled a terrestrial humic-like fluorescence peak and has been observed in various aquatic systems (Coble 2007). Although the proportional contribution of the component C5 was observed to be similar in the Ganges and the Pearl Rivers, yet significant differences were shown when months were included as factors (Fig. 4.5). In the Ganges River, C5 was highest in the month of January (12.96 ± 0.30%) and lowest in the month of July (9.18 ± 0.83%). C5 concentration was intermediate in both August (10.30 ± 0.59%) and December (11.55 ± 0.65%) in the Pearl River (Table 4.1). Higher values of C5 in January in the Ganges River and in December in the Pearl River suggest that terrestrial sources contributed to DOM pool during winter

months due to limited heterotrophic activity due to lower temperatures. In contrast, elevated temperature levels in the months of July and August supported bacterial activity and enhanced microbial degradation of terrestrial DOM, which caused lower proportional contribution of this type of DOM. Additionally, photochemical breakdown of terrestrial DOM during summer periods potentially reduced the fluorescence levels of this component. The abundance of this component in many environments is controlled by simultaneous production and degradation of DOM (Yamashita et al. 2008; Cawley et al. 2014; Chen and Jaffé 2016). Some studies have also suggested this component to be somewhat refractory in character because it is protected by other molecules that bind to it (Cory and Kaplan 2012; Cawley et al. 2014).

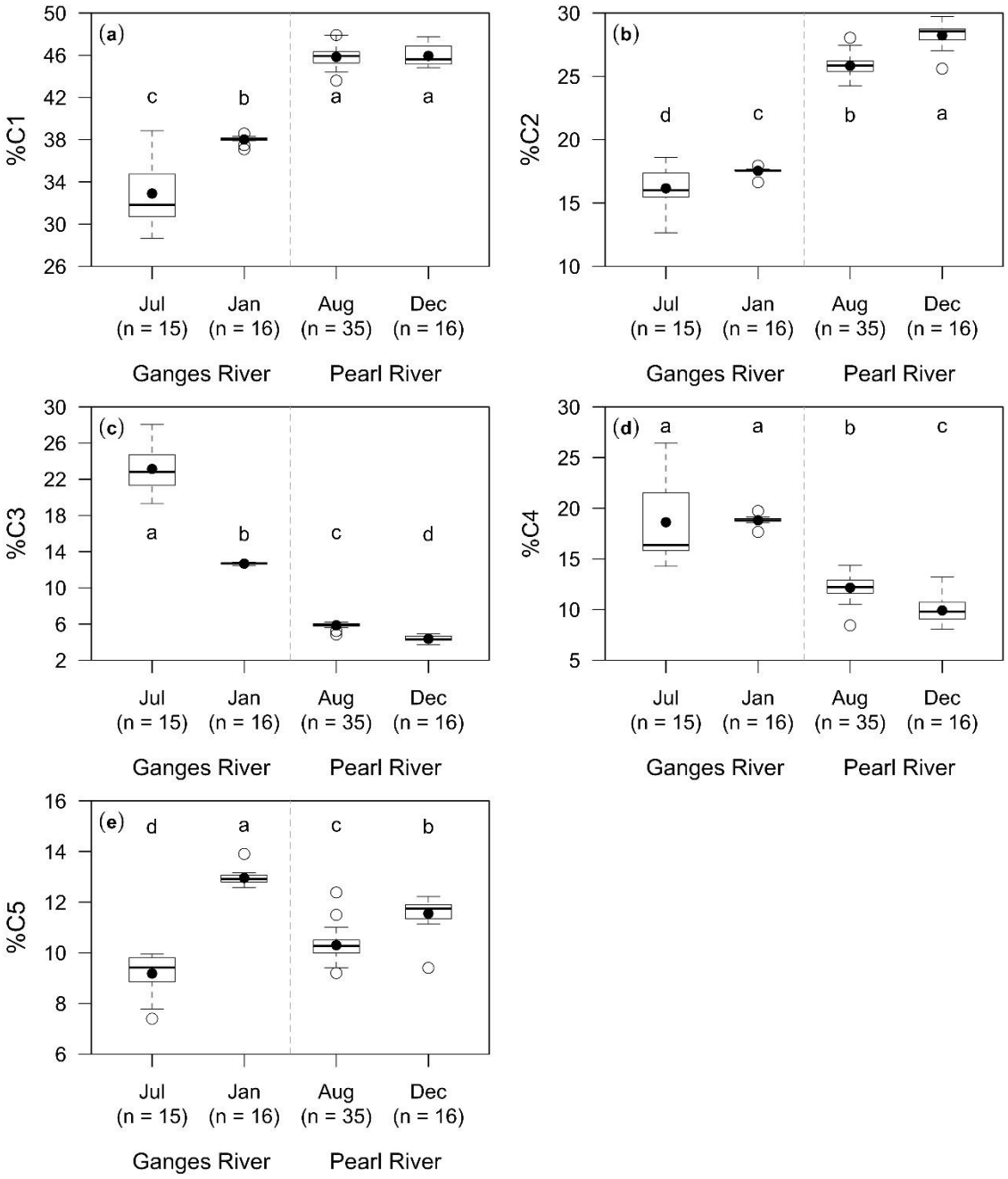

Figure 4.5 Distributions of EEM-PARAFAC modeled five DOM compositions in the Ganges and the Pearl River samples. Same letters represent no significant difference at alpha = 0.05.

4.3.3 DOM optical proxies in the Ganges and the Pearl Rivers

The spectroscopic indices measured in this study displayed clear spatial and temporal patterns in DOM distribution in the Ganges River as well as in the Pearl River. In general, BIX and a_{254} showed an inverse relationship (Fig. 4.6). In the Ganges River, a_{254} was significantly lower compared to the Pearl River. A clear distinction between July and January samples was also evident. The aromaticity optical proxy (a_{254}) suggested highly aromatic DOM in the month of July in the Ganges River but BIX values were also observed to be high in the same month. The high aromaticity in the Ganges River samples in the month of July with corresponding high BIX values suggests that autochthonous production or biological origin of DOM were in elevated levels of aromaticity in the Ganges River samples in the month of July. This finding is unlikely to observe in many aquatic systems. Generally, increase in aromaticity is related to terrestrial inputs of DOM while high BIX values are associated with autochthonous production or DOM of biological origin, which contains lower aromaticity in DOM molecules (Coble 2007; Fellman et al. 2010a; Jaffé et al. 2014). Thus, observing an increase in both these parameters in the month of July suggest that sources of DOM were either mostly autochthonous or fresher organic material but were highly aromatic. High aromaticity in N-rich DOM molecules has been reported in previous studies (Yamashita and Tanoue, 2003). In the Ganges River samples, high TDN concentrations were observed (Fig. 4.3), which suggests that highly aromatic N-rich DOM molecules were exported from terrestrial landscape, especially in runoff from untreated sewage and industrial effluents (Engelhaupt et al. 2003; Yamashita and Tanoue 2003; Murphy et al. 2011; Carstea et al. 2014). Another source of this type of DOM could be from upstream

agricultural fields where both organic and inorganic fertilizers are used and may have entered into the channel in runoff during monsoonal rains (Jordan et al. 2003; Naden et al. 2010). In contrast, low BIX and high a_{254} values were observed for the Pearl River with high average a_{254} value in the month of December and high average BIX in the month of August indicating reduction in terrestrial inputs of DOM in August following a general low-flow period in this watershed. Most of the DOM exports in the Pearl River follow rain events and hydrological disconnection occurs in the summer between the river and its flood plain (Duan et al. 2007a; Cai et al. 2016). This may have declined the terrestrial organic inputs to enter the river and hence lower aromaticity of DOM was observed. Because of comparatively high autochthonous (e.g., macrophyte and periphyton) production and/or microbial activity during summer (August) in the Pearl River in addition to photochemical cleaving of DOM molecules owing to high temperature and UV radiation levels, high average value of BIX is an expected finding.

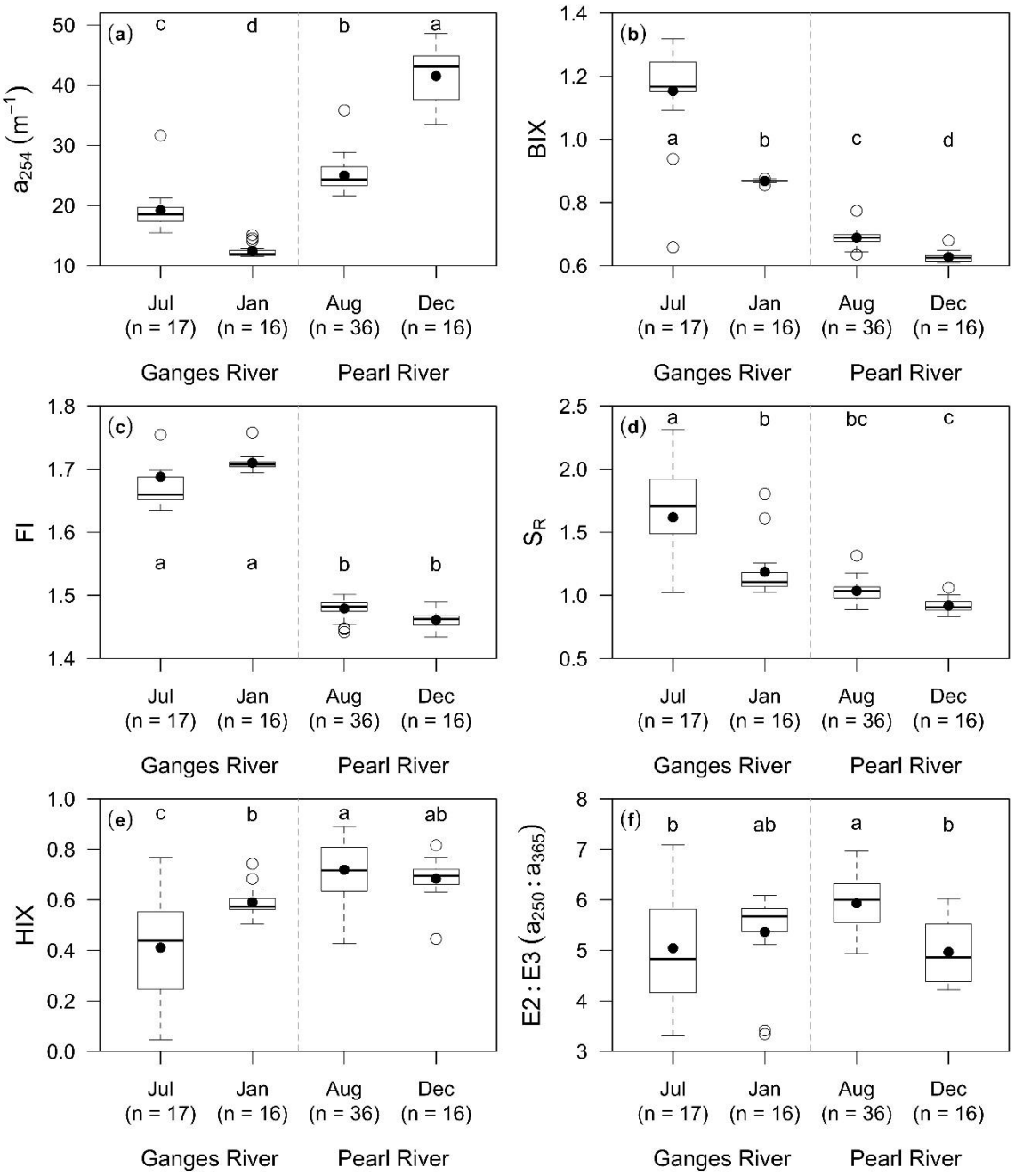

Figure 4.6 Distributions of DOM optical proxies in the Ganges and the Pearl River samples. Same letters represent no significant difference at alpha = 0.05.

The FI and S_R show higher values in the Ganges River compared to those in the Pearl River (Fig. 4.6 and Table 4.1). High values of FI in the Ganges River suggest that

the DOM had precursor material from microbial origin. No significant differences across months were observed for both the Ganges and Pearl River. The average values of FI in the months of July and January were 1.69 and 1.71, respectively in the Ganges River, while FI average values in the Pearl River were 1.48 and 1.46 in the months of August and December, respectively. These results were found to be similar as observed earlier in large rivers in the US where lower FI values (1.4-1.5) were reported indicating a dominance of terrestrial derived DOM (McKnight et al. 2001). In comparison, the lakes in the US had FI values between 1.6 to 1.9 suggesting autochthonous production and/or microbially generated DOM (McKnight et al. 2001). In contrast, a few studies suggested that FI does not strongly correspond to terrestrial DOM pools, hence this index itself might not be a very good indicator in separating DOM pools in terrestrial systems (Hood et al. 2006; Roelke et al. 2006). Spectral slope ratio, S_R, is extremely useful in differentiating between high molecular weight (HMW) and low molecular weight (LMW) organic materials. Additionally, it is useful in tracking the influence of photo bleaching on DOM molecules (Helms et al. 2008; Helms et al. 2013). The high S_R value indicates a LMW DOM suggesting high primary production in aquatic systems and possibly photo bleached DOM. Lower S_R values are usually dominant in terrestrial DOM pools where high organic inputs are generated from terrestrial sources with refractory character (Helms et al. 2008; Singh et al. 2014b). Nevertheless, both these indices (i.e., FI and BIX) together explained the distribution of DOM qualitatively in the Ganges River and in the Pearl River. Elevated microbial influence on the DOM quality in the Ganges River suggests that it potentially has originated from anthropogenic inputs.

The high HIX and E2:E3 ratio were 0.71 and 5.63, respectively, in the Pearl River. These suggested the occurrence of highly humified HMW DOM in the Pearl River while the lower values of HIX and E2:E3 ratio (0.50 and 5.20, respectively), in the Ganges River suggest the occurrence of relatively unstable LMW DOM in the Ganges River (Fig. 4.6). Low HIX values in large rivers are commonly observed phenomena and have been attributed to dilution of humified DOM due to large discharge (Chen et al. 2011; Sun et al. 2014). In contrast, high HIX in small streams is often associated with rapid response to precipitation events resulting in high discharge (Graeber et al. 2012; Halbedel et al. 2012; Singh et al. 2014b). Moreover, higher HIX values are usually associated with a higher degree of aromaticity, a lower rate of mineralization, and a lower percentage of oxygen-containing functional groups of DOM (Fuentes et al. 2006; Hur 2011). Changes in HIX value from July to January from 0.41 to 0.59, respectively, in the Ganges samples could be attributed to high discharge during summer associated with monsoon rains, which diluted the humic DOM. While in the month of January, when the base flow conditions dominate during winter, a relatively highly humified DOM export may occur. A high variability of E2:E3 (Fig. 4.6) in the month of July (5.04) in the Ganges River suggests that the sources of LMW DOM could be many that include autochthonous production of periphyton and variable inputs of anthropogenic DOM. Nonetheless, these optical indices in conjunction with other above stated indices clearly displayed a distinct character of DOM in the Ganges and the Pearl River samples, and suggest completely different sources of DOM in these two water bodies. Also, many physicochemical processes such as hydrological connection/disconnection causing mixing or dissolution, photo- and bio-degradation, and autochthonous (or microbial)

production to name a few have contributed to temporal distributions of DOM in these water bodies.

4.3.4 Correlations and principal component analysis

The correlation analyses of DOM concentrations and compositions revealed strong associations between the DOM components and the optical indices supporting the findings from DOM optical proxies and further suggesting the potential origin and character of DOM in the Ganges and Pearl River watersheds (Table 4.3). The strong correlation, r = 0.92, between the components C1, a microbial humic-like, and C2, a soil-derived terrestrial humic-like components suggest a similar DOM source for both these components. The source for C1 and C2 were riparian soils and sediments that were mineralized by the microbial communities, leaving relatively simpler DOM molecules for further biochemical degradation. The source material for these fluorescence signatures was rich in organic carbon fractions of DOM. Terrestrially derived humic-like DOM (C1 and C2) were more aromatic owing to their high correlations with a_{254} and HIX. They also had higher average molecular weight as evident by their inverse relationship with S_R. Moreover, these materials were diagenetically altered before entering into the streams and were aged, while the DOM that was either microbially altered or autochthonously produced within streams was relatively fresh and less humified as evidenced by their direct relationship with BIX. In a study by Lu et al. (2013), the diagenetic status of DOM was found as a major control of DOM dynamics in urbanized watersheds of mid-Atlantic region of USA. The authors also found strong associations between diagenetic status of DOM and photochemical and biological degradation processes. The correlation between C3 and C4 was also fairly strong, r = 0.73. Both C3 and C4 were strongly correlated with

TDN, r = 0.88 and 0.82 respectively, which indicates increased N-rich DOM molecules were responsible for these fluorescence signals (Table 4.3). Strong correlations of FI with the components C3 and C4 suggest that microbes played an important role in modifying DOM character. While the sources of these microbially generated DOM were tracked to anthropogenic inputs in the Ganges River from multiple sources, which included agricultural runoff, industrial and municipal waste discharge, and biomass burning. Lower contributions of the same fluorescence signals in the Pearl River could not be ascertained in this study.

The principal component analysis of DOM absorption and fluorescence characteristics based on EEM-PARAFAC analysis revealed discernible differences in the DOM character in the Ganges and Pearl Rivers, and difference in DOM property owing to the water sample collection in two seasons (Fig. 4.7). PCA identified two principal components that together explained 78% of the variation in the DOM dataset. The loadings for the first PCA axis were most strongly affected by the PARAFAC components C3, a microbial humic-like component, and C4, a protein-like component. The loadings for the second PCA axis were most strongly influenced by the PARAFAC components C1 and C2, which were microbial humic-like and soil-derived terrestrial humic-like components, respectively. First PCA axis separated the DOM based on refractory (the negative side on first axis) and labile character (the positive side of the first axis). The second axis separated the DOM based on young or old stages. Especially for the Ganges River samples, where fresh DOM was possibly introduced during high discharge periods in the month of July (monsoon rain with snow-melt waters) and in the

month of January the DOM was comparatively older organic material from terrestrial sources.

The humic-like aromatic DOM was pronounced in the Pearl River, which suggests that aged terrestrial organic materials were flushed into the streams mostly after the rain events. Because water discharge due to local rainstorms usually controls the DOM supply to the Pearl River system, local inputs of DOM from forest soils and riparian wetlands could cause the greater variability in DOM concentration in the Pearl River (Duan et al. 2007a; Duan and Bianchi 2007). In the Pearl River watershed, late fall and winter (December) period usually characterized by an increased storm activity causing increased levels of hydrologic discharge. Moreover, reduced discharge during summer (August) base-flow period transforms DOM abundance via microbial and photochemical degradation processes with more light availability and elevated temperatures (Moran et al. 2000; Lu et al. 2013; Singh et al. 2017). Hence, temporal DOM distributions could be ascribed to hydrological transport of local inputs and dominant biogeochemical processes such as photochemical degradation in the Pearl River system.

Table 4.3 Correlation analysis between PARAFAC modeled components (C1-C5), DOC and TDN concentrations, and DOM indices. Non-significant correlations at $\alpha = 0.05$ are represented as "–".

	C1	**C2**	**C3**	**C4**	**C5**	**DOC**	**TDN**	**a_{254}**	**SUVA**	**HIXO**	**FI**	**BIX**	**SR**
C2	**0.92**												
C3	**-0.94**	**-0.89**											
C4	**-0.86**	**-0.92**	**0.73**										
C5	–	–	-0.27	–									
DOC	0.70	0.68	-0.70	-0.68	-0.48								
TDN	**-0.89**	**-0.86**	**0.88**	**0.82**	**0.77**	-0.55							
a_{254}	0.61	**0.80**	-0.59	**-0.75**	–	0.63	-0.60						
SUVA	0.34	0.44	-0.42	-0.46	–	–	-0.31	0.59					
HIXO	0.63	0.66	-0.61	-0.67	–	–	-0.40	0.30	–				
FI	**-0.87**	**-0.96**	**0.79**	**0.88**	0.23	-0.65	**0.91**	-0.66	-0.35	-0.57			
BIX	**-0.94**	**-0.89**	**0.99**	**0.74**	-0.32	-0.66	**0.84**	-0.59	-0.44	-0.60	0.68		
S_R	**-0.72**	**-0.71**	**0.83**	0.55	-0.37	-0.42	0.42	-0.46	-0.33	-0.38	0.42	**0.81**	
E2:E3	0.30	–	-0.26	–	–	–	–	–	-0.25	–	–	-0.23	-0.51

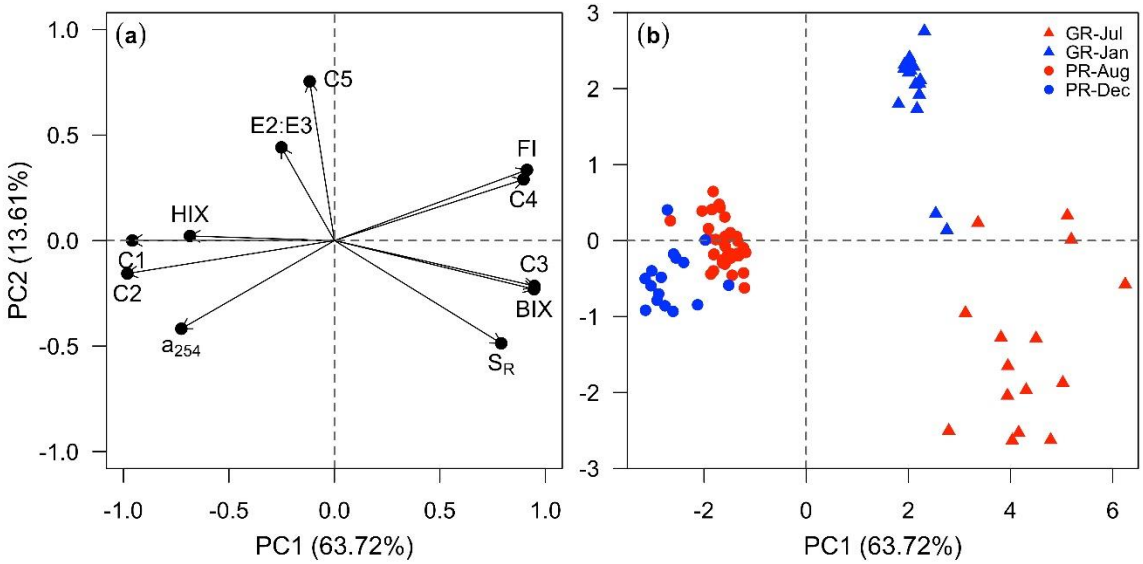

Figure 4.7 Principal component analysis of DOM dataset that include PARAFAC modeled (C1-C5) components, and DOM indices. Sampling locations and timings are referred in the legend of the score plot.

In large rivers like the Ganges River, in-situ DOM processing is a dominant mechanism that changes the character and composition of DOM (Striegl et al. 2007; Raymond and Spencer 2014). Contribution and dilution from autochthonous production, runoff from point and non-point sources, and longer residence time as a result of dams can potentially affect the DOM character and quality in large rivers (Kaushal et al. 2011; Zurbrügg et al. 2013; Leech et al. 2016). However, the present analysis suggests that the DOM in the Ganges River is relatively labile and less aromatic low molecular weight N-rich (high TDN). The source could be tracked back to anthropogenic inputs from agricultural runoff, industrial and municipal waste discharge, biomass burning and untreated sewage effluents, because DOM from these sources are generally highly bioavailable and labile than the DOM from natural landscapes such as forests. Moreover,

high BIX and FI loadings on the positive axis 1 in PCA suggest that the DOM in the Ganges River was relatively fresh. The summer (July) samples show high inputs of this fresh organic material into the river from runoff during monsoonal rains that transported the organic material from upstream as well as from adjacent urban areas of the river (Pandey et al. 2015). During winter (January), when light availability and temperatures are at the lower levels, riverine processing decreases due to dormancy in microbial activity and decreased autochthonous production. Additionally, water level drops causing base-flow, which causes not much alteration of the terrestrial organic materials that are in the river. Nonetheless, principal component analysis clearly separated the samples from both the locations, the Ganges and the Pearl Rivers, and temporal differences in DOM character were also distinctly observed in this analysis, especially in the Ganges River.

4.4 Conclusions

The DOM concentration and composition via spectral absorption and fluorescence properties were studied for a large river (the Ganges River, India) and a small pristine black water river (the Pearl River, USA). The spatial and temporal patterns for DOM abundance and properties were examined using DOC and TDN concentrations, EEM-PARAFAC modeled DOM compositions and a suite of DOM indices. Five distinct DOM compositions (C1-C5) were modeled using EEM-PARAFAC approach. The Ganges River showed distinctly different DOM character between July and January with increased fresher terrestrial and anthropogenic inputs in the month of July when monsoon rains flood the river. The wash-off materials from the riverbanks, point-source inputs of urban, industrial, and municipal wastes characterized this DOM. Autochthonous production also contributed to elevated DOM levels in the month of July during summer.

In comparison, reduced DOM levels were observed during colder month, January. High riverine processing as well as microbial and photochemical processes dominated the DOM character in the Ganges River, while temporal patterns of DOM abundance and composition in the Pearl River was mostly controlled by hydrological discharge following local rainfall events. Highly aromatic and humic-rich DOM inputs from forest soils and wetlands were the dominant contributor of DOM in this river system. Also, removal of these local inputs of DOM through photo bleaching was prominent in the hot season (August) in the Pearl River. Nevertheless, the temporal patterns of DOM concentration and composition in both these river systems demonstrated the complexity of the carbon and nutrient cycling in a large river system in comparison to a small pristine river.

Thus the supply and removal of DOM in aquatic systems depend on a range of processes such as mixing water masses, microbial and photo degradation, autochthonous production, removal of natural forests and wetlands, construction of dams among many other factors (Aiken et al. 2011; Guéguen et al. 2016). Seasonal variability with multitude of sources that include both natural and anthropogenic sources can significantly influence the DOM character and its dynamics in these systems. However, many of these complex processes and their interactions could be deciphered with high-resolution spatial and temporal measurements. Additionally, this study emphasized the application of optical techniques in monitoring and measuring molecular level changes in DOM. These understandings of the DOM properties are critical for a comprehensive assessment of biogeochemical processes undergoing in important water bodies on which our society is heavily dependent upon.

CHAPTER V

CONCLUSIONS

This project was carried out in multiple watersheds located in the Gulf-Atlantic Coastal Plain Physiographic region of the southeast USA and Indo-Gangetic Plain of India. UV-visible absorption and fluorescence spectroscopy in conjunction with statistical tools (i.e., PARAFAC, PCA etc.) were used to study the character of dissolved organic matter (DOM) in these watersheds. In this study, spatial and temporal dynamics of dissolved organic matter were explored to understand water biogeochemistry influenced by land use and land cover during low-flow and high-flow conditions. Watershed intrinsic properties such as proportion of wetland coverage, proportion of agricultural land, and natural and anthropogenic processes were evaluated to determine their influence on the DOM properties. Generally, watersheds with greater wetland coverage contributed larger DOM exports with aromatic and humic-rich DOM character while the watersheds with greater agricultural and urban coverage showed a distinct DOM response with bioavailable and non-humic DOM. Principal component analysis and regression analyses of DOM data indicated that the northern Mississippi lakes were majorly influenced by agricultural land use, estuarine region was affected by natural DOM export from forests and wetlands, while the coastal waters were affected by a mix of anthropogenic and natural inputs of DOM. Temporal variations in DOM properties suggested variable DOM dynamics across seasons. Spring showed a high DOM

concentration concurrent with high-flow periods in the small river system while DOM during summer (low-flow) season was highly influenced by photochemical and biological degradation processes. DOM quality changed across hydrologic conditions (e.g., high-flow *versus* low-flow) and seasons (e.g., spring *versus* summer) reflecting variable DOM dynamics at different times of the year. Anthropogenic loads mainly influenced DOM in a densely populated and urbanized large river system.

In summary, this study emphasized the application of optical techniques in monitoring and measuring molecular level changes in DOM, as these are rapid and inexpensive techniques. Understanding these changes to DOM properties are critical to study biogeochemical processes related to ecologically sensitive water bodies for a comprehensive assessment over a range of spatial and temporal scales.

5.1 Significance of this study

This dissertation research focused on investigating the sources, transformations, and spatial and temporal variations of DOM in multiple aquatic ecosystems primarily using optical and multivariate statistical techniques. An understanding of the dominant controls and factors responsible for the sources, transport, transformations, and fate of DOM helped in advancing our knowledge about the influence of DOM quality and quantity on the overall water quality of these ecosystems. The role of DOM in carbon and nutrient cycling with water movement is critical to understand. As future climate change scenarios predict a greater variation in temperature and precipitation patterns, the flux and transport of DOM from inland water bodies to receiving coastal waters will change (Karl et al. 2009; Harvey et al. 2015; Dieleman et al. 2016). These changes in DOM amount and flux will have significant bearing on the regional and global change in carbon

movement between various pools (Battin et al. 2008; Bianchi 2011). To study and manage water quality issues and resources, biogeochemical and hydrodynamic models for mass circulation and transport are currently being developed (Massicotte and Frenette 2013; Sharip et al. 2016). Hence, an increased understanding of DOM movement between various pools needs to be included in developing these regional and global biogeochemical and hydrodynamic models to simulate circulation and estimate information of mass transport of organic materials with expected/modeled changes in climate conditions.

REFERENCES

Adrian R, O'Reilly CM, Zagarese H, et al (2009) Lakes as sentinels of climate change. Limnol Oceanogr 54:2283–2297. doi: 10.4319/lo.2009.54.6_part_2.2283

Ågren A, Buffam I, Berggren M, et al (2008) Dissolved organic carbon characteristics in boreal streams in a forest-wetland gradient during the transition between winter and summer. J Geophys Res 113:1–11. doi: 10.1029/2007JG000674

Aiken GR, Gilmour CC, Krabbenhoft DP, Orem W (2011) Dissolved Organic Matter in the Florida Everglades: Implications for Ecosystem Restoration. Crit Rev Environ Sci Technol 41:217–248. doi: 10.1080/10643389.2010.530934

Aitkenhead-Peterson JA, McDowell WH, Neff JC (2003) Sources, Production, and Regulation of Allochthonous Dissolved Organic Matter Inputs to Surface Waters. In: Findlay SEG, Sinsabaugh RL (eds) Aquatic Ecosystems: Interactivity of Dissolved Organic Matter. Academic Press, Amsterdam, The Netherlands, pp 25–70

Amon RMW, Benner R (1996) Bacterial utilization of different size classes of dissolved organic matter. Limnol Oceanogr 41:41–51. doi: 10.4319/lo.1996.41.1.0041

Anderson, JR, Hardy EE, Roach JT, Witmer RE (1976) A Land Use and Land Cover Classification System For Use With Remote Sensor Data. USGS Professional Paper 964. A revision of the land use classification system as presented in the USGS Circular 671.

Arellano AR, Coble PG (2015) Assessing carbon and nutrient inputs in a spring-fed estuary using fluorescence spectroscopy and discriminatory classification. Limnol Oceanogr 60:789–804. doi: 10.1002/lno.10078

Baghoth SA, Sharma SK, Amy GL (2011) Tracking natural organic matter (NOM) in a drinking water treatment plant using fluorescence excitation-emission matrices and PARAFAC. Water Res 45:797–809. doi: 10.1016/j.watres.2010.09.005

Baker A (2002) Fluorescence properties of some farm wastes: implications for water quality monitoring. Water Res 36:189–195.

Baker A, Inverarity R (2004) Protein-like fluorescence intensity as a possible tool for determining river water quality. Hydrol Process 18:2927–2945. doi: 10.1002/hyp.5597

Baker A, Inverarity R, Charlton M, Richmond S (2003) Detecting river pollution using fluorescence spectrophotometry: case studies from the Ouseburn, NE England. Environ Pollut 124:57–70.

Balcarczyk KL, Jones Jr. JB, Jaffé R, Maie N (2009) Stream dissolved organic matter bioavailability and composition in watersheds underlain with discontinuous permafrost. Biogeochemistry 94:255–270. doi: 10.1007/s10533-009-9324-x

Banaitis MR, Waldrip-Dail H, Diehl MS, et al (2006) Investigating sorption-driven dissolved organic matter fractionation by multidimensional fluorescence spectroscopy and PARAFAC. J Colloid Interface Sci 304:271–276. doi: 10.1016/j.jcis.2006.07.035

Bano N, Moran MA, Hodson RE (1997) Bacterial utilization of dissolved humic substances from a freshwater swamp. Aquat Microb Ecol 12:233–238. doi: 10.3354/ame012233

Battin TJ, Kaplan LA, Findlay S, et al (2008) Biophysical controls on organic carbon fluxes in fluvial networks. Nat Geosci 1:95–100. doi: 10.1038/ngeo602

Beggs KMH, Summers RS (2011) Character and chlorine reactivity of dissolved organic matter from a mountain pine beetle impacted watershed. Environ Sci Technol 45:5717–5724. doi: 10.1021/es1042436

Bertilsson S, Tranvik LJ (2000) Photochemical transformation of dissolved organic matter in lakes. Limnol Oceanogr 45:753–762. doi: 10.4319/lo.2000.45.4.0753

Bianchi TS (2011) The role of terrestrially derived organic carbon in the coastal ocean: A changing paradigm and the priming effect. Proc Natl Acad Sci 108:19473–19481. doi: 10.1073/pnas.1017982108

Bittar TB, Berger SA, Birsa LM, et al (2016) Seasonal dynamics of dissolved, particulate and microbial components of a tidal saltmarsh-dominated estuary under contrasting levels of freshwater discharge. Estuar Coast Shelf Sci 182:72–85. doi: 10.1016/j.ecss.2016.08.046

Blanchet M, Pringault O, Panagiotopoulos C, et al (2017) When riverine dissolved organic matter (DOM) meets labile DOM in coastal waters: changes in bacterial community activity and composition. Aquat Sci 1–17. doi: 10.1007/s00027-016-0477-0

Bolan NS, Adriano DC, De-la-Luz M (2004) Dynamics and environmental significance of dissolved organic matter in soil. In: 3rd Australian New Zealand Soils Conference. pp 1–8

Bolan NS, Adriano DC, Kunhikrishnan A, et al (2011) Dissolved Organic Matter: Biogeochemistry, Dynamics, and Environmental Significance in Soils. In: Sparks D (ed) Advances in Agronomy, 1st edn. Elsevier Inc., pp 1–75

Borisover M, Laor Y, Saadi I, et al (2011) Tracing Organic Footprints from Industrial Effluent Discharge in Recalcitrant Riverine Chromophoric Dissolved Organic Matter. Water Air Soil Pollut 222:255–269. doi: 10.1007/s11270-011-0821-x

Boyer JN, Dailey SK, Gibson PJ, et al (2006) The role of dissolved organic matter bioavailability in promoting phytoplankton blooms in Florida Bay. Hydrobiologia 569:71–85. doi: 10.1007/s10750-006-0123-2

Bracchini L, Cózar A, Dattilo AM, et al (2006) The role of wetlands in the chromophoric dissolved organic matter release and its relation to aquatic ecosystems optical properties. A case of study: Katonga and Bunjako Bays (Victoria Lake; Uganda). Chemosphere 63:1170–1178. doi: 10.1016/j.chemosphere.2005.09.045

Brooks PD, Mcknight DM, Bencala KE (1999) The relationship between soil heterotrophic activity, soil dissolved organic carbon (DOC) leachate, and catchment-scale DOC export in headwater catchments. Water Resour Res 35:1895–1902.

Buffam I, Galloway JN, Blum LK, McGlathery KJ (2001) A stormflow/baseflow comparison of dissolved organic matter concentrations and bioavailability in an Appalachian stream. Biogeochemistry 53:269–306.

Buffam I, Laudon H, Temnerud J, et al (2007) Landscape-scale variability of acidity and dissolved organic carbon during spring flood in a boreal stream network. J Geophys Res 112:1–11. doi: 10.1029/2006JG000218

Bushaw KL, Zepp RG, Tarr MA, et al (1996) Photochemical relaease of biologically available nitrogen from aquatic dissolved organic matter. Nature 381:404–407.

Bushaw-Newton KL, Moran MA (1999) Photochemical formation of biologically available nitrogen from dissolved humic substances in coastal marine systems. Aquat Microb Ecol 18:285–292. doi: 10.3354/ame018285

Butman D, Raymond PA (2011) Significant efflux of carbon dioxide from streams and rivers in the United States. Nat Geosci 4:839–842. doi: 10.1038/ngeo1294

Butturini A, Guarch A, Romani AM, et al (2016) Hydrological conditions control in situ DOM retention and release along a Mediterranean river. Water Res 99:33–45. doi: 10.1016/j.watres.2016.04.036

Caffrey JM, Murrell MC, Amacker KS, et al (2014) Seasonal and Inter-annual Patterns in Primary Production, Respiration, and Net Ecosystem Metabolism in Three Estuaries in the Northeast Gulf of Mexico. Estuaries and Coasts 37:222–241. doi: 10.1007/s12237-013-9701-5

Cai Y, Guo L, Wang X, et al (2013) Effects of tropical cyclones on river chemistry: A case study of the lower Pearl River during Hurricanes Gustav and Ike. Estuar Coast Shelf Sci 129:180–188. doi: 10.1016/j.ecss.2013.05.019

Cai Y, Shim M-J, Guo L, Shiller A (2016) Floodplain influence on carbon speciation and fluxes from the lower Pearl River, Mississippi. Geochim Cosmochim Acta 186:189–206. doi: 10.1016/j.gca.2016.05.007

Carstea EM, Baker A, Bieroza M, et al (2014) Characterisation of dissolved organic matter fluorescence properties by PARAFAC analysis and thermal quenching. Water Res 61:152–161. doi: 10.1016/j.watres.2014.05.013

Catalán N, Kellerman AM, Peter H, et al (2015) Absence of a priming effect on dissolved organic carbon degradation in lake water. Limnol Oceanogr 60:159–168. doi: 10.1002/lno.10016

Catalán N, Marcé R, Kothawala DN, Tranvik LJ (2016) Organic carbon decomposition rates controlled by water retention time across inland waters. Nat Geosci 9:1–7. doi: 10.1038/ngeo2720

Catalán N, Obrador B, Alomar C, Pretus JL (2013) Seasonality and landscape factors drive dissolved organic matter properties in Mediterranean ephemeral washes. Biogeochemistry 112:261–274. doi: 10.1007/s10533-012-9723-2

Catalán N, Obrador B, Felip M, Pretus JL (2013) Higher reactivity of allochthonous vs. autochthonous DOC sources in a shallow lake. Aquat Sci. doi: 10.1007/s00027-013-0302-y

Cawley KM, Ding Y, Fourqurean J, Jaffé R (2012) Characterising the sources and fate of dissolved organic matter in Shark Bay, Australia: A preliminary study using optical properties and stable carbon isotopes. Mar Freshw Res 63:1098–1107. doi: 10.1071/MF12028

Cawley KM, Yamashita Y, Maie N, Jaffé R (2014) Using Optical Properties to Quantify Fringe Mangrove Inputs to the Dissolved Organic Matter (DOM) Pool in a Subtropical Estuary. Estuaries and Coasts 37:399–410. doi: 10.1007/s12237-013-9681-5

Chauhan MS, Dikshit PKS, Dwivedi SB (2015) Modeling of Discharge Distribution in Bend of Ganga River at Varanasi. Comput Water, Energy, Environ Eng 25–37.

Chen H, Lei K, Wang X (2016) Terrestrial humic substances in Daliao River and its estuary: optical signatures and photoreactivity to UVA light. Environ Sci Pollut Res 23:6459–6471. doi: 10.1007/s11356-015-5876-6

Chen H, Meng W, Zheng B, et al (2013a) Optical signatures of dissolved organic matter in the watershed of a globally large river (Yangtze River, China). Limnologica 43:482–491. doi: 10.1016/j.limno.2013.04.004

Chen H, Zheng B, Song Y, Qin Y (2011) Correlation between molecular absorption spectral slope ratios and fluorescence humification indices in characterizing CDOM. Aquat Sci 73:103–112. doi: 10.1007/s00027-010-0164-5

Chen M, Jaffé R (2014) Photo- and bio-reactivity patterns of dissolved organic matter from biomass and soil leachates and surface waters in a subtropical wetland. Water Res 61:181–190. doi: 10.1016/j.watres.2014.03.075

Chen M, Jaffé R (2016) Quantitative assessment of photo- and bio-reactivity of chromophoric and fluorescent dissolved organic matter from biomass and soil leachates and from surface waters in a subtropical wetland. Biogeochemistry 129:273–289. doi: 10.1007/s10533-016-0231-7

Chen M, Maie N, Parish K, Jaffé R (2013b) Spatial and temporal variability of dissolved organic matter quantity and composition in an oligotrophic subtropical coastal wetland. Biogeochemistry. doi: 10.1007/s10533-013-9826-4

Chen M, Price RM, Yamashita Y, Jaffé R (2010) Comparative study of dissolved organic matter from groundwater and surface water in the Florida coastal Everglades using multi-dimensional spectrofluorometry combined with multivariate statistics. Appl Geochemistry 25:872–880. doi: 10.1016/j.apgeochem.2010.03.005

Chow AT, Dai J, Conner WH, et al (2012) Dissolved organic matter and nutrient dynamics of a coastal freshwater forested wetland in Winyah Bay, South Carolina. Biogeochemistry 1–17. doi: 10.1007/s10533-012-9750-z

Church MJ, Hutchins DA, Hugh W (2000) Limitation of Bacterial Growth by Dissolved Organic Matter and Iron in the Southern Ocean. Appl Environ Microbiol 66:455–466. doi: 10.1128/AEM.66.2.455-466.2000.Updated

Coble PG (1996) Characterization of marine and terrestrial DOM in seawater using excitation-emission matrix spectroscopy. Mar Chem 51:325–346. doi: 10.1016/0304-4203(95)00062-3

Coble PG (2007) Marine Optical Biogeochemistry : The Chemistry of Ocean Color. Chem Rev 107:402–418. doi: 10.1021/cr050350

Coble PG (2008) Cycling coloured carbon. Nat Geosci 1:575–576.

Coble PG, Del Castillo CE, Avril B (1998) Distribution and optical properties of CDOM in the Arabian Sea during the 1995 Southwest Monsoon. Deep Sea Res II 45:2195–2223. doi: 10.1016/S0967-0645(98)00068-X

Coble PG, Green SA, Blough N V., Gagosian RB (1990) Characterization of dissolved organic matter in the Black Sea by fluorescence spectroscopy. Nature 348:432–435.

Cole JJ, Prairie YT, Caraco NF, et al (2007) Plumbing the Global Carbon Cycle: Integrating Inland Waters into the Terrestrial Carbon Budget. Ecosystems 10:172–185. doi: 10.1007/s10021-006-9013-8

Coleman DC (1994) The microbial loop concept as used in terrestrial soil ecology studies. Microb Ecol 28:245–250.

Cory RM, Boyer EW, McKnight DM (2011) Spectral Methods to Advance Understanding of Dissolved Organic Carbon Dynamics in Forested Catchments. In: Levia DF, Carlyle-Moses D, Tanaka T (eds) Forest Hydrology and Biogeochemistry: Synthesis of Past Research and Future Directions. Springer Netherlands, Dordrecht, pp 117–136

Cory RM, Kaplan LA (2012) Biological lability of streamwater fluorescent dissolved organic matter. Limnol Oceanogr 57:1347–1360. doi: 10.4319/lo.2012.57.5.1347

Cory RM, McKnight DM (2005) Fluorescence Spectroscopy Reveals Ubiquitous Presence of Oxidized and Reduced Quinones in Dissolved Organic Matter. Environ Sci Technol 39:8142–8149. doi: 10.1021/es0506962

Cory RM, McKnight DM, Chin Y-PP, et al (2007) Chemical characteristics of fulvic acids from Arctic surface waters: Microbial contributions and photochemical transformations. J Geophys Res 112:1–14. doi: 10.1029/2006JG000343

Cory RM, Miller MP, Mcknight DM, et al (2010) Effect of instrument-specific response on the analysis of fulvic acid fluorescence spectra. Limnol Oceanogr Methods 8:67–78.

Cronan CS (2012) Biogeochemistry of the Penobscot River watershed, Maine, USA: nutrient export patterns for carbon, nitrogen, and phosphorus. Environ Monit Assess 184:4279–4288. doi: 10.1007/s10661-011-2263-8

D'Amore DV, Fellman JB, Edwards RT, Hood E (2010) Controls on dissolved organic matter concentrations in soils and streams from a forested wetland and sloping bog in southeast Alaska. Ecohydrology 3:249–261. doi: 10.1002/eco

Dalrymple RM, Carfagno AK, Sharpless CM (2010) Correlations between Dissolved Organic Matter Optical Properties and Quantum Yields of Singlet Oxygen and Hydrogen Peroxide. Environ Sci Technol 44:5824–5829. doi: Doi 10.1021/Es101005u

Dalzell BJ, Filley TR, Harbor JM (2007) The role of hydrology in annual organic carbon loads and terrestrial organic matter export from a midwestern agricultural watershed. Geochim Cosmochim Acta 71:1448–1462. doi: 10.1016/j.gca.2006.12.009

Das P, Tamminga KR (2012) The ganges and the GAP: An assessment of efforts to clean a sacred river. Sustainability 4:1647–1668. doi: 10.3390/su4081647

Dash P, Silwal S, Ikenga JO, et al (2015) Water Quality of Four Major Lakes in Mississippi, USA: Impacts on Human and Aquatic Ecosystem Health. Water 7:4999–5030. doi: 10.3390/w7094999

Dash P, Walker ND, Mishra DR, et al (2011) Estimation of cyanobacterial pigments in a freshwater lake using OCM satellite data. Remote Sens Environ 115:3409–3423. doi: 10.1016/j.rse.2011.08.004

Del Vecchio R, Blough N V. (2004) Spatial and seasonal distribution of chromophoric dissolved organic matter and dissolved organic carbon in the Middle Atlantic Bight. Mar Chem 89:169–187. doi: 10.1016/j.marchem.2004.02.027

Del Vecchio R, Blough N V. (2006) Influence of ultraviolet radiation on the chromophoric dissolved organic matter in natural waters. In: Environmental UV Radiation: Impact on Ecosystems and Human Health and Predictive Models. Springer Netherlands, pp 203–216

DeVilbiss SE, Zhou Z, Klump JV, Guo L (2016) Spatiotemporal variations in the abundance and composition of bulk and chromophoric dissolved organic matter in seasonally hypoxia-influenced Green Bay, Lake Michigan, USA. Sci Total Environ 565:742–757. doi: 10.1016/j.scitotenv.2016.05.015

Dieleman CM, Lindo Z, McLaughlin JW, et al (2016) Climate change effects on peatland decomposition and porewater dissolved organic carbon biogeochemistry. Biogeochemistry 128:385–396. doi: 10.1007/s10533-016-0214-8

Duan S, Bianchi TS (2006) Seasonal Changes in the Abundance and Composition of Plant Pigments in Particulate Organic Carbon in the Lower Mississippi and Pearl Rivers. Estuaries and Coasts 29:427–442.

Duan S, Bianchi TS (2007) Particulate and dissolved amino acids in the lower Mississippi and Pearl Rivers (USA). Mar Chem 107:214–229. doi: 10.1016/j.marchem.2007.07.003

Duan S, Bianchi TS, Sampere TP (2007a) Temporal variability in the composition and abundance of terrestrially-derived dissolved organic matter in the lower Mississippi and Pearl Rivers. Mar Chem 103:172–184. doi: 10.1016/j.marchem.2006.07.003

Duan S, Bianchi TS, Shiller AM, et al (2007b) Variability in the bulk composition and abundance of dissolved organic matter in the lower Mississippi and Pearl rivers. J Geophys Res 112:1–12. doi: 10.1029/2006JG000206

Duan S, Chen N, Kaushal SS, et al (2015) Dynamics of dissolved organic carbon and total dissolved nitrogen in Maryland's coastal bays. Estuar Coast Shelf Sci 164:451–462. doi: 10.1016/j.ecss.2015.08.004

Dyer J, Mercer A (2013) Assessment of Spatial Rainfall Variability over the Lower Mississippi River Alluvial Valley. J Hydrometeorol 14:1826–1843. doi: 10.1175/JHM-D-12-0163.1

Eimers MC, Buttle J, Watmough SA (2008) Influence of seasonal changes in runoff and extreme events on dissolved organic carbon trends in wetland- and upland-draining streams. Can J Fish Aquat Sci 65:796–808. doi: 10.1139/F07-194

Engelhaupt E, Bianchi TS, Wetzel RG, Tarr MA (2003) Photochemical transformations and bacterial utilization of high-molecular-weight dissolved organic carbon in a southern Louisiana tidal stream (Bayou Trepagnier). Biogeochemistry 62:39–58. doi: 10.1023/A:1021176531598

Fellman JB, D'Amore DV, Hood E, Boone RD (2008) Fluorescence characteristics and biodegradability of dissolved organic matter in forest and wetland soils from coastal temperate watersheds in southeast Alaska. Biogeochemistry 88:169–184. doi: 10.1007/s10533-008-9203-x

Fellman JB, Dogramaci S, Skrzypek G, et al (2011) Hydrologic control of dissolved organic matter biogeochemistry in pools of a subtropical dryland river. Water Resour Res 47:1–13. doi: 10.1029/2010WR010275

Fellman JB, Hood E, D'Amore DV, et al (2009) Seasonal changes in the chemical quality and biodegradability of dissolved organic matter exported from soils to streams in coastal temperate rainforest watersheds. Biogeochemistry 95:277–293. doi: 10.1007/s10533-009-9336-6

Fellman JB, Hood E, Spencer RGM (2010a) Fluorescence spectroscopy opens new windows into dissolved organic matter dynamics in freshwater ecosystems: A review. Limnol Oceanogr 55:2452–2462. doi: 10.4319/lo.2010.55.6.2452

Fellman JB, Miller MP, Cory RM, et al (2009) Characterizing dissolved organic matter using PARAFAC modeling of fluorescence spectroscopy: a comparison of two models. Environ Sci Technol 43:6228–6234.

Fellman JB, Spencer RGM, Hernes PJ, et al (2010b) The impact of glacier runoff on the biodegradability and biochemical composition of terrigenous dissolved organic matter in near-shore marine ecosystems. Mar Chem 121:112–122. doi: 10.1016/j.marchem.2010.03.009

Findlay S (2010) Stream microbial ecology. J North Am Benthol Soc 29:170–181. doi: 10.1899/09-023.1

Fuentes M, González-Gaitano G, García-Mina JM (2006) The usefulness of UV–visible and fluorescence spectroscopies to study the chemical nature of humic substances from soils and composts. Org Geochem 37:1949–1959. doi: 10.1016/j.orggeochem.2006.07.024

Gao C, Zhu JG, Zhu JY, et al (2004) Nitrogen export from an agriculture watershed in the Taihu Lake area, China. Environ Geochem Health 26:199–207.

Graeber D, Boëchat IG, Encina-montoya F, et al (2015) Global effects of agriculture on fluvial dissolved organic matter. Sci Rep 5:16328. doi: 10.1038/srep16328

Graeber D, Gelbrecht J, Pusch MT, et al (2012) Agriculture has changed the amount and composition of dissolved organic matter in Central European headwater streams. Sci Total Environ 438:435–446. doi: 10.1016/j.scitotenv.2012.08.087

Gremm TJ, Kaplan LA (1998) Dissolved Carbohydrate Concentration, Composition, and Bioavailability to Microbial Heterotrophs in Stream Water. Acta Hydrochim Hydrobiol 26:167–171. doi: 10.1002/(SICI)1521-401X(199805)26:3<167::AID-AHEH167>3.0.CO;2-Q

Guéguen C, Mokhtar M, Perroud A, et al (2016) Mixing and photoreactivity of dissolved organic matter in the Nelson/Hayes estuarine system (Hudson Bay, Canada). J Mar Syst 161:42–48. doi: 10.1016/j.jmarsys.2016.05.005

Guenet B, Danger M, Abbadie L, Lacroix G (2010) Priming effect: bridging the gap between terrestrial and aquatic ecology. Ecology 91:2850–2861.

Guo W, Yang L, Hong H, et al (2011) Assessing the dynamics of chromophoric dissolved organic matter in a subtropical estuary using parallel factor analysis. Mar Chem 124:125–133. doi: 10.1016/j.marchem.2011.01.003

Halbedel S, Büttner O, Weitere M (2012) Linkage between the temporal and spatial variability of dissolved organic matter and whole stream metabolism. Biogeosciences Discuss 9:18253–18293. doi: 10.5194/bgd-9-18253-2012

Hanley KW, Wollheim WM, Salisbury J, et al (2013) Controls on dissolved organic carbon quantity and chemical character in temperate rivers of North America. Global Biogeochem Cycles 27:492–504. doi: 10.1002/gbc.20044

Hansen AM, Kraus TEC, Pellerin BA, et al (2016) Optical properties of dissolved organic matter (DOM): Effects of biological and photolytic degradation. Limnol Oceanogr 61:1015–1032. doi: 10.1002/lno.10270

Harvey ET, Kratzer S, Andersson A (2015) Relationships between colored dissolved organic matter and dissolved organic carbon in different coastal gradients of the Baltic Sea. Ambio 44:392–401. doi: 10.1007/s13280-015-0658-4

Hedges JI, Keil RG, Benner R (1997) What happens to terrestrial organic matter in the ocean? Org Geochem 27:195–212. doi: 10.1016/S0146-6380(97)00066-1

Helms JR, Stubbins A, Perdue EM, et al (2013) Photochemical bleaching of oceanic dissolved organic matter and its effect on absorption spectral slope and fluorescence. Mar Chem 155:81–91. doi: 10.1016/j.marchem.2013.05.015

Helms JR, Stubbins A, Ritchie JD, et al (2008) Absorption spectral slopes and slope ratios as indicators of molecular weight, source, and photobleaching of chromophoric dissolved organic matter. Limnol Oceanogr 53:955–969. doi: 10.4319/lo.2008.53.3.0955

Hernes PJ, Spencer RGM, Dyda RY, et al (2008) The role of hydrologic regimes on dissolved organic carbon composition in an agricultural watershed. Geochim Cosmochim Acta 72:5266–5277. doi: 10.1016/j.gca.2008.07.031

Hiriart-Baer VP, Binding C, Howell TE (2013) Dissolved organic matter quantity and quality in Lake Simcoe compared to two other large lakes in southern Ontario. Inl Waters 3:139–152. doi: 10.5268/IW-3.2.535

Hong H, Yang L, Guo W, et al (2012) Characterization of dissolved organic matter under contrasting hydrologic regimes in a subtropical watershed using PARAFAC model. Biogeochemistry 109:163–174. doi: 10.1007/s10533-011-9617-8

Hood E, Gooseff MN, Johnson SL (2006) Changes in the character of stream water dissolved organic carbon during flushing in three small watersheds, Oregon. J Geophys Res 111:1–8. doi: 10.1029/2005JG000082

Hopkinson CS, Vallino JJ (2005) Efficient export of carbon to the deep ocean through dissolved organic matter. Nature 433:142–145. doi: 10.1038/nature03191

Hosen JD, McDonough OT, Febria CM, Palmer MA (2014) Dissolved organic matter quality and bioavailability changes across an urbanization gradient in headwater streams. Environ Sci Technol 48:7817–7824. doi: 10.1021/es501422z

Hudson N, Baker A, Reynolds D (2007) Fluorescence analysis of dissolved organic matter in natural, waste, and polluted waters - A review. River Res Appl 23:631–649. doi: 10.1002/rra.1005

Huguet A, Vacher L, Relexans S, et al (2009) Properties of fluorescent dissolved organic matter in the Gironde Estuary. Org Geochem 40:706–719. doi: 10.1016/j.orggeochem.2009.03.002

Hur J (2011) Microbial Changes in Selected Operational Descriptors of Dissolved Organic Matters From Various Sources in a Watershed. Water Air Soil Pollut 215:465–476. doi: 10.1007/s11270-010-0491-0

Ingram KT, Dow K, Carter L, Anderson J (Eds.) (2013) Climate of the Southeast United States: Variability, Change, Impacts, and Vulnerability. Island Press, Washington, DC

Jaffé R, Boyer JN, Lu X, et al (2004) Source characterization of dissolved organic matter in a subtropical mangrove-dominated estuary by fluorescence analysis. Mar Chem 84:195–210. doi: 10.1016/j.marchem.2003.08.001

Jaffé R, Cawley KM, Yamashita Y (2014) Applications of excitation emission matrix fluorescence with parallel factor analysis (EEM-PARAFAC) in assessing environmental dynamics of natural dissolved organic matter (DOM) in aquatic environments: A review. ACS Symp Ser 1160:27–73. doi: 10.1021/bk-2014-1160.ch003

Jaffé R, McKnight D, Maie N, et al (2008) Spatial and temporal variations in DOM composition in ecosystems: The importance of long-term monitoring of optical properties. J Geophys Res 113:1–15. doi: 10.1029/2008JG000683

Jaffé R, Yamashita Y, Maie N, et al (2012) Dissolved Organic Matter in Headwater Streams: Compositional Variability across Climatic Regions of North America. Geochim Cosmochim Acta 94:95–108. doi: 10.1016/j.gca.2012.06.031

Jansen B, Kalbitz K, McDowell WH (2014) Dissolved Organic Matter: Linking Soils and Aquatic Systems. Vadose Zo J 13:0. doi: 10.2136/vzj2014.05.0051

Johnson D, Mueller R (2010) The 2009 cropland data layer. Photogramm Eng Remote Sens 76(11):1201-1205.

Jordan TE, Whigham DF, Hofmockel KH, Pittek MA (2003) Nutrient and sediment removal by a restored wetland receiving agricultural runoff. J Environ Qual 32:1534–1547.

Kaiser K, Kalbitz K (2012) Cycling downwards – dissolved organic matter in soils. Soil Biol Biochem 52:29–32. doi: 10.1016/j.soilbio.2012.04.002

Kalscheur KN, Penskar RR, Daley AD, et al (2012) Effects of anthropogenic inputs on the organic quality of urbanized streams. Water Res 46:2515–2524. doi: 10.1016/j.watres.2012.01.043

Karl TR, Melillo JM, Peterson TC (2009) Global Climate Change Impacts in the United States. Cambridge University Press, New Yok, USA

Kaushal SS, Groffman PM, Band LE, et al (2011) Tracking nonpoint source nitrogen pollution in human-impacted watersheds. Environ Sci Technol 45:8225–8232. doi: 10.1021/es200779e

Keller DP, Hood RR (2011) Modeling the seasonal autochthonous sources of dissolved organic carbon and nitrogen in the upper Chesapeake Bay. Ecol Modell 222:1139–1162. doi: 10.1016/j.ecolmodel.2010.12.014

Kellerman AM, Dittmar T, Kothawala DN, Tranvik LJ (2014) Chemodiversity of dissolved organic matter in lakes driven by climate and hydrology. Nat Commun 5:3804. doi: 10.1038/ncomms4804

Korak JA, Dotson AD, Summers RS, Rosario-Ortiz FL (2014) Critical analysis of commonly used fluorescence metrics to characterize dissolved organic matter. Water Res 49:327–338. doi: 10.1016/j.watres.2013.11.025

Kothawala DN, Stedmon CA, Müller RA, et al (2014) Controls of dissolved organic matter quality: evidence from a large-scale boreal lake survey. Glob Chang Biol 20:1101–1114. doi: 10.1111/gcb.12488

Kottek M, Grieser J, Beck C, et al (2006) World map of the Köppen-Geiger climate classification updated. Meteorol Zeitschrift 15:259–263. doi: 10.1127/0941-2948/2006/0130

Kowalczuk P, Cooper WJ, Durako MJ, et al (2010) Characterization of dissolved organic matter fluorescence in the South Atlantic Bight with use of PARAFAC model: Relationships between fluorescence and its components, absorption coefficients and organic carbon concentrations. Mar Chem 118:22–36. doi: 10.1016/j.marchem.2009.10.002

Kraus TEC, Bergamaschi BA, Hernes PJ, et al (2008) Assessing the contribution of wetlands and subsided islands to dissolved organic matter and disinfection byproduct precursors in the Sacramento–San Joaquin River Delta: A geochemical approach. Org Geochem 39:1302–1318. doi: 10.1016/j.orggeochem.2008.05.012

Krishna MS, Prasad VR, Sarma VVSS, et al (2015) Fluxes of dissolved organic carbon and nitrogen to the northern Indian Ocean from the Indian monsoonal rivers. J Geophys Res G Biogeosciences 120:2067–2080. doi: 10.1002/2015JG002912

Lapierre J-F, Frenette J-J (2009) Effects of macrophytes and terrestrial inputs on fluorescent dissolved organic matter in a large river system. Aquat Sci 71:15–24. doi: 10.1007/s00027-009-9133-2

Larsen LG, Aiken GR, Harvey JW, et al (2010) Using fluorescence spectroscopy to trace seasonal DOM dynamics, disturbance effects, and hydrologic transport in the Florida Everglades. J Geophys Res 115:1–14. doi: 10.1029/2009JG001140

Lawaetz AJ, Stedmon CA (2009) Fluorescence Intensity Calibration Using the Raman Scatter Peak of Water. Appl Spectrosc 63:936–940.

Leech DM, Ensign SH, Piehler MF (2016) Spatiotemporal patterns in the export of dissolved organic carbon and chromophoric dissolved organic matter from a coastal, blackwater river. Aquat Sci 78:1–14. doi: 10.1007/s00027-016-0474-3

Leenheer JA (2009) Systematic Approaches to Comprehensive Analyses of Natural Organic Matter. Ann Environ Sci 3:1–130.

Leenheer JA, Croué J-P (2003) Characterizing aquatic dissolved organic matter. Environ Sci Technol 37:18A–26A. doi: 10.1021/es032333c

Liu L, Song C, Yan Z, Li F (2009) Characterizing the release of different composition of dissolved organic matter in soil under acid rain leaching using three-dimensional excitation-emission matrix spectroscopy. Chemosphere 77:15–21. doi: 10.1016/j.chemosphere.2009.06.026

Lochmuller CH, Saavedra SS (1986) Conformational Changes in a Soil Fulvic Acid Measured by Time-Dependent Fluorescence Depolarization. Anal Chem 58:1978–1981.

Lønborg C, Álvarez-Salgado XA, Davidson K, et al (2010) Assessing the microbial bioavailability and degradation rate constants of dissolved organic matter by fluorescence spectroscopy in the coastal upwelling system of the Ria de Vigo. Mar Chem 119:121–129. doi: 10.1016/j.marchem.2010.02.001

Lottig NR, Stanley EH, Maxted JT (2012) Assessing the influence of upstream drainage lakes on fluvial organic carbon in a wetland-rich region. J Geophys Res Biogeosciences 117:1–10. doi: 10.1029/2012JG001983

Lovley DR, Coates JD, BluntHarris EL, et al (1996) Humic substances as electron acceptors for microbial respiration. Nature 382:445–448. doi: 10.1038/382445a0

Lu Y, Bauer JE, Canuel E a., et al (2014a) Effects of land use on sources and ages of inorganic and organic carbon in temperate headwater streams. Biogeochemistry 119:275–292. doi: 10.1007/s10533-014-9965-2

Lu Y, Bauer JE, Canuel EA, et al (2013) Photochemical and microbial alteration of dissolved organic matter in temperate headwater streams associated with different land use. J Geophys Res Biogeosciences 118:566–580. doi: 10.1002/jgrg.20048

Lu Y, Edmonds JW, Yamashita Y, et al (2014b) Spatial variation in the origin and reactivity of dissolved organic matter in Oregon-Washington coastal waters. Ocean Dyn 65:17–32. doi: 10.1007/s10236-014-0793-7

Maie N, Boyer JN, Yang C, Jaffé R (2006a) Spatial, geomorphological, and seasonal variability of CDOM in estuaries of the Florida Coastal Everglades. Hydrobiologia 569:135–150. doi: 10.1007/s10750-006-0128-x

Maie N, Jaffé R, Miyoshi T, Childers DL (2006b) Quantitative and Qualitative Aspects of Dissolved Organic Carbon Leached from Senescent Plants in an Oligotrophic Wetland. Biogeochemistry 78:285–314. doi: 10.1007/s10533-005-4329-6

Maie N, Yamashita Y, Cory RM, et al (2012) Application of excitation emission matrix fluorescence monitoring in the assessment of spatial and seasonal drivers of dissolved organic matter composition: Sources and physical disturbance controls. Appl Geochemistry 27:917–929. doi: 10.1016/j.apgeochem.2011.12.021

Mann PJ, Davydova a., Zimov N, et al (2012) Controls on the composition and lability of dissolved organic matter in Siberia's Kolyma River basin. J Geophys Res Biogeosciences 117:1–15. doi: 10.1029/2011JG001798

Markager S, Vincent WF (2000) Spectral light attenuation and the absorption of UV and blue light in natural waters. Limnol Oceanogr 45:642–650.

Marschner B, Kalbitz K (2003) Controls of bioavailability and biodegradability of dissolved organic matter in soils. Geoderma 113:211–235. doi: 10.1016/S0016-7061(02)00362-2

Massicotte P, Frenette J-J (2013) A mechanistic-based framework to understand how dissolved organic carbon is processed in a large fluvial lake. Limnol Oceanogr Fluids Environ 3:139–155. doi: 10.1215/21573689-2372976

Mayer LM, Thornton KH, Schick LL (2011) Bioavailability of organic matter photodissolved from coastal sediments. Aquat. Microb. Ecol. 64, 275–284. doi:10.3354/ame01530

McCallister SL, Bauer JE, Kelly J, Ducklow HW (2005) Effects of sunlight on decomposition of estuarine dissolved organic C, N and P and bacterial metabolism. Aquat Microb Ecol 40:25–35. doi: 10.3354/ame040025

McKnight DM, Boyer EW, Westerhoff PK, et al (2001) Spectrofluorometric Characterization of Dissolved Organic Matter for Indication of Precursor Organic Material and Aromaticity. Limnol Oceanogr 46:38–48. doi: 10.4319/lo.2001.46.1.0038

McKnight DM, Hood E, Klapper L (2003) Trace organic moieties of dissolved organic material in natural waters. In: Findlay SEG, Sinsabaugh RL (eds) Aquatic Ecosystems: Interactivity of Dissolved Organic Matter. Academic Press, Amsterdam, The Netherlands, pp 71–96

McKnight DM, Hornberger GM, Bencala KE, Boyer EW (2002) In-stream sorption of fulvic acid in an acidic stream: A stream-scale transport experiment. Water Resour Res 38:1–12. doi: 10.1029/2001WR000269

Meng F, Huang G, Yang X, et al (2013) Identifying the sources and fate of anthropogenically impacted dissolved organic matter (DOM) in urbanized rivers. Water Res 47:5027–5039. doi: 10.1016/j.watres.2013.05.043

Milbrandt EC, Coble PG, Conmy RN, et al (2010) Evidence for the production of marine fluorescent dissolved organic matter in coastal environments and a possible mechanism for formation and dispersion. Limnol Oceanogr 55:2037–2051. doi: 10.4319/lo.2010.55.5.2037

Miller MP, Boyer EW, McKnight DM, et al (2016) Variation of organic matter quantity and quality in streams at Critical Zone Observatory watersheds. Water Resour Res 52:600–612. doi: 10.1002/2016WR018970

Miller MP, McKnight DM (2010) Comparison of seasonal changes in fluorescent dissolved organic matter among aquatic lake and stream sites in the Green Lakes Valley. J Geophys Res 115:1–14. doi: 10.1029/2009JG000985

Mladenov N, Zheng Y, Miller MP, et al (2010) Dissolved organic matter sources and consequences for iron and arsenic mobilization in Bangladesh aquifers. Environ Sci Technol 44:123–128. doi: 10.1021/es901472g

Molinero J, Burke RA (2009) Effects of land use on dissolved organic matter biogeochemistry in Piedmont headwater streams of the southeastern united states. Hydrobiologia 635:289–308. doi: 10.1007/s10750-009-9921-7

Mopper K, Kieber DJ, Stubbins A (2015) Marine Photochemistry of Organic Matter : Processes and Impacts. In: Hansell DA, Carlson CA (eds) Biogeochemistry of Marine Dissolved Organic Matter, Second. Academic Press, New York, USA, pp 389–450

Mopper K, Zhou X, Kieber RJ, et al (1991) Photochemical degradation of dissolved organic carbon and its impact on oceanic carbon cycle. Nature 353:60–62.

Moran MA, Sheldon Jr. WM, Zepp RG (2000) Carbon loss and optical property changes during long-term photochemical and biological degradation of estuarine dissolved organic matter. Limnol Oceanogr 45:1254–1264.

Moran MA, Zepp RG (1997) Role of Photoreactions in the Formation of Biologically Labile Compounds from Dissolved Organic Matter. Limnol Oceanogr 42:1307–1316. doi: 10.4319/lo.1997.42.6.1307

Mulholland MR, Glibert PM, Berg GM, et al (1998) Extracellular amino acid oxidation by microplankton: A cross-ecosystem comparison. Aquat Microb Ecol 15:141–152. doi: 10.3354/ame015141

Mulholland PJ (2003) Large-scale patterns of dissolved organic carbon concentration, flux and sources. In: Findlay SEG, Sinsabaugh RL (eds) Aquatic Ecosystems: Interactivity of Dissolved Organic Matter. Academic Press, Burlington, pp 139–159

Mulholland PJ, Hill WR (1997) Seasonal patterns in streamwater nutrient and dissolved organic carbon concentrations: Separating catchment flow path and in-stream effects. Water Resour Res 33:1297–1306. doi: 10.1029/97WR00490

Murphy KR, Butler KD, Spencer RGM, et al (2010) Measurement of dissolved organic matter fluorescence in aquatic environments: an interlaboratory comparison. Environ Sci Technol 44:9405–9412. doi: 10.1021/es102362t

Murphy KR, Hambly A, Singh S, et al (2011) Organic matter fluorescence in municipal water recycling schemes: toward a unified PARAFAC model. Environ Sci Technol 45:2909–2916. doi: 10.1021/es103015e

Murphy KR, Stedmon CA, Graeber D, Bro R (2013) Fluorescence spectroscopy and multi-way techniques. PARAFAC. Anal Methods 5:6557. doi: 10.1039/c3ay41160e

Naden PS, Old GH, Eliot-Laize C, et al (2010) Assessment of natural fluorescence as a tracer of diffuse agricultural pollution from slurry spreading on intensely-farmed grasslands. Water Res 44:1701–1712. doi: 10.1016/j.watres.2009.11.038

Nelson CE, Wear EK (2014) Microbial diversity and the lability of dissolved organic carbon. Proc Natl Acad Sci U S A 111:7166–7167. doi: 10.1073/pnas.1405751111

O'Donnell JA, Aiken GR, Kane ES, Jones JB (2010) Source water controls on the character and origin of dissolved organic matter in streams of the Yukon River basin, Alaska. J Geophys Res 115:1–12. doi: 10.1029/2009JG001153

Obernosterer I, Benner R (2004) Competition between biological and photochemical processes in the mineralization of dissolved organic carbon. Limnol Oceanogr 49:117–124. doi: 10.4319/lo.2004.49.1.0117

Oestreich WK, Ganju NK, Pohlman JW, Suttles SE (2016) Colored dissolved organic matter in shallow estuaries: Relationships between carbon sources and light attenuation. Biogeosciences 13:583–595. doi: 10.5194/bg-13-583-2016

Ohno T (2002) Fluorescence Inner-Filtering Correction for Determining the Humification Index of Dissolved Organic Matter. Environ Sci Technol 36:742–746. doi: 10.1021/es0155276

Olefeldt D, Turetsky MR, Blodau C (2013) Altered Composition and Microbial versus UV-Mediated Degradation of Dissolved Organic Matter in Boreal Soils Following Wildfire. Ecosystems 16:1396–1412. doi: 10.1007/s10021-013-9691-y

Opsahl S, Benner R (1998) Photochemical reactivity of dissolved lignin in river and ocean waters. Limnol Oceanogr 43:1297–1304. doi: 10.4319/lo.1998.43.6.1297

Osburn CL, Boyd TJ, Montgomery MT, et al (2016) Optical Proxies for Terrestrial Dissolved Organic Matter in Estuaries and Coastal Waters. Front Mar Sci 2:127. doi: 10.3389/fmars.2015.00127

Osburn CL, Mikan MP, Etheridge JR, et al (2015) Seasonal variation in the quality of dissolved and particulate organic matter exchanged between a salt marsh and its adjacent estuary. J Geophys Res G Biogeosciences 120:1430–1449. doi: 10.1002/2014JG002897

Paerl HW, Valdes LM, Peierls BL, et al (2006) Anthropogenic and climatic influences on the eutrophication of large estuarine ecosystems. Limnol Oceanogr 51:448–462. doi: 10.4319/lo.2006.51.1_part_2.0448

Pandey M, Pandey AK, Mishra A, Tripathi BD (2015) Assessment of metal species in river Ganga sediment at Varanasi, India using sequential extraction procedure and SEM-EDS. Chemosphere 134:466–474. doi: 10.1016/j.chemosphere.2015.04.047

Pandey U (2013) The influence of DOC trends on light climate and periphyton biomass in the Ganga River, Varanasi, India. Bull Environ Contam Toxicol 90:143–147. doi: 10.1007/s00128-012-0879-1

Para J, Coble PG, Charriere B, et al (2010) Fluorescence and absorption properties of chromophoric dissolved organic matter (CDOM) in coastal surface waters of the northwestern Mediterranean Sea, influence of the Rhone River. Biogeosciences 7:4083–4103. doi: 10.5194/bg-7-4083-2010

Pellerin BA, Saraceno JF, Shanley JB, et al (2011) Taking the pulse of snowmelt: in situ sensors reveal seasonal, event and diurnal patterns of nitrate and dissolved organic matter variability in an upland forest stream. Biogeochemistry 108:183–198. doi: 10.1007/s10533-011-9589-8

Petrone KC, Fellman JB, Hood E, et al (2011) The origin and function of dissolved organic matter in agro-urban coastal streams. J Geophys Res 116:1–13. doi: 10.1029/2010JG001537

Peuravuori J, Pihlaja K (1997) Molecular size distribution and spectroscopic properties of aquatic humic substances. Anal Chim Acta 337: 133-149.

Pinckney JL, Wee JL, Hou A, Walker ND (2009) Phytoplankton community structure responses to urban effluent inputs following Hurricanes Katrina and Rita. Mar Ecol Prog Ser 387:137–146. doi: 10.3354/meps08091

Post WM, Kwon KC (2000) Soil carbon sequestration and land-use change: processes and potential. Glob Chang Biol 6:317–327. doi: 10.1046/j.1365-2486.2000.00308.x

Prasad AK, Singh RP, Singh S, Nanda DS (2007) GPS and satellite meteorology for understanding monsoon dynamics over the Indian sub-continent. In: Quantification and Reduction of Predictive Uncertainty for Sustainable Water Resources Management. IAHS Publications, Perugia, Italy, pp 33–39

Qualls RG (2013) Dissolved Organic Matter. In: DeLaune RD, Reddy KR, Richardson CJ, Megonigal P (eds) Methods in Biogeochemistry of Wetlands, SSSA Book . Soil Science Society of America, Madison, WI, USA, pp 1–14

Qualls RG, Haines BL, Swank WT, Tyler SW (2002) Retention of soluble organic nutrients by a forested. Biogeochemistry 61:135–171.

Rai PK, Mishra a, Tripathi BD (2010) Heavy metal and microbial pollution of the River Ganga: A case study of water quality at Varanasi. Aquat Ecosyst Health Manag 13:352–361. doi: 10.1080/14634988.2010.528739

Raymond PA, Spencer RGM (2014) Riverine DOM. Biogeochem Mar Dissolved Org Matter Second Ed 509–533. doi: 10.1016/B978-0-12-405940-5.00011-X

Roelke DL, Cotner JB, Montoya J V., et al (2006) Optically determined sources of allochthonous organic matter and metabolic characterizations in a tropical oligotrophic river and associated lagoon. J North Am Benthol Soc 25:185–197. doi: 10.1899/0887-3593(2006)25

Romera-Castillo C, Sarmento H, Alvarez-Salgado XA, et al (2011) Net production/consumption of fluorescent colored dissolved organic matter by natural bacterial assemblages growing on marine phytoplankton exudates. Appl Environ Microbiol 77:7490–7498. doi: 10.1128/AEM.00200-11

Santín C, Yamashita Y, Otero XL, et al (2009) Characterizing humic substances from estuarine soils and sediments by excitation-emission matrix spectroscopy and parallel factor analysis. Biogeochemistry 96:131–147. doi: 10.1007/s10533-009-9349-1

Santos L, Pinto A, Filipe O, et al (2016) Insights on the Optical Properties of Estuarine DOM – Hydrological and Biological Influences. PLoS One 11:e0154519. doi: 10.1371/journal.pone.0154519

Santos L, Santos EBH, Dias JM, et al (2014) Photochemical and microbial alterations of DOM spectroscopic properties in the estuarine system Ria de Aveiro. Photochem Photobiol Sci 1146–1159. doi: 10.1039/c4pp00005f

Schiebel HN, Wang X, Chen RF, Peri F (2015) Photochemical Release of Dissolved Organic Matter from Resuspended Salt Marsh Sediments. Estuaries and Coasts 38:1692–1705. doi: 10.1007/s12237-014-9893-3

Schrumpf M, Zech W, Lehmann J, Lyaruu HVC (2006) TOC, TON, TOS and TOP in Rainfall, Throughfall, Litter Percolate and Soil Solution of a Montane Rainforest Succession at Mt. Kilimanjaro, Tanzania. Biogeochemistry 78:361–387. doi: 10.1007/s10533-005-4428-4

Schuster PF, Shanley JB, Marvin-Dipasquale M, et al (2008) Mercury and Organic Carbon Dynamics During Runoff Episodes from a Northeastern USA Watershed. Water Air Soil Pollut 187:89–108. doi: 10.1007/s11270-007-9500-3

Seager R, Tzanova A, Nakamura J (2009) Drought in the Southeastern United States: Causes, variability over the last millennium, and the potential for future hydroclimate change. J Clim 22:5021–5045. doi: 10.1175/2009JCLI2683.1

Sebestyen SD, Boyer EW, Shanley JB, et al (2008) Sources, transformations, and hydrological processes that control stream nitrate and dissolved organic matter concentrations during snowmelt in an upland forest. Water Resour Res 44:1–14. doi: 10.1029/2008WR006983

Shank GC, Evans A, Yamashita Y, Jaffé R (2011) Solar radiation-enhanced dissolution of particulate organic matter from coastal marine sediments. Limnol Oceanogr 56:577–588. doi: 10.4319/lo.2011.56.2.0577

Shank GC, Nelson K, Montagna PA (2009) Importance of CDOM distribution and photoreactivity in a shallow Texas estuary. Estuaries and Coasts 32:661–677. doi: 10.1007/s12237-009-9159-7

Shank GC, Zepp RG, Vähätalo A, et al (2010) Photobleaching kinetics of chromophoric dissolved organic matter derived from mangrove leaf litter and floating Sargassum colonies. Mar Chem 119:162–171. doi: 10.1016/j.marchem.2010.01.003

Shank GC, Zepp RG, Whitehead RF, Moran MA (2005) Variations in the spectral properties of freshwater and estuarine CDOM caused by partitioning onto river and estuarine sediments. Estuar Coast Shelf Sci 65:289–301. doi: 10.1016/j.ecss.2005.06.009

Sharip Z, Yanagawa R, Terasawa T (2016) Eco-hydrodynamic Modelling of Chini Lake: Model Description. Environ Model Assess 21:193–210. doi: 10.1007/s10666-015-9464-4

Sharma S, Roy A, Agrawal M (2016) Spatial variations in water quality of river Ganga with respect to land uses in Varanasi. Environ Sci Pollut Res. doi: 10.1007/s11356-016-7411-9

Sharma Y (1997) Case Study 1 - The Ganga, India. Water Pollut Control - A Guide to Use Water Qual Manag Princ 12.

Shiller AM, Duan S, Erp P van, et al (2006) Photo-oxidation of dissolved organic matter in river water and its effect on trace element speciation. Limnol Oceanogr 51:1716–1728. doi: 10.4319/lo.2006.51.4.1716

Singh M, Singh AK (2007) Bibliography of environmental studies in natural characteristics and anthropogenic influences on the Ganga River. Environ Monit Assess 129:421–432. doi: 10.1007/s10661-006-9374-7

Singh N (2010) Physicochemical properties of polluted water of river Ganga at Varanasi. Int J Energy Environ 1:823–832.

Singh S, D'Sa E, Swenson E (2010b) Seasonal variability in CDOM absorption and fluorescence properties in the Barataria Basin, Louisiana, USA. J Environ Sci 22:1481–1490. doi: 10.1016/S1001-0742(09)60279-5

Singh S, D'Sa EJ, Swenson EM (2010a) Chromophoric dissolved organic matter (CDOM) variability in Barataria Basin using excitation-emission matrix (EEM) fluorescence and parallel factor analysis (PARAFAC). Sci Total Environ 408:3211–3222. doi: 10.1016/j.scitotenv.2010.03.044

Singh S, Dash P, Silwal S, et al (2017) Influence of land use and land cover on the spatial variability of dissolved organic matter in multiple aquatic environments. Environ Sci Pollut Res 24(16):14124-14141. doi: 10.1007/s11356-017-8917-5

Singh S, Dutta S, Inamdar S (2014a) Land application of poultry manure and its influence on spectrofluorometric characteristics of dissolved organic matter. Agric Ecosyst Environ 193:25–36. doi: 10.1016/j.agee.2014.04.019

Singh S, Inamdar S, Mitchell M (2015) Changes in dissolved organic matter (DOM) amount and composition along nested headwater stream locations during baseflow and stormflow. Hydrol Process 29:1505–1520. doi: 10.1002/hyp.10286

Singh S, Inamdar S, Mitchell M, McHale P (2014b) Seasonal pattern of dissolved organic matter (DOM) in watershed sources: influence of hydrologic flow paths and autumn leaf fall. Biogeochemistry 118:321–337. doi: 10.1007/s10533-013-9934-1

Singh S, Inamdar S, Scott D (2013) Comparison of Two PARAFAC Models of Dissolved Organic Matter Fluorescence for a Mid-Atlantic Forested Watershed in the USA. J Ecosyst 2013:1–16. doi: 10.1155/2013/532424

Spencer RGM, Aiken GR, Dornblaser MM, et al (2013) Chromophoric dissolved organic matter export from U.S. rivers. Geophys Res Lett 40:1575–1579. doi: 10.1002/grl.50357

Spencer RGM, Baker A, Ahad JME, et al (2007) Discriminatory classification of natural and anthropogenic waters in two U.K. estuaries. Sci Total Environ 373:305–323. doi: 10.1016/j.scitotenv.2006.10.052

Spencer RGM, Stubbins A, Hernes PJ, et al (2009) Photochemical degradation of dissolved organic matter and dissolved lignin phenols from the Congo River. J Geophys Res Biogeosciences 114:1–12. doi: 10.1029/2009JG000968

Stedmon CA, Markager S, Sondergaard M, et al (2006) Dissolved organic matter (DOM) export to a temperate estuary: Seasonal variations and implications of land use. Estuaries and Coasts 29:388–400. doi: 10.1007/BF02784988

Stedmon CA, Bro R (2008) Characterizing dissolved organic matter fluorescence with parallel factor analysis: a tutorial. Limnol Oceanogr Methods 6:572–579.

Stedmon CA, Markager S (2005) Resolving the variability in dissolved organic matter fluorescence in a temperate estuary and its catchment using PARAFAC analysis. Limnol Oceanogr 50:686–697. doi: 10.4319/lo.2005.50.2.0686

Stedmon CA, Markager S (2005) Tracing the production and degradation of autochthonous fractions of dissolved organic matter using fluorescence analysis. Limnol Oceanogr 50:1415–1426. doi: 10.4319/lo.2005.50.5.1415

Stedmon CA, Markager S, Bro R (2003) Tracing dissolved organic matter in aquatic environments using a new approach to fluorescence spectroscopy. Mar Chem 82:239–254. doi: 10.1016/S0304-4203(03)00072-0

Stedmon CA, Markager S, Tranvik L, et al (2007) Photochemical production of ammonium and transformation of dissolved organic matter in the Baltic Sea. Mar Chem 104:227–240. doi: 10.1016/j.marchem.2006.11.005

Stedmon CA, Thomas DN, Papadimitriou S, et al (2011) Using fluorescence to characterize dissolved organic matter in Antarctic sea ice brines. J Geophys Res 116:1–24. doi: 10.1029/2011JG001716

Striegl RG, Dornblaser MM, Aiken GR, et al (2007) Carbon export and cycling by the Yukon, Tanana, and Porcupine rivers, Alaska, 2001-2005. Water Resour Res 43:1–9. doi: 10.1029/2006WR005201

Stubbins A, Spencer RGM, Chen H, et al (2010) Illuminated darkness: Molecular signatures of Congo River dissolved organic matter and its photochemical alteration as revealed by ultrahigh precision mass spectrometry. Limnol Oceanogr 55:1467–1477. doi: 10.4319/lo.2010.55.4.1467

Sun L, Mopper K (2016) Studies on Hydroxyl Radical Formation and Correlated Photoflocculation Process Using Degraded Wood Leachate as a CDOM Source. Front Mar Sci 2:117. doi: 10.3389/fmars.2015.00117

Sun Q, Wang C, Wang P, et al (2014) Absorption and fluorescence characteristics of chromophoric dissolved organic matter in the Yangtze Estuary. Environ Sci Pollut Res 21:3460–3473. doi: 10.1007/s11356-013-2287-4

Tank SE, Lesack LFW, Gareis JAL, et al (2011) Multiple tracers demonstrate distinct sources of dissolved organic matter to lakes of the Mackenzie Delta, western Canadian Arctic. Limnol Oceanogr 56:1297–1309. doi: 10.4319/lo.2011.56.4.1297

Tedetti M, Cuet P, Guigue C, Goutx M (2011) Characterization of dissolved organic matter in a coral reef ecosystem subjected to anthropogenic pressures (La Réunion Island, Indian Ocean) using multi-dimensional fluorescence spectroscopy. Sci Total Environ 409:2198–2210. doi: 10.1016/j.scitotenv.2011.01.058

Thurman EM (1985) Organic Geochemistry of Natural Waters. Martinus Nijhoff / Dr W. Junk Publishers, Dordrecht, The Netherlands

Tiwari A, Dwivedi AC, Mayank P (2016) Time Scale Changes in the Water Quality of the Ganga River, India and Estimation of Suitability for Exotic and Hardy Fishes. Hydrol Curr Res 7:1–8. doi: 10.4172/2157-7587.1000254

Toosi ER, Schmidt JP, Castellano MJ (2014) Land use and hydrologic flowpaths interact to affect dissolved organic matter and nitrate dynamics. Biogeochemistry 120:89–104. doi: 10.1007/s10533-014-9983-0

Tranvik LJ, Downing J a., Cotner JB, et al (2009) Lakes and reservoirs as regulators of carbon cycling and climate. Limnol Oceanogr 54:2298–2314. doi: 10.4319/lo.2009.54.6_part_2.2298

Uher G, Hughes C, Henry G, Upstill-Goddard RC (2001) Non-conservative mixing behavior of colored dissolved organic matter in a humic-rich, turbid estuary. Geophys Res Lett 28:3309–3312.

USDA (2017) web: https://gdg.sc.egov.usda.gov/GDGOrder.aspx accessed in February 2017.

USDA (2015) web: https://gdg.sc.egov.usda.gov/GDGOrder.aspx accessed in November 2015.

Vähätalo A V, Zepp RG (2005) Photochemical Mineralization of Dissolved Organic Nitrogen to Ammonium in the Baltic Sea Photochemical Mineralization of Dissolved Organic Nitrogen to Ammonium in the Baltic Sea. Environ Sci Technol 39:6985–6992. doi: 10.1021/es050142z

Vähätalo A V., Aarnos H, Hoikkala L, Lignell R (2011) Photochemical transformation of terrestrial dissolved organic matter supports hetero- and autotrophic production in coastal waters. Mar Ecol Prog Ser 423:1–14. doi: 10.3354/meps09010

Vannote RL, Minshall GW, Cummins KW, et al (1980) The River Continuum Concept. Can J Fish Aquat Sci 37:130–137.

Vazquez E, Amalfitano S, Fazi S, Butturini A (2010) Dissolved organic matter composition in a fragmented Mediterranean fluvial system under severe drought conditions. Biogeochemistry 102:59–72. doi: 10.1007/s10533-010-9421-x

Vodacek A, Hoge FE, Swift RN, et al (1995) The use of in situ and airborne fluorescence measurements to determine UV absorption coefficients and DOC concentrations in surface waters. Limnol Oceanogr 40:411–415. doi: 10.4319/lo.1995.40.2.0411

von Schiller D, Graeber D, Ribot M, et al (2015) Hyrological transitions drive dissolved organic matter quantity and composition in a temporary Mediterranean stream. Biogeochemistry 123:429–446. doi: 10.1007/s10533-015-0077-4

Wachenfeldt E von, Sobek S, Bastviken D, Tranvik LJ (2008) Linking allochthonous dissolved organic matter and boreal lake sediment carbon sequestration: The role of light-mediated flocculation. Limnol Oceanogr 53:2416–2426, doi:10.4319/lo.2008.53.6.2416. doi: 10.4319/lo.2008.53.6.2416

Wagner LE, Vidon P, Tedesco LP, Gray M (2008) Stream nitrate and DOC dynamics during three spring storms across land uses in glaciated landscapes of the Midwest. J Hydrol 362:177–190. doi: 10.1016/j.jhydrol.2008.08.013

Walsh J, Wuebbles D, Hayhoe K, et al (2014) Our changing climate. In: Melillo JM, Richmond T, Yohe GW (eds) Climate Change Impacts in the United States: The Third National Climate Assessment. U.S. Global Change Research Program, pp 19–67

Wang L, Wu F, Zhang R, et al (2009) Characterization of dissolved organic matter fractions from Lake Hongfeng, Southwestern China Plateau. J Environ Sci 21:581–588. doi: 10.1016/S1001-0742(08)62311-6

Wang X, Chen RF, Cable JE, Cherrier J (2014) Leaching and microbial degradation of dissolved organic matter from salt marsh plants and seagrasses. Aquat Sci 76:595–609. doi: 10.1007/s00027-014-0357-4

Watanabe A, Moroi K, Sato H, et al (2012) Contributions of humic substances to the dissolved organic carbon pool in wetlands from different climates. Chemosphere 88:1265–1268. doi: 10.1016/j.chemosphere.2012.04.005

Wehr JD, Lonergan SP, Thorp JH (1997) Concentrations and controls of dissolved organic matter in a constricted-channel region of the Ohio River. Biogeochemistry 38:41–65. doi: 10.1023/A:1005708326368

Weishaar JL, Aiken GR, Bergamaschi BA, et al (2003) Evaluation of specific ultraviolet absorbance as an indicator of the chemical composition and reactivity of dissolved organic carbon. Environ Sci Technol 37:4702–4708. doi: 10.1021/es030360x

Westerhoff P, Chen W, Esparza M (2001) Fluorescence analysis of a standard fulvic acid and tertiary treated wastewater. J Environ Qual 30:2037–2046.

Wiegner TN, Seitzinger SP (2001) Photochemical and microbial degradation of external dissolved organic matter inputs to rivers. Aquat Microb Ecol 24:27–40. doi: 10.3354/ame024027

Wiegner TN, Seitzinger SP (2004) Seasonal bioavailability of dissolved organic carbon and nitrogen from pristine and polluted freshwater wetlands. Limnol Oceanogr 49:1703–1712. doi: 10.4319/lo.2004.49.5.1703

Williams CJ, Yamashita Y, Wilson HF, et al (2010) Unraveling the role of land use and microbial activity in shaping dissolved organic matter characteristics in stream ecosystems. Limnol Oceanogr 55:1159–1171. doi: 10.4319/lo.2010.55.3.1159

Williams MW, Knauf M, Cory R, et al (2006) Nitrate Content and Potential Microbial Signature of Rock Glacier Outflow, Colorado Front Range. Earth Surf Process Landforms 1–16. doi: 10.1002/esp.1455

Wilson HF, Xenopoulos MA (2009) Effects of agricultural land use on the composition of fluvial dissolved organic matter. Nat Geosci 2:37–41. doi: 10.1038/ngeo391

Wilson HF, Xenopoulos MA (2008) Ecosystem and Seasonal Control of Stream Dissolved Organic Carbon Along a Gradient of Land Use. Ecosystems 11:555–568. doi: 10.1007/s10021-008-9142-3

Xue J, Lee C, Wakeham SG, Armstrong, RA (2011). Using principal component analysis (PCA) of sinking particles in the ocean. Org Geochem 42:356-367. doi:10.1016/j.orggeochem.2011.01.012

Ya C, Anderson W, Jaffé R (2015) Assessing dissolved organic matter dynamics and source strengths in a subtropical estuary: Application of stable carbon isotopes and optical properties. Cont Shelf Res 92:98–107. doi: 10.1016/j.csr.2014.10.005

Yamashita Y, Jaffé R (2008) Characterizing the Interactions between Trace Metals and Dissolved Organic Matter Using Excitation-Emission Matrix and Parallel Factor Analysis. Environ Sci Technol 42:7374–7379. doi: 10.1021/es801357h

Yamashita Y, Jaffé R, Maie N, Tanoue E (2008) Assessing the dynamics of dissolved organic matter (DOM) in coastal environments by excitation emission matrix fluorescence and parallel factor analysis (EEM-PARAFAC). Limnol Oceanogr 53:1900–1908. doi: 10.4319/lo.2008.53.5.1900

Yamashita Y, Maie N, Briceño H, Jaffé R (2010) Optical characterization of dissolved organic matter in tropical rivers of the Guayana Shield, Venezuela. J Geophys Res 115:1–15. doi: 10.1029/2009JG000987

Yamashita Y, Nosaka Y, Suzuki K, et al (2013) Photobleaching as a factor controlling spectral characteristics of chromophoric dissolved organic matter in open ocean. Biogeosciences 10:7207–7217. doi: 10.5194/bg-10-7207-2013

Yamashita Y, Tanoue E (2003) Chemical characterization of protein-like fluorophores in DOM in relation to aromatic amino acids. Mar Chem 82:255–271. doi: 10.1016/S0304-4203(03)00073-2

Yang L, Chen C-TA, Lui H-K, et al (2016) Effects of microbial transformation on dissolved organic matter in the east Taiwan Strait and implications for carbon and nutrient cycling. Estuar Coast Shelf Sci 180:59–68. doi: 10.1016/j.ecss.2016.06.021

Yang L, Hong H, Guo W, et al (2012) Effects of changing land use on dissolved organic matter in a subtropical river watershed, southeast China. Reg Environ Chang 12:145–151. doi: 10.1007/s10113-011-0250-9

Yang X, Meng F, Huang G, et al (2014) Sunlight-induced changes in chromophores and fluorophores of wastewater-derived organic matter in receiving waters--the role of salinity. Water Res 62:281–92. doi: 10.1016/j.watres.2014.05.050

Yates CA, Johnes PJ, Spencer RGM (2016) Assessing the drivers of dissolved organic matter export from two contrasting lowland catchments, U.K. Sci Total Environ. doi: 10.1016/j.scitotenv.2016.06.211

Zepp RG, Erickson III DJ, Paul ND, Sulzberger B (2006) Interactive effects of solar UV radiation and climate change on biogeochemical cycling.

Zhang Y, Liu M, Qin B, Feng S (2009) Photochemical degradation of chromophoric-dissolved organic matter exposed to simulated UV-B and natural solar radiation. Hydrobiologia 627:159–168. doi: 10.1007/s10750-009-9722-z

Zhang Y, Zhang E, Yin Y, et al (2010) Characteristics and sources of chromophoric dissolved organic matter in lakes of the Yungui Plateau, China, differing in trophic state and altitude. Limnol Oceanogr 55:2645–2659. doi: 10.4319/lo.2010.55.6.2645

Zsolnay A (2003) Dissolved organic matter: artefacts, definitions, and functions. Geoderma 113:187–209. doi: 10.1016/S0016-7061(02)00361-0

Zsolnay A, Baigar E, Jimenez M, et al (1999) Differentiating with fluorescence spectroscopy the sources of dissolved organic matter in soils subjected to drying. Chemosphere 38:45–50.

Zurbrügg R, Suter S, Lehmann MF, et al (2013) Organic carbon and nitrogen export from a tropical dam-impacted floodplain system. Biogeosciences 10:23–38. doi: 10.5194/bg-10-23-2013

APPENDIX A

TABLE

Table A.1 Distribution of all variables including PARAFAC components, optical indices, biochemical, and physical parameters measured for five lakes, an estuary, and a coastal region (eastern Mississippi Sound) in the Mississippi, USA in the study. The number of samples (n) for each water body is shown in the brackets in the top row.

Water Body **Parameters computed / measured**	**Lakes** **(n = 149)**	**Estuary** **(n = 61)**	**Coastal** **(n = 65)**
PARAFAC Components			
Component 1, C1	0.71 ± 0.05^{b} (0.62 − 0.82)	0.77 ± 0.03^{a} (0.73 − 0.83)	0.64 ± 0.02^{c} (0.60 − 0.70)
Component 2, C2	0.47 ± 0.04^{b} (0.39 − 0.56)	0.45 ± 0.05^{c} (0.36 − 0.51)	0.52 ± 0.02^{a} (0.49 − 0.56)
Component 3, C3	0.17 ± 0.02^{c} (0.13 − 0.23)	0.23 ± 0.02^{a} (0.21 − 0.28)	0.19 ± 0.01^{b} (0.15 − 0.21)
Component 4, C4	0.16 ± 0.06^{b} (0.08 − 0.36)	0.21 ± 0.10^{a} (0.08 − 0.40)	0.22 ± 0.04^{a} (0.14 − 0.37)
Component 5, C5	0.09 ± 0.04^{b} (0.00 − 0.18)	0.03 ± 0.01^{c} (0.00 − 0.06)	0.16 ± 0.02^{a} (0.12 − 0.20)
Optical Indices			
Humification Indices, HIX	4.00 ± 3.33^{b} (0.15 − 23.06)	5.64 ± 3.98^{a} (1.41 − 28.19)	4.77 ± 3.76^{ab} (0.60 − 17.18)
Biological Indices, BIX	0.66 ± 0.05^{b} (0.57 − 0.80)	0.62 ± 0.07^{c} (0.54 − 0.71)	0.76 ± 0.03^{a} (0.66 − 0.80)
Fluorescence Indices, FI	1.46 ± 0.05^{b} (1.37 − 1.58)	1.44 ± 0.05^{c} (1.32 − 1.51)	1.48 ± 0.02^{a} (1.43 − 1.54)
Absorption Coefficients, a_{254} (m^{-1})	41.38 ± 16.95^{b} (13.20 − 89.37)	50.16 ± 27.27^{a} (21.09 − 138.56)	18.65 ± 7.14^{c} (7.37 − 50.54)
Spectral Slope Ratio, S_R	1.01 ± 0.25^{b} (0.52 − 2.19)	0.80 ± 0.09^{b} (0.69 − 1.03)	1.79 ± 2.44^{a} (0.74 − 14.32)
Spectral Slope, $S_{254-436}$ (nm^{-1})	0.016 ± 0.002^{b} (0.013 − 0.028)	0.015 ± 0.001^{c} (0.014 − 0.018)	0.018 ± 0.003^{a} (0.014 − 0.035)
Biochemical Parameters			
NH_4-N (mg L^{-1})	0.08 ± 0.06^{b} (0.00 − 0.33)	0.05 ± 0.03^{c} (0.00 − 0.15)	0.13 ± 0.05^{a} (0.01 − 0.29)
NO_3-N (mg L^{-1})	0.24 ± 0.28^{a} (0.00 − 1.94)	0.28 ± 0.18^{a} (0.06 − 1.04)	0.10 ± 0.08^{b} (0.00 − 0.34)
TDP (mg L^{-1})	0.008 ± 0.009^{b} (0.000 − 0.047)	0.007 ± 0.006^{b} (0.000 − 0.027)	0.032 ± 0.018^{a} (0.009 − 0.086)

Table A.1 (Continued)

Total Chlorophyll-*a*, Chl-*a*, (µg L^{-1})	15.5 ± 9.1[a] (1.5 − 39.3)	8.1 ± 7.0[b] (1.0 − 26.5)	3.2 ± 1.6[c] (0.4 − 9.2)
Physical Parameters			
Temperature, T (°C)	26.7 ± 6.5[a] (6.5 − 34.5)	16.9 ± 2.3[b] (13.7 − 22.6)	28.4 ± 2.7[a] (16.6 − 31.7)
Salinity (psu)	0.0 ± 0.0[c] (0.0 − 0.1)	2.9 ± 3.8[b] (0.0 − 12.6)	23.4 ± 3.3[a] (15.6 − 31.9)
pH	8.1 ± 1.2[b] (6.3 − 11.9)	9.5 ± 0.8[a] (8.1 − 11.3)	8.1 ± 0.3[b] (7.1 − 8.6)
Dissolved Oxygen, DO (mg L^{-1})	7.0 ± 1.4[a] (3.6 − 10.7)	6.7 ± 1.8[ab] (0.7 − 10.5)	6.2 ± 1.7[b] (3.4 − 9.6)

The values are shown as Mean ± Std. Dev. Range of the values are shown as (Min − Max). Levels not connected by the "same" letter are significantly different ($p \leq 0.05$).

APPENDIX B

PERMISSION

SPRINGER LICENSE
TERMS AND CONDITIONS

Jun 14, 2017

This Agreement between Dr. Padmanava Dash ("You") and Springer ("Springer") consists of your license details and the terms and conditions provided by Springer and Copyright Clearance Center.

License Number	4127960384012
License date	Jun 14, 2017
Licensed Content Publisher	Springer
Licensed Content Publication	Environmental Science and Pollution Research
Licensed Content Title	Influence of land use and land cover on the spatial variability of dissolved organic matter in multiple aquatic environments
Licensed Content Author	Shatrughan Singh
Licensed Content Date	Jan 1, 2017
Licensed Content Volume	24
Licensed Content Issue	16
Type of Use	Thesis/Dissertation
Portion	Full text
Number of copies	1
Author of this Springer article	Yes and you are a contributor of the new work
Order reference number	
Title of your thesis / dissertation	Influence of land use, land cover, and hydrology on the spatial and temporal characteristics of dissolved organic matter (DOM) in multiple aquatic ecosystems
Expected completion date	Aug 2017
Estimated size(pages)	170
Requestor Location	Dr. Padmanava Dash 109 Hilbun Hall MISSISSIPPI STATE, MS 39762 United States Attn: Dr. Padmanava Dash
Billing Type	Invoice
Billing Address	Dr. Padmanava Dash 109 Hilbun Hall MISSISSIPPI STATE, MS 39762 United States Attn: Dr. Padmanava Dash
Total	0.00 USD
Terms and Conditions	